Light delivery and light dosimetry for photodynamic therapy of bronchogenic carcinoma

Lars H.P. Murrer

Cover: Light dosimetry and thermometry device developed by the author and Jerry van der Ploeg for (pre-)clinical measurements.

Light delivery and light dosimetry for photodynamic therapy of bronchogenic carcinoma

Lichtapplicatie en lichtdosimetrie voor fotodynamische therapie van kanker van de bovenste luchtwegen

Proefschrift

Ter verkrijging van de graad van doctor
aan de Erasmus Universiteit Rotterdam
op gezag van de rector magnificus

Prof. dr P.W.C. Akkermans M.A.

en volgens het besluit van het college voor promoties.

De openbare verdediging zal plaatsvinden op

woensdag 4 februari 1998 om 13^{45} uur

door

Lars Henri Petra Murrer

geboren 12 april 1966 te Maastricht

Promotiecommissie

Promotor	Prof. dr P.C. Levendag
Overige Leden	Prof. dr ir M.J.C. Van Gemert
	Prof. dr B. Löwenberg
	Dr ir G.J. Puppels
Co-Promotor	Dr W.M. Star

Voor Ann en Stijn

This thesis has been prepared at:

Department of Clinical Physics
Daniel den Hoed Cancer Centre
University Hospital Rotterdam
The Netherlands

This work was kindly sponsored by:


DUTCH CANCER SOCIETY


RARE EARTH MEDICAL, INC.

QuantaNova

Address for correspondence:

Lars HP Murrer
Dept. of Clinical Physics
Daniel den Hoed Cancer Centre
University Hospital Rotterdam
PO Box 5201
3008 AE Rotterdam
The Netherlands
Phone: +31 10 4391746
Fax: +31 10 4864561
E-mail: murrer@kfih.azr.nl

Contents

Chapter 1

General Introduction

Photodynamic Therapy

Photodynamic therapy (PDT) is a treatment modality for malignant (and benign) diseases that combines administration of a chemical compound (photosensitiser) and irradiation with (visible) light of the proper wavelength and fluence to induce tissue necrosis. The mechanisms by which PDT induces cell death are not yet fully understood. The basic principle is that the illumination of the sensitiser causes excitation of the oxygen present in the tissue to the very reactive singlet state that induces damage to the tissue. The oxygen supply in the treated tissue is therefore of paramount importance for the final damage induced. Two types of damage are thought to be most important for the induced necrosis. Firstly, important (tumour)cell structures such as mitochondrial and cellular membranes are damaged with consequent direct cell death. Secondly, through damage of the endothelium of the blood vessels vascular stasis occurs which causes tissue damage as a secondary process.

The photosensitiser can be one single molecule like mTHPC (meta-Tetra-Hydroxy-Phenyl-Chlorin) or a mixture of several photo-active compounds as is the case with Photofrin. Instead of using exogenous photosensitisers, photosensitivity can also be generated in the living tissue by the induction of the formation of an endogenous photosensitiser ProtoPorphyrin IX (PPIX). This is achieved by administering ALA (5-amino-levulinic-acid), which intervenes in a feedback mechanism of the cycle of haem synthesis, thereby inducing excess formation of PPIX, which can then be used for photodynamic therapy.

The majority of the sensitisers is activated with red light ($\approx$ 630 nm for PPIX and Photofrin, 652 nm for mTHPC). Sometimes green light (514 nm) is also applied because some sensitisers (eg. Photofrin, PPIX) have stronger absorption at that wavelength. The penetration of green light in tissue is very limited ($\approx$ 1 mm) because of the strong absorption by blood. For the treatment of thick lesions this is a disadvantage but for the treatment of the superficial lesions in the oesophagus, however, the limited penetration depth of the green light is an advantage because it prevents perforations.

In the ideal case, the photosensitiser accumulates preferentially in the target tissue, and selective treatment of the target (tumour) tissue is possible. Unfortunately, most photosensitisers do not show these ideal localisation properties. A drawback of the use of photosensitisers is the fact that the clearance of the compound from the body can take some time (up to months with Photofrin), and during this period precautions most be taken to avoid

exposure to bright daylight, because the drug can accumulate in the skin (especially Photofrin). In the development of new sensitisers for clinical use, much effort is put into reducing the clearance time, which is, for example, reduced to two weeks for mTHPC.

Fluorescence

In parallel with the generation of singlet oxygen, the photosensitiser may show fluorescence. This fluorescence light can be used to estimate the amount of sensitiser present. This can be used to study the pharmacokinetics of the sensitiser, which knowledge helps to optimize treatment parameters such as the interval between administration of the sensitiser and illumination. During illumination the amount of sensitiser present can be reduced by photo-degradation, which can be monitored by a fluorescence measurement.

In the case of a sensitiser with good selective uptake in the tumour it might be possible to use the fluorescence to find pre-malignant tissue that is not yet visible with conventional techniques. There is a great need for methods for early detection of malignant tissue, because this generally enhances the chances of a successful treatment considerably.

Applications

The majority of the current applications of PDT concerns the treatment of malignant diseases. The light penetration in tissue is limited to a maximum of $\approx$ 1 cm, depending on the wavelength of illumination and the optical properties of the tissue. A consequence of this is that mostly superficial lesions are treated, although interstitial illumination of e.g. liver metastases is being investigated. In principle all tumours in areas that can be accessed either directly or by endoscopic techniques are eligible for treatment such as the skin, mouth, bladder, prostate, the digestive tract (oesophagus) and the upper respiratory tract. Sometimes intra-operative illuminations are performed e.g. in the thorax for treatment of malignant mesothelioma and in the peritoneum for treatment of ovarian cancer mestatases. Also benign diseases can be treated with PDT, for example warts and age related macular degeneration. Another interesting application is the disinfection of donor-blood with PDT.

PDT is often used for recurrent tumors, because in such cases the maximum tolerable radiation therapy dose has already been applied. The advantage of PDT is that it can be applied more than once, if necessary several illuminations can be performed with one single photosensitiser dose.

This thesis focuses on the treatment of cancer of the upper respiratory tract. PDT is used with curative intent on early lesions (carcinoma *in situ*) as well as for palliative means in the case of (partly) obstructing tumours.

Light delivery

Lasers are often used as a light source for PDT treatment, because they offer the possibility to tune the wavelength to an absorption maximum of the sensitiser. A second advantage of a Laser as a light source is that the light can be easily transported through fiber-optics, so that the light can be delivered at every place that is accessible by endoscopic techniques. For skin lesions sometimes conventional (halogen) lamps are used in combination with filters.

For the illumination of lesions three types of light delivery systems are commonly applied (figure 1). In the case of a localised lesion on a flat surface such as the skin or inside a hollow structure such as the upper respiratory tract a microlens is used that projects a divergent beam of light on the surface, causing a circular homogeneous illumination field if the beam's axis is perpendicular to the surface. In the case of the illumination of a hollow organ the output characteristics of the light applicator are adjusted to the geometry of the organ. For use in cylinder-like organs such as the trachea, the oesophagus and the prostate a linear (or cylindrical) diffuser is used that emits diffuse light over some length that can be chosen to fit to the dimensions of the treated lesion. For a sphere-like organ such as the bladder a spherical diffuser is used that acts as a diffuse point source.

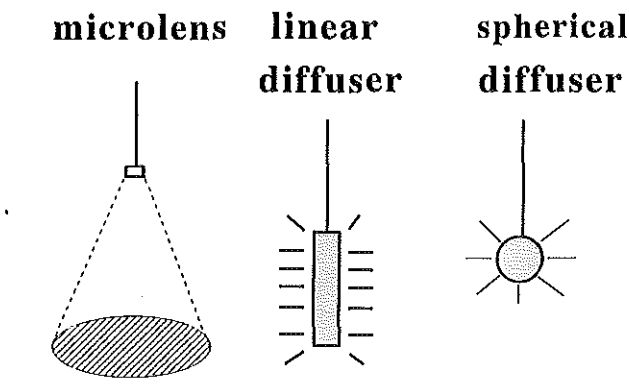

Figure 1.1: Overview of the light delivery systems used in PDT

Light dosimetry

The applied light fluence is one of the important factors for the final effect of the treatment. The applied fluence can be measured *in situ* with a fiberoptic isotropic probe. This detector measures the incoming light from all directions (fluence rate), which is a measure for the amount of optical energy available for absorption by the photosensitiser. This detector does not only measure the light incident on the tissue from the light delivery system, but also accounts for the light that is backscattered from the tissue. An isotropic probe is very similar to a spherical diffuser (figure 1), with this difference that the light is collected and sent through the fibre to a photodiode, instead of the light coming from the laser and being emitted.

A fluence measurement is of vital importance because large variations in the measured fluence can be observed for different patients treated with the same applicator with the same output. These variations are caused by inter-patient variations in the optical properties of the tissues.

Aim of the study

The aim of this study is well described by the title of this thesis, which was also the title of the project funded by the Dutch Cancer Society that provided the financial means to perform these investigations. Besides the importance of understanding the bio-distribution of the photosensitiser and the oxygenation of the tissue, the other aspect of paramount importance for the therapeutic effect is to deliver the light to the right place in the right amount. By conforming the illumination field to the tumor and tumor bed dimensions through proper light delivery techniques, the disadvantages of less-than-ideal bio-distribution of the photosensitiser can be diminished. The absolute levels and distribution of the fluence rate in the target tissues are highly dependent on the optical properties of the tissue leading to large inter-tissue and inter-patient variations. In order to perform well-defined fluence-response studies that yield readily comparable results it is a necessity to combine *in situ* measurements with knowledge gained from experiments and mathematical and Monte Carlo models.

This thesis focuses on light delivery and light dosimetry for PDT of the upper respiratory tracts, an area in which the light dosimetry was not very advanced until recently. Topics that are dealt with are: the influence of the quality of the linear diffusers used, of the optical properties of the bronchial tissue, of the position and length of the light source and of the diameter of the treated lumen. An applicator for the delivery and measurement of light was developed to put the knowledge to clinical practice.

Outline of the thesis

Chapter 2 describes measurements in *ex vivo* pig tracheas in which we measured the fluence rate in the tissue when the trachea was illuminated with a linear diffuser. The total fluence rate in the bronchial mucosa is considerably more than the fluence rate incident on the tissue from the linear diffuser. This is caused by backscattering from the tissue and multiple reflections in the cylindrical cavity of the trachea. Also the influence of the positioning of the light source was investigated. The measured fluence rate profiles are compared to the profiles simulated with a Monte Carlo model.

In chapter 3 a device is presented that measures the output characteristics of the linear diffusers used for endobronchial PDT. The consequences of those characteristics for illumination in a cavity and for interstitial illumination are evaluated. Chapter 4 shows improved designs of linear diffusers that were given to us after the publication of chapter 3.

In chapter 5 a design of an applicator for light delivery and light dosimetry is presented that incorporates a linear diffuser, a fixation system and an isotropic probe for *in situ* light dosimetry. Also the first *in vivo* measurements with this applicator are discussed.

The Monte Carlo model that is validated in chapter 2 is used to gain more insight in the fluence rate profiles resulting from varying diffusers in varying lumen diameters in tissue with varying optical properties. In chapter 6 the results of the simulations are presented, with an attempt to extend the findings to rules of thumb for clinical use.

The applicator for endobronchial PDT is used to perform a fluence-response study on the normal tissue of the pig trachea. In chapter 7 a short-term fluence finding experiment is described for maximum tolerable normal tissue damage with the use of the sensitisers Photofrin and mTHPC. Also the long-term recovery of the bronchial mucosa is evaluated with the fluence found in the short-term experiment.

An application of in *in vivo*, clinical use of light dosimetry is evaluated in chapter 8. The feasibility of intra-operative PDT of Malignant Mesothelioma in an entire hemithorax with mTHPC is investigated. Data of the first 5 patients are discussed.

Suggested reading

A comprehensive overview of clinical and preclinical Photodynamic Therapy is given by Fisher *et al* (1995). Lam (1994) presents an overview of PDT for lung cancer. Henderson and Dougherty (1992) provide information about the mechanisms involved in PDT tissue destruction. An overview of the clinical use of *in vivo* fluorescence can be found in Andersson-Engels and Wilson (1992)

An overview of the principles and applications of *in vivo* light dosimetry can be found in Star (1997). A complete overview of several aspects important for light dosimetry is offered by Welch and van Gemert (1995). In this book attention is paid to the mathematical modelling of light propagation in tissue and measurement of the optical properties of biological tissue. Also an overview is given of light delivery systems for PDT and other medical laser applications.

References

1. Andersson-Engels S, Wilson B C. (1992) In vivo fluorescence in clinical oncology: Fundamental and practical issues. *J. Cell Pharmacology* **3** *66-79*

2. Fisher A M R, Murphree A L, Gomer C J. (1995) Clinical and preclinical Photodynamic Therapy. *Lasers Surg. Med.* **17** *2-31*

3. Henderson B W, Dougherty T J. (1992) How does Photodynamic Therapy work? *Photochem. Photobiol.* **55** *145-157*

4. Lam S. (1994) Photodynamic therapy of lung cancer. *Semin. Oncol.* **21** *(suppl. 15) 15-19*

5. Star W M. (1997) Light dosimetry *in vivo*. *Phys. Med. Biol.* **42** *763-787*

6. Welch A J, van Gemert M J C *eds.* (1995) Optical-thermal response of laser-irradiated tissue. *New York: Plenum*

Chapter 2

Ex vivo light dosimetry and Monte Carlo simulations for endobronchial Photodynamic Therapy

(1995) Phys. Med. Biol. **40** *1807-1817.*

L.H.P. Murrer J.P.A. Marijnissen W.M. Star

Abstract

The light distribution during Photodynamic Therapy of the bronchial tree has been estimated by measuring the fluence rate in ex vivo experiments on dissected pig bronchi. The trachea was illuminated (630 nm) with a cylindrical diffuser and the fluence rate was measured with a fiberoptic isotropic probe. The experiment with the diffuser on the central axis was also simulated with Monte Carlo techniques using the optical properties that were determined with a double-integrating-sphere setup. The results from ex vivo experiments and the Monte Carlo simulations were found to agree within the error of measurement (15%), indicating that the Monte Carlo technique can be used to estimate the light distribution for varying geometries and optical properties. The results showed that the light fluence rate in the mucosa of the tracheal tract may increase by a factor of 6 compared to the fluence rate in air (in the absence of tissue). This is due to the scattering properties of the tissue and the multiple reflections within the cavity. Further ex vivo experiments showed that the positioning of the diffuser is critical for the fluence rate in the lesion to be treated. When the position of the diffuser was changed from the central axis to nearby the lesion, the fluence rate in the mucosa increased significantly by several orders of magnitude as compared to the initial (central) illumination. The inter- and intra- specimen variations in this increase were large ($\pm$ 35 %) because of variations in optical and geometrical properties and light source positioning, respectively. These variations might cause under- or overdosage resulting in either insufficient tumour-necrosis or excessive normal-tissue damage.

Introduction

Light dosimetry in tissue is essential for the proper evaluation of the effect of PhotoDynamic Therapy (PDT). For bladder, esophagus and skin, attempts have been made to perform dosimetry during treatment (Marijnissen *et al* 1993a, Overholt *et al* 1994, Hudson *et al* 1994). Except for the skin treatment, where it is possible to use invasive methods, light dosimetry is limited to measurements of the fluence rate at the surface. The penetration of light in the tissue has to be estimated with the aid of radiative transfer models (diffusion theory) (Star 1995) and Monte Carlo simulations (Keijzer *et al* 1991). These methods rely on measurements of optical properties which should ideally be performed in vivo and non-invasively (Patterson

et al 1989). In the bronchus, the dosimetry during treatment is seriously hampered by the requirement of a measurement technique that does not block the air flow. The lesion is illuminated through a cylindrical diffuser of which the length (typically 2 cm) can be adapted to the size of the lesion. In clinical practice, dosimetry has been limited to specification of the total output per unit length of the diffuser (typically 200 J/cm at 630 nm). Few studies on the influence of the geometry and optical properties of the illuminated lumen of the bronchus have been published (Marijnissen *et al* 1993b).

The first objective of this study is to assess the influence of the placement of the light source in the lumen. Even though most clinical protocols prescribe that the cylindrical light source be placed on the central axis of the lumen, clinicians are often tempted to place the source close to the visible part of the lesion. The motive for this is to increase the light dose in the lesion and spare the normal tissue at the opposite side. The light dosimetry for such a geometry has never been evaluated. In this study PDT in the bronchus is mimicked by ex-vivo experiments on pig bronchi.

The second aim is to estimate the light distribution in the mucosal layer at the inside of the trachea during endobronchial PDT by combining ex-vivo experiments on pig bronchi with Monte Carlo simulations for the same optical properties and geometry as the experiment. Once agreement between ex vivo and Monte Carlo data is reached, the latter can be used to estimate the light distribution for varying optical properties and lumen diameters. This provides a tool for evaluating light dosimetry during treatment.

Materials and Methods

Ex-Vivo Fluence Rate Measurements

Experiments were performed in the trachea of a fresh, dissected pig-bronchus. The trachea was excised and mounted vertically on a stand. For the delivery of light we used a 2 cm cylindrical diffusing light source (Quadra Logic Technologies, Canada) that was connected to an argon pumped dye-laser (Spectra Physics model 2040E/375B) that produced light of 630 nm. The light source was positioned in the trachea either on the central axis (central) of the trachea, against (proximal) or opposite the site of measurement (distal) (figure 1) (in contact with the tissue). The output of the diffuser was measured with an integrating sphere power meter and adjusted to 800

mW, corresponding to the clinically used output of 400 mW/cm diffuser length.

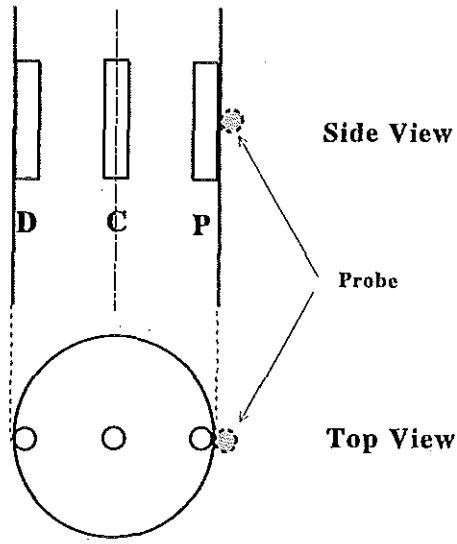

Figure 2.1: *Schematic drawing of three possible positions of the light source. C=central, D=distal and P=proximal to the site of measurement (probe position indicated).*

The light fluence rate was measured with an isotropic probe (accuracy ± 15%) constructed with a small (diameter 0.9 mm) scattering sphere mounted on a quartz fiber (core diameter 200 μm), of which the directional sensitivity showed a ± 15% deviation from mean for angles from -160 to 160 degrees relative to forward incidence (van Staveren *et al* 1995a).

The probe was calibrated in air in a home-made integrating sphere with built-in laser diodes that provided a stable diffuse light field at a wavelength of 680 nm. With an appropriate conversion factor this provided a reference light field of 7.0 mW/cm^2 for calibration at 630 nm (van Staveren *et al* 1995a). When the probe is calibrated in air, the fluence rate measured in tissue has to be multiplied by a factor 1.7 to account for the losses due to the change of refractive index (Marijnissen *et al* 1987). This correction factor was determined empirically by comparing the detector response to a uniform beam in air and in water. Water serves as a phantom for tissue in this instance because it has a refractive index close to tissue (water: n=1.33,

tissue (mucosa, see section Optical Properties): n=1.37). The correction for measurement while pressing the detector against the mucosa reduces to 1.07 (sd 0.03) and was determined in a similar way by immersing the probe halfway into the water.

The probe was placed either in the trachea on the mucosa or gradually inserted from the outside in between the cartilage rings until the probe was positioned below the mucosa. Measurements were made at 4 different positions, viz. (1) on the mucosa inside the trachea, (2) just below the mucosa on the edge of the cartilage, (3) in the tissue between the cartilage rings and (4) in the tissue just outside the cartilage rings (figure 2). The measurement made with the probe pressed against the mucosa yields an average value of the fluence rate in the mucosa and in air. Those fluence rates will be different because of the change of refractive index.

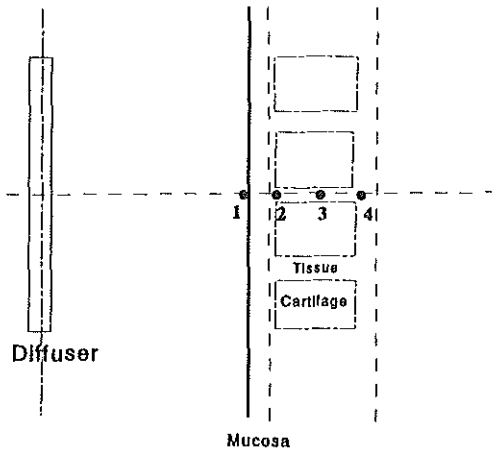

Figure 2.2: *Places of measurement on and in the trachea wall. (1) on the mucosa inside the trachea,(2) just underneath the mucosa, (3) in between the cartilage rings and (4) in the tissue just outside the cartilage rings. The mean depths (n=5) of positions 1..4 are 0, 0.9(0.1), 2.7(0.5) and 3.5(0.4) mm respectively (sd in parentheses).*

In some experiments the position of the probe in the tissue relative to the diffuser was varied to measure at the tip, the centre and the bottom of the

diffuser. The influence of limited tissue thickness outside the trachea was investigated by comparing the readings at position 4 without and with some extra tissue added at that position. The variations found were only minor compared to the error in the measurement, and therefore the influence of the tissue thickness is only minor.

Optical Properties

The optical properties of the mucosa were determined with a double-integrating-sphere setup combined with an Inverse Adding Doubling (IAD) algorithm (Pickering *et al* 1993). This setup yields values for the scattering coefficient μ_s and the absorption coefficient μ_a as well as the anisotropy factor g. The index of refraction of the mucosa was found to be n=1.37 ($\pm$ 0.01 for 450 nm $< \lambda <$ 650 nm), by measurement of the critical angle of interface between tissue and glass (n=1.73, λ = 630 nm (van Staveren 1995b)). The optical properties were measured after the ex-vivo experiment. The mucosa was seperated from the cartilage and and the tissue samples were either measured immediately or after keeping them refrigerated in saline overnight. The optical properties of the supporting cartilage rings were also measured.

From μ_a, μ_s and g the other relevant optical properties can be derived, according to $\mu_t = \mu_s + \mu_a$, $\mu_{tr} = \mu_a + \mu_s(1-g)$ and $\mu_{eff} = \sqrt{3\mu_a\mu_{tr}}$, which are the total-, transport- and effective attenuation coefficients, respectively.

Monte Carlo Simulation

The Monte Carlo code was adapted from the code used to simulate whole bladder wall illumination (Keijzer *et al* 1991). The geometry of the experiment was modelled as a cylinder of air (diameter typically r=18-20 mm) embedded in a cylindrically symmetric semi-infinite medium (height h=50 mm, outer radius $r \rightarrow \infty$). The chosen height was typical for the length of trachea that is used in an experiment. Making the slab thicker resulted in no significant changes in light distribution and for the sake of spatial resolution the slab thickness was kept limited. The air in the cylinder has negligible absorption and scattering, and the index of refraction is 1. The semi-infinite medium has the optical properties of the mucosa layer at the inner side of the trachea at λ=630 nm. The linear light source with a length of 2 cm is modelled as a continuous distribution of ideal isotropic point sources placed on the central axis of the cylinder (figure 3). An

estimate of the error in the simulation is calculated from the standard deviation of 5 consecutive runs of 25000 photons each. The total output (i.e. the summed contributions of all point sources) of the source was adjusted to fit the output of the source in the ex vivo experiment as measured with an integrating sphere.

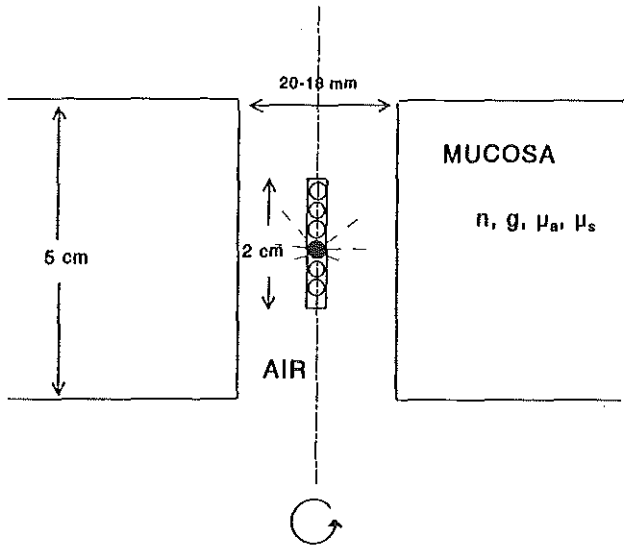

Figure 2.3: *Schematic representation of the cylindrical Monte-Carlo model. One layer of mucosa was simulated, of thickness 5 cm and a radius* $r \rightarrow \infty$. *The 2 cm light source consist of homogeneously distributed isotropic point sources. The cavity has a diameter of typically 18-20 mm and is filled with air as is the space outside the slab of mucosa.*

In the tissue, the measured and simulated fluence rate may be readily compared. The measurement at the surface (position 1) with the probe partly in the tissue is approximated by a volume element on the border of the tissue, with one surface facing the air in the cavity. In general however, the optical properties of the probe material differ from those of the tissue. This causes local changes in the light distribution and introduces inaccuracies (Marijnissen 1993c).

Results

Ex vivo measurements

The fluence rate measured in the mucosa and the tissue in between the cartilage rings for one trachea is shown in figure 4. The fluence rate in air was measured beforehand with an isotropic probe, at a distance from the diffuser equivalent to position 1 (figure 2) in the absence of tissue. This value ϕ_0 is used to define a fluence rate build-up factor β in analogy with earlier work in the bladder (van Staveren *et al* 1994). This factor relates the true fluence rate ϕ_{true} in the mucosa to the unscattered incident light coming directly from the linear diffuser.

$$\beta = \frac{\phi_{true}}{\phi_0} \tag{2.1}$$

The measured ϕ_0 is in reasonable agreement with calculations of simple models with either a linear light source that emits light only perpendicularly to its length or a superposition of isotropic point sources (see below). In the first case ϕ_0 is described by

$$\phi_0(r) = \frac{P^*}{(2\pi r)} \qquad mW/cm^2 \tag{2.2}$$

and in the second case

$$\phi_0(r,l) = \frac{P^*}{(2\pi r)} \arctan(l/2r) \qquad mW/cm^2 \tag{2.3}$$

where r is the radial distance from the diffuser $[cm]$ and l is the length of the diffuser $[cm]$. P^* is the radiant power per cm diffuser length $[mW/cm]$. For the experiments $l = 2$ cm, $r \approx 1$ cm and $P^* = 400$ mW/cm, which yields a fluence rate of $\phi_0 \approx 64\,mW/cm^2$ in the first, and $\phi_0 \approx 50\,mW/cm^2$ in the second case. On average (n=7), both formulas underestimate the measured (non-scattered) fluence rate by 7% and 22%, respectively, which is of the same order of magnitude ($\pm$15%) as the error in the measurement.

The data in figure 4 are for a trachea with a diameter of 20(1) mm. The measured ϕ_0 was 56 mW/cm^2. The fluence rate in air as a function of

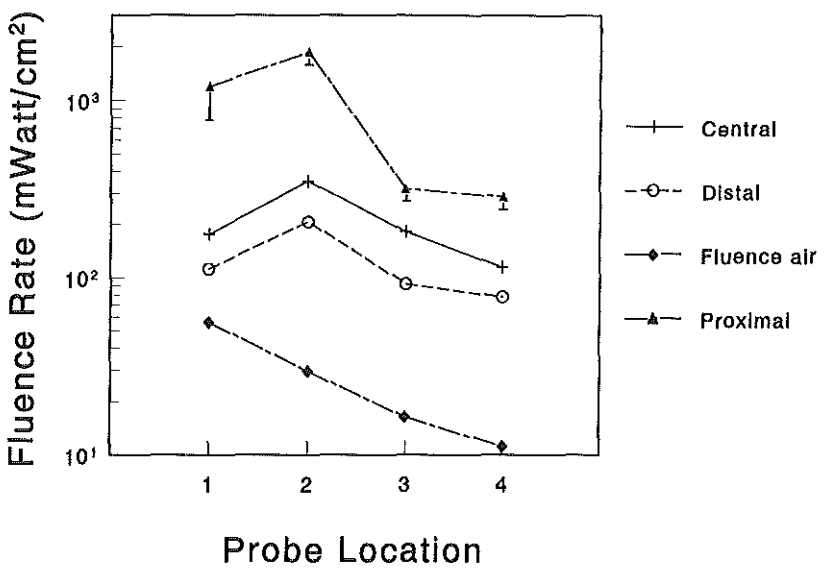

Figure 2.4: *Fluence rate measured on and in the trachea wall, on positions 1-4 described in the methods section. The linear diffusing light source of 2 cm length emits 800 mWatt of light at λ=630 nm. The light source was placed either centrally, distally or proximally. The estimated error in measurement is 15%, except for the measurement on position 1, proximal (see text).*

distance is also indicated for reference. It can be roughly described by a $1/r$ relationship (r = radial distance between diffuser and probe). When the diffuser was placed centrally, we observed a build up factor $\beta = 3.1$ on the mucosa (position 1) and $\beta = 6.3$ just underneath (position 2). Further in the tissue (positions 3,4) the fluence rate decreases, though not as rapidly as in air.

The fluence rate build-up for the distal placement showed the same dependency on distance in the tissue with an amplitude of about half that of the central illumination. The ratio β on position 1 and 2 now is 2.0 and 3.7, respectively.

Proximal illumination increased the fluence rate considerably. β values of 21.4 and 33.4 are a factor 6.9 and 5.3 higher on position 1 and 2 as compared to the central illumination. The error in the measurement of the fluence rate on position 1 was rather large (35%) because small variations in diffuser postioning caused rather large variations in the measured fluence rate. This error implied an uncertainty in delivered fluence rate of a factor of $\approx 2(35\% \times 6.9)$. These fluctuations were absent when we measured on position 2. Deeper in the tissue the fluence rate decreases similarly to the first two cases.

Figure 5 shows data from 6 tracheas. To make an inter-specimen comparison to evaluate the influence of diffuser positioning, we normalized the fluence rates to a reference value, ϕ_{ref}. This is the fluence rate observed on position 1 and central illumination. We chose this value for normalisation because this will be the only value that might be measured during treatment.

The fluence rate was significantly lower in the distal case, as the average on position 1 is 0.64 (sd 0.02). Proximal positioning caused an increase of a factor 4.0 with a standard deviation = 0.9, indicating an overall fluence rate uncertainty of 90%. On average a slight, though not significant, increase of fluence rate could be observed just underneath the mucosa. The fluence rate measured just outside the cartilage rings (position 4) is still considerable. The measured fluence rates were 49(8)%, 43(5)% and 137(29)% of ϕ_{ref} for central, distal and proximal illumination respectively.

The mean values for β for central illumination are summarized in table I. The true fluence rates on positions 1-4 have been divided by ϕ_0 for each

Position	1	2	3	4
β	4.9(1.7)	6.2(2.9)	4.9(3.1)	2.1(0.5)

Table 2.1: *Mean (n=6) β values (Eq. 1) for positions 1-4 (figure 2) in the trachea wall, standard deviation in parentheses.*

individual specimen. The fluence rate tended to be built up to a maximum just below the mucosa (position 2).

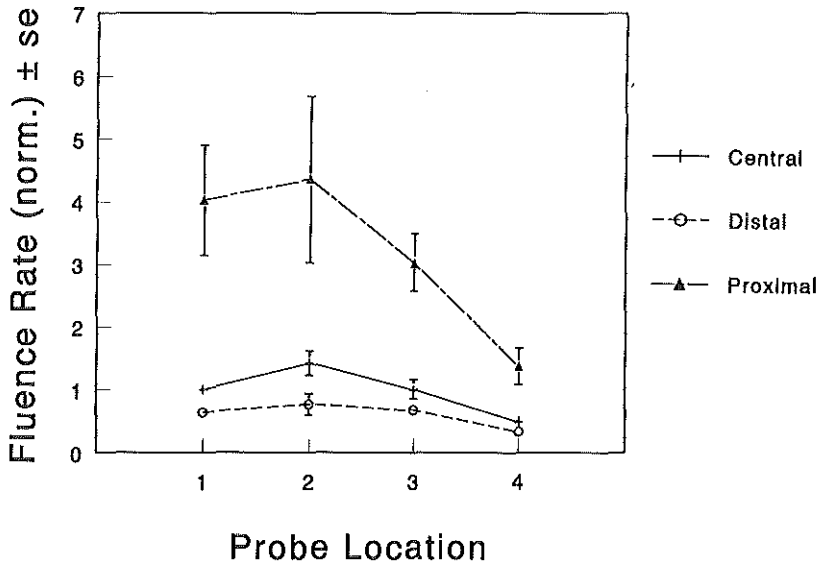

Figure 2.5: *Average of the measured fluence rate in different tracheas (n=6) with a diameter varying from 18-20 mm. The fluence rates for each individual trachea were normalised to the fluence rate measured on position 1 for each specimen, centrally to correspond with the normal treatment protocol. Fluence rates were measured on positions 1-4 (see Methods) with the light source placed centrally, distally or proximally.*

Monte Carlo Simulations

Optical properties

The averaged (n=5) optical properties of lung mucosa and cartilage are summarized in table II. The specimens were taken from 5 of the 6 tracheas used for the ex vivo dosimetry experiment. The mean thicknesses of the mucosa and cartilage layers were 0.9(0.1) mm and 2.6(0.4)mm. The inter-specimen variation of optical properties is rather large which is reflected in

Tissue type	absorption μ_a (cm^{-1})	scattering μ_s (cm^{-1})	anisotropy g(-)
mucosa	0.22 (0.17)	113 (19)	0.80 (0.06)
cartilage	0.10 (0.06)	43 (17)	0.56 (0.11)

Tissue type	total attenuation μ_t (cm^{-1})	transport attenuation μ_{tr} (cm^{-1})	effective attenuation μ_{eff} (cm^{-1})
mucosa	113 (19)	22 (5)	3.9 (0.9)
cartilage	43 (17)	19 (5)	2.2 (0.6)

Table 2.2: *Mean values of optical properties of bronchial mucosa and cartilage for λ =630 nm. Standard deviations for n=5 specimens in parentheses.*

high standard deviations. The variation of μ_a is most prominent (77% and 60% for mucosa and cartilage, respectively).

Cartilage tends (though not significantly) to be less absorbing, and is significantly less scattering than mucosa. On the other hand, cartilage is a more isotropic scatterer. This is reflected in the g value, which is significantly lower for cartilage. The g and μ_s values combine to about equal transport attenuation coefficients (μ_{tr}) for both tissue types. The low absorption of cartilage results in a lower effective attenuation (μ_{eff}).

The optical properties for mucosa and cartilage of the trachea that was simulated are summarized in table III. These values were measured for a different trachea than that used for the data of figure 4. The values are comparable to the average values in table II within the error of measurement. The lumen diameter was 20(1) mm, the mucosa thickness was 1.0(0.1) mm and the cartilage thickness was 3.2(0.1) mm.

Simulations

The calculated and the measured fluence rate in this trachea are shown in figures 6 A and B. Generally speaking, the measured and simulated data were in agreement. This in spite of the fact that the trachea was modelled as consisiting only of mucosa without accounting for the cartilage. The

Tissue type	absorption μ_a (cm^{-1})	scattering μ_s (cm^{-1})	anisotropy g (-)
mucosa	0.15 (0.02)	81.2 (0.9)	0.77 (0.01)
cartilage	0.040 (0.006)	29.4 (0.5)	0.45 (0.01)

Tissue type	total attenuation μ_t (cm^{-1})	transport attenuation μ_{tr} (cm^{-1})	effective attenuation μ_{eff} (cm^{-1})
mucosa	81.4 (0.9)	18.7(0.5)	2.9 (0.2)
cartilage	29.4 (0.5)	16.2(0.8)	1.4 (0.1)

Table 2.3: *Optical properties of bronchial mucosa and cartilage of simulated trachea for λ = 630 nm. Standard deviations for n=4 spots on the specimen in parentheses.*

error in the measurement (15%) is larger than the statistical fluctuations in the simulation (2-3%).

In figure 6 A the fluence rate in the tissue is presented. The measured and Monte Carlo data agree in the mucosa layer, but start to deviate in the cartilage region as is to be expected. The simulated fluence rate is 50% lower than the measured fluence rate at the outer edge of the cartilage.

In figure 6 B the fluence rate inside the trachea on the mucosa surface is presented. The measurements were made opposite the tip (-10mm), the middle (0 mm) and the tail (10 mm) of the diffuser. The measured fluence rate opposite the tip was higher than that opposite the tail. This was probably caused by the (non-ideal) output characteristics of the linear diffuser. The effective length of treatment is longer than the diffuser length. If the 37% (1/e) value of the maximum fluence rate is taken as a measure, the treated length is $\approx$ 32 mm.

We calculated the influence of the error in the measurement of the optical properties on the outcome of the Monte Carlo simulation by performing simulations with the above used values plus or minus the standard deviations. We found that the influence of variations in g and μ_s were only minor (5% and 2%, respectively). The influence of the variations in μ_a were larger, especially when the value was lowered by 1 standard deviation. This yielded an error of 12 %. Varying the diameter of the lumen by 1 mm,

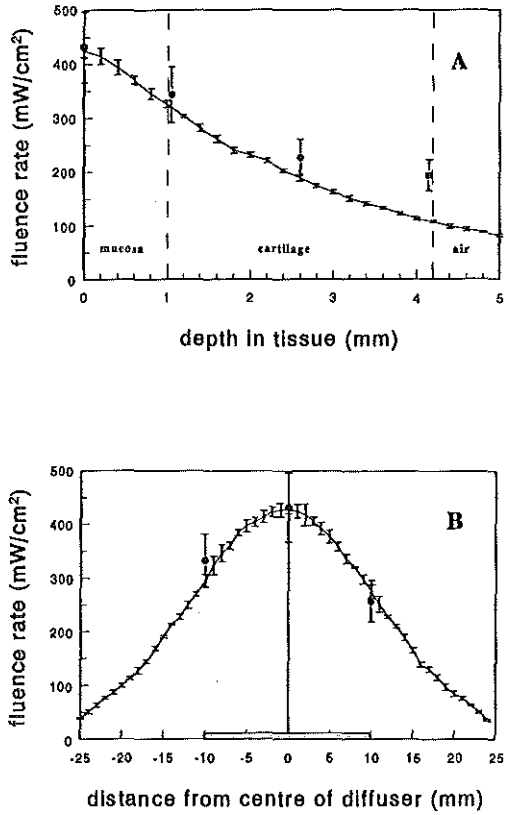

Figure 2.6: *Comparison of measured fluence rate (dots) and Monte Carlo simulated data (solid line) for central illumination with 2 cm linear diffuser emitting 800 mWatt of light at λ=630nm. Measured data are ± sd (15%) and the Monte Carlo data ± sd calculated from 5 consecutive runs of 25.000 photons each. A: Measurements in the trachea wall, opposite the middle of the light source. Positions of measurement 1-4 with real distance, for mucosa thickness of 1(0.1) mm and cartilage thickness 3.2(0.1) mm. The stippled lines indicate the borders between air, mucosa and cartilage in the ex vivo experiment. B: Measurements on the mucosa inside the trachea opposite the middle (0 mm), top (-10 mm) and bottom (10 mm) of the diffuser. The diffuser position is indicated on the x-axis.*

which is the estimated measurement error, resulted in a 6% variation.

Discussion

The light dose delivered to the tissue strongly depends on the positioning of the diffuser in the lumen. If the diffuser is fixed in the centre of the lumen a reproducible and rotationally uniform illumination can be achieved. Moving the diffuser towards the visible part of the lesion causes a high and variable increase in the light dose in the lesion and is accompanied by a decrease of dose in the tissue at the opposite side. The disadvantage of such a procedure is that the light dose in the lesion is not controllable, which hampers interpretation of dose-response data. Furthermore, the light dose is not distributed uniformly across the lumen, thereby underdosing possible pre-malignant cells at other sites. Therefore, we strongly recommend that during endobronchial PDT the linear diffuser always be fixed at the centre of the lumen.

The scattering nature of the tissue helps to broaden the treated area and increases the light dose by a maximum factor of 6.2 just underneath the mucosa (table I) when compared to the incident unscattered illumination. This factor is of the same order of magnitude as observed in pig bladder ($\beta = 5.0$) (van Staveren *et al* 1994), which has approximately the same optical properties but a different geometry. Lesions that invade between the cartilage rings may also be treated, as the fluence rate decreases only slowly with increasing depth (figure 5).

The measured optical properties (table II) for the mucosa were different from the $\mu_{eff} = 9.1\ cm^{-1}$ for human mucosa reported by Cheong *et al* (1990). Nevertheless, with our set of optical properties we were able to obtain agreement between the Monte Carlo simulation and the ex vivo experiment, especially in the mucosa.

The measurent of μ_a is the most critical. The outcome of the simulation strongly depends on the value of μ_a, and table II shows a large inter-specimen variation of the absorption. This indicates that there is a great need for non-invasive in vivo methods for the accurate determination of optical properties (e.g. Patterson *et al* 1989).

The measured fluence rate outside the mucosa, in between the cartilage rings, is higher than the simulated fluence rate. This is caused by the inadequate modelling of a semi-infinite medium consisting of only mucosa.

The underestimation of the true fluence rate can be understood qualitatively by taking the properties of the cartilage into account. The cartilage of the example trachea is less absorbing and more isotropically scattering than the mucosa (see table III), which may result in a higher light dose. An additional factor is the change of refractive index from tissue (n=1.37) to air (n=1.00) outside the cartilage, which causes internal reflections and thereby an increase in light dose.

On average, we observed an increase in fluence rate just below the mucosa (figure 5, table I) in the ex vivo experiment. This phenomenon did not occur in our Monte Carlo simulations. This observation might be explained by the same arguments as above. Indeed, on average the cartilage is less absorbing and more isotropically scattering than the mucosa (table II). Despite the inadequate modelling we were able to predict the light dose in the mucosa, and we expect that further improvement of the model will allow prediction of the fluence rate in the cartilage region.

Acknowledgments

The authors wish to thank Jerry van der Ploeg for the development and maintenance of the dosimetry equipment and Marleen Keijzer for supplying the basic Pascal code for the Monte Carlo simulations. The Laser Centre at the Amsterdam Medical Centre kindly provided access to the double-integrating-sphere setup.

References

1. Cheong W F, Prahl S A, Welch A J. (1990) A review of optical properties of biological tissues. *IEEE J. Quantum Electron.* **26(12)** *2166-2185*

2. Hudson E J, Stringer M R, Cairnduff F, Ash D V, Smith M A. (1994) The optical properties of skin tumors measured during superficial photodynamic therapy. *Lasers Med. Sci.* **9** *99-103*

3. Keijzer M, Pickering J W and van Gemert M J C. (1991) Laser beam diameter for port wine stain treatment. *Lasers Surg. Med.* **11** *601-605*

4. Marijnissen J P A, Star W M. (1987) Quantitative light dosimetry in vitro and in vivo. *Lasers Med. Sci.* **2** *235-242*

5. Marijnissen J P A, Star W M, In 't Zandt H J A, D'Hallewin M A, Baert L. (1993a) In situ light dosimetry during whole bladder wall photodynamic

therapy: clinical results and experimental verification. *Phys. Med. Biol.* **38** *567-582*

6. Marijnissen J P A, Baas P, Beek J F,van Moll J H, van Zandwijk N, Star W M. (1993b) Pilot study on light dosimetry for endobronchial photodynamic therapy. *Photochem. Photobiol.* **58** *92-98*

7. Marijnissen J P A. (1993c) Optimization of light delivery and light dosimetry for photodynamic therapy. *PhD. Thesis, Univ. of Amsterdam*

8. Overholt B F, Panjehpour M, Denovo R C, Petersen M G. (1994) Photodynamic therapy for esophageal cancer using a 180° windowed esophageal balloon. *Lasers Surg. Med.* **14** *27-33*

9. Patterson M S, Chance B, Wilson B C. (1989) Time resolved reflectance and transmittance for the non-invasive measurement of tissue optical properties. *Appl. Opt.* **28(12)** *2331-2336*

10. Pickering J W , Prahl S A , van Wieringen N, Beek J F and van Gemert M J C. (1993) Double-integrating-sphere system for measuring the optical properties of tissue. *Appl. Opt.* **32** *399-410*

11. Star W M. (1995) Diffusion theory of light transport. *In: 'Optical-thermal response of laser-irradiated tissue', chapter 6, ed. Welch A J, van Gemert M J C (Plenum: New York)*

12. van Staveren H J, Beek J F, Ramaekers J W H, Keijzer M, and Star W M. (1994) Integrating Sphere effect in whole bladder wall photodynamic therapy: I. 532 nm versus 630 nm optical irradiation. *Phys. Med. Biol.* **39** *947-959*

13. van Staveren H J, Marijnissen J P A, Aalders M C G and Star W M. (1995a) Construction, quality control and calibration of spherical isotropic fibre-optic light diffusers. *Lasers Med. Sci.* **10** *137-147*

14. van Staveren H J. (1995b) The physics of photodynamic therapy for bladder carcinoma. *PhD. Thesis, Univ. of Amsterdam*

Chapter 3

Light distribution by linear diffusing sources for Photodynamic Therapy

(1996) Phys. Med. Biol. **41** *951-961*

L.H.P. Murrer , J.P.A. Marijnissen, W.M. Star

Abstract

The distribution of the light emitted by linear light diffusers commonly employed in PhotoDynamic Therapy (PDT) has been investigated. A device is presented which measures the angular distribution of the exiting light at each point of the diffuser. With these data the fluence rate in air or in a cavity at some distance from the diffuser can be predicted. The results show that the light is scattered from the diffuser predominantly in the forward direction. Experiments and calculations show that the fluence rate in air and in a cavity of scattering tissue at some distance from the diffuser has a maximum near the tip of the diffuser, instead of near the middle. However, the fluence rate resulting from an interstitial diffuser in a purely scattering tissue phantom shows a maximum in the bisecting plane of the diffuser as would be predicted when the diffuser emitted light isotropically. The scattering nature of the tissue is expected to cancel the anisotropy of the diffuser.

Introduction

Linearly diffusing light sources are commonly employed for PhotoDynamic Therapy (PDT) in cylinder-like hollow organs such as the bronchus (Marijnissen *et al* 1993) and the oesophagus (Overholt *et al* 1994). Interstitial illumination is also employed, e.g. in the brain (Ji *et al* 1992) and more frequently in animal models (e.g. Cairnduff *et al* 1995). The dosimetry in these treatment modalities is limited to the specification of the radiant power per cm diffuser length, without specification of the angular power-distribution of the emitted light. Monte-Carlo simulations and radiative transfer theories for these treatments mostly employ a model of a linear light source that consists of a row of ideal isotropic point sources (e.g. Murrer *et al* 1995). The present study investigates the influence of the expected non-isotropy of these point sources.

In clinical practice, during treatment of a hollow organ like the trachea, the output of the diffusers is assumed to be a cylindrically symmetric, uniform field along the length of the diffuser, which is too simple an approach. Indeed, measurements of the fluence rate at some distance from the diffuser have shown a forward directed scattering from the diffuser (Feather *et al* 1994), with a non-uniform distribution parallel to the diffuser. During interstitial application, the scattering and absorbing properties of the tissue

will also determine the light distribution in the tissue.

In this paper we present a device that provides a means of checking the quality of a linear light diffuser by measuring the angular distribution of the emitted light from the diffuser, and an algorithm to determine the fluence rate in air at some distance from the diffuser. Also the influence of the presence of scattering tissue (bulk or a cavity wall) has been investigated.

Materials and Methods

The angular distribution of the light emitted by a linear diffuser is measured by the apparatus shown in figure 1. A (black) measuring head is mounted on a rail and can be moved by computer-control. In this head 5 detectors are mounted at different angles with respect to the surface that will be measured, viz. at 30, 60, 90, 120 and 150 degrees. The angles are defined relative to the direction of the incoming light from the fibre. The detector at 30 degrees therefore measures light that is emitted in a forward direction.

The detectors are constructed with a lens (diameter 2 mm) mounted at a fixed distance from a cleaved bare fibre, in such a way that an image of the measured surface is formed on the fibre surface. The light is then transported through the fibre to photodiodes (Photop^T 455, United Detector Technologies), and the signal of the diodes is A/D-converted and stored on the PC's hard-disk. The light source we used for all experiments and calibrations is a HeNe-laser ($\lambda = 632.8$), with an output of several mWatts. The setup with 5 fixed angles offers a quick method for measurement of the output of a linear diffuser, which is desirable for clinical use.

We used a lens with a focal distance of $f = +3.5\ mm$, fixed on the image distance of $d_i = 7\ mm\ (2f)$ of the fibre (figure 1). Using the lens-formula $(1/f = 1/d_i + 1/d_o)$ this means that the fibre surface has to be placed at the object distance ($d_o = 7\ mm\ (2f)$), while measuring the output of the fibre in air. Such a setup measures the radiance at a point of the surface ($Watt/(sr\ m^2)$). The detectors are calibrated relative to each-other by measuring the radiance of an isotropic spherical diffuser, which should yield the same reading for each detector (see figure 1).

The 5 detectors sample one common point on the diffuser surface. By moving the head parallel to the diffuser the entire diffuser surface is sampled. The surface is divided into sections by making measurements at 0.5 mm intervals. The diffuser is also rotated 90 degrees along its axis, and the

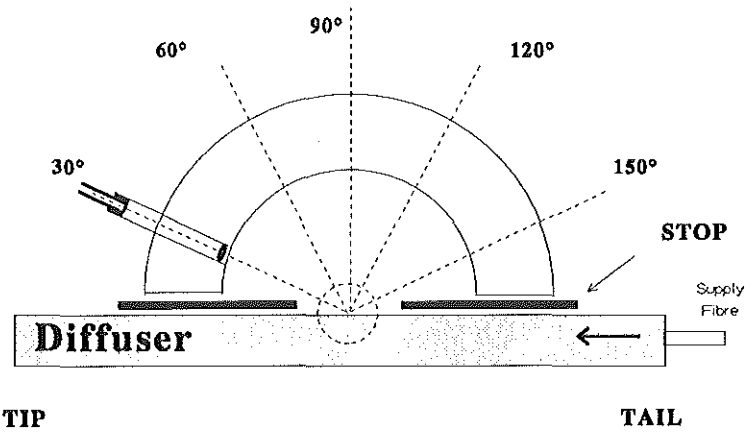

Figure 3.1: *Schematic representation of the measurement device. The light enters the diffuser from the right side (arrow) through a supply fibre. The side where the light enters the diffuser is denoted as the tail, the distal end of the diffuseris denoted as the tip. These conventions are maintained in all figures. One point of the diffusing surface is sampled from 5 angles (30°..150°) by 5 lenses. The measuring head can be moved parallel to the diffuser. The stop reduces scattered light from other parts of the diffuser surface. The dashed circle indicates the position of the isotropic spherical diffuser for calibration.*

measurement is repeated to check for cylindrical symmetry of the emitted radiation pattern. To check for intra- and inter measurement variations we performed a series of measurements with and without removing and repositioning the fibre between measurements. Influence of scattered light from other than the sampled part is minimized by putting a stop (diameter 2 mm) over the diffuser surface which leaves only the sampled part visible (figure 1).

The radiance measured at 30,..,150 degrees is used to estimate the radiance in the directions that were not measured by fitting a sixth-degree Lagrange interpolation polynomial (Abramowitz and Stegun, 1970) through the measurements at 5 angles and assuming that the radiance at 0° and 180° is

zero. This yields a curve for each element n of the surface that is measured for each angle α, denoted as $L_{6,n}(\alpha)$ (figure 2, part B). This polynomial does occasionally result in small negative values for the radiance, which is not realistic. In such a case, the absolute value of this radiance is used, but this does not represent a large contribution to the total.

From the results of the diffuser-tester the measured fluence rate $\phi(d, z)$ (Watt/cm^2) at a certain distance d from the linear diffuser and a distance z from the tip of the diffuser can be predicted. This is achieved by summing the contributions $\phi_n(d, z)$ of the N separate sections that are measured (Eq. 3.1).

$$\phi[d, z] = \sum_{n=1}^{N} \phi_n[d, z] \tag{3.1}$$

These sections have the co-ordinate X_n as indicated in figure 2 (part B). The contribution of one section to the fluence rate is the irradiance caused by this section on the surface perpendicular to the direction of the incoming light. The radiance in this direction is determined by the interpolation polynomial $L_{6,n}(\alpha_n[d, z])$ (figure 2, part A).

The irradiance in the direction of the measurement is then determined by firstly multiplying the radiance by the cosine of the angle α_n (Eq.3.2) with the normal to the surface and by the projection of the diffuser surface A_n of each element (in a plane perpendicular to the plane of figure 2 B). Assuming a cylindrically symmetric emission pattern, this projected surface becomes equal to the surface of the section parallel to the axis of the linear light source which is the length of the section (L/N) multiplied by the diameter of the diffuser D (Eq. 3.3). Secondly, the radiance is divided by the square of the distance r_n (Eq. 3.4) from measurement site to section surface to go from power per solid angle (W/sr) to power per surface area (W/m^2). This leads to a contribution of each section according to Eq. 3.5.

$$\alpha_n[d, z] = \arctan((z - x_n)/d) \tag{3.2}$$

$$A_n = \frac{L}{N} D \tag{3.3}$$

$$r_n^2[z, d] = (z - x_n)^2 + d^2 \tag{3.4}$$

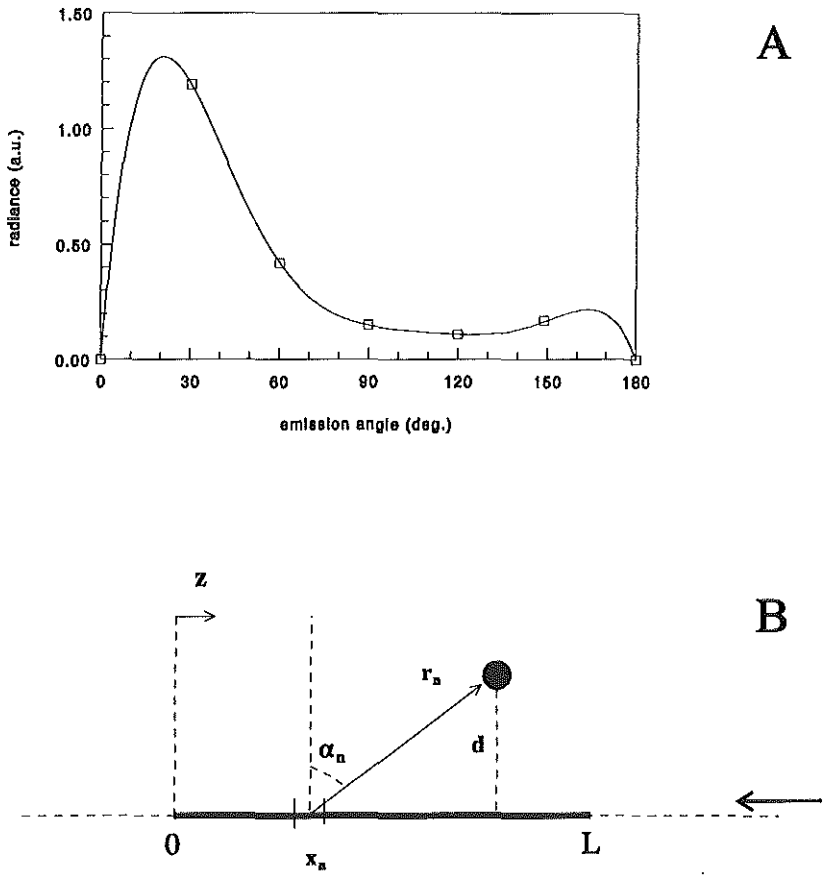

Figure 3.2: **A** *: Example of a sixth-degree polynomial fit through the measurements at 5 angles (30°..150°) and the assumed values of 0 for 0° and 180°. Measurements are from a section in the middle of a typical diffuser with strongly forward scattering.* **B** *: Definition of the geometry for calculating the fluence rate in air at a perpendicular distance d from a diffuser of length L and a distance z from the tip of the diffuser. X_n is the center-coordinate of one section, which is at a distance r_n from the point of measurement. α_n represents the angle of the vector r_n with the normal to the surface of the section n. The light enters the diffuser from the right side (arrow).*

$$\phi_n(d,z) = L_{6,n}(\alpha_n[d,z])\ \cos(\alpha_n[d,z])\ \frac{1}{r_n^2[d,z]}\ A_n \qquad (3.5)$$

The error introduced by the assumption that the radiance at 0 and 180 degrees is zero is reduced by the fact that the cosine of α is small in this region. Therefore the contribution to the total fluence rate at these angles is small.

The calculations of the distribution of the fluence rate are verified with a measurement of the actual fluence rate at a distance d from the diffuser on an axis parallel to the diffuser (figure 3, part A). The fluence rate is measured with a fibre-optic isotropic probe, of which the construction and calibration have been described by Marijnissen and Star (1987, 1996) and Van Staveren *et al* (1995). The influence of the presence of a cavity-wall of scattering tissue has been examined by repeating the same procedure as above inside a dissected pig trachea with a radius $r \approx d$ (figure 3 part B).

Interstitial treatment was simulated by immersing the linear diffuser in a liquid phantom (water with Intralipid^T). This 33 ml/l 10% Intralipid^T in water solution has a scattering coefficient $\mu_s = 16\ cm^{-1}$ and an anistropy factor $g = 0.768$ with very small absorption (van Staveren *et al* 1991). This phantom served as an example to look at the influence of scattering only, which serves as an indication for the phenomena that can be expected in real tissue. The influence of added absorber is beyond the scope of this article. The fluence rate was measured with an isotropic probe which was also immersed in the phantom at a distance d from the diffuser. Before the Intralipid was added, the fluence rate was also measured to investigate the influence of the refractive index of the surrounding medium (water, $n = 1.33$).

Results

The diffusers we tested were kindly provided by PDT Systems (Santa Barbara CA, USA), Quadra Logic Technologies (Vancouver, Canada) and Rare Earth Medical (Dennis MA, USA). Their diameters varied from 0.5 to 2.5 mm, and their lengths from 1.0 to 3.4 cm. A typical example of the radiance pattern from a commercially available diffuser is presented in figure 4. This diffuser has a diffusing tip that is emitting light from a length of 34 mm long (PDT System's specification: 30 mm) and has a diameter of 1.2 mm. We will use this diffuser throughout this paper, as it is representative

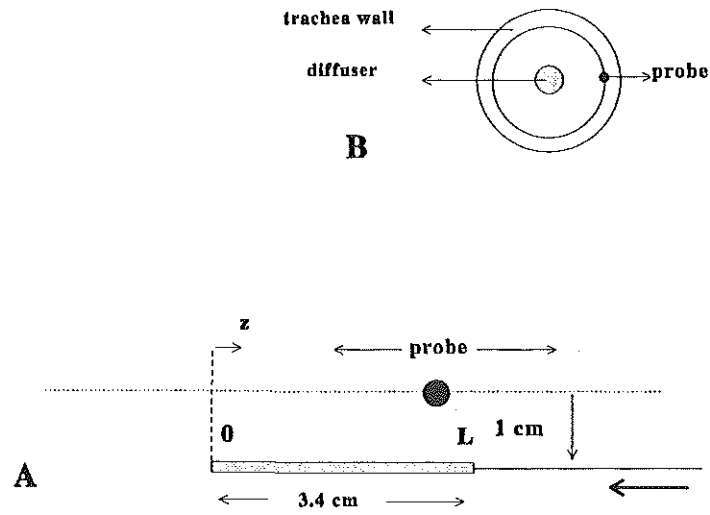

Figure 3.3: **A**: *Geometry for the measurement of the fluence rate at 1 cm perpendicular distance from a linear diffuser of 3.4 cm length. The isotropic probe is moved parallel to the diffuser, with the light entering from the right side (arrow). This setup is employed for measurement in air, water and a tissue simulating phantom where both diffuser and detector are in the medium.* **B**: *The measurement in the trachea is performed with the linear diffuser in air (at the centre of the lumen) and the isotropic probe embedded halfway in the mucosa of the trachea, as shown in the cross-section drawing.*

for most diffusers because it shows strongly forward scattering.

The most striking feature of this and other diffusers is that the radiance in the forward directions (30° and 60°) is much higher than in the other directions. The radiance in the 90°, 120° and 150° directions are much alike. Diffusers are often tested by moving a photodiode or a bare fibre with a stop parallel to the diffuser surface and then measuring the (ir)radiance. This more or less corresponds to our 90° measurement. Compared to the 90° radiance, the 30° radiance is ≈10 times higher. This and other diffusers were also rotated around the fibre axis and measured again. The readings then showed differences that were as large as the measurement error, therefore it is reasonable to assume rotational symmetry.

The diffuser appears to have a part (27 to 34 mm) where the radiance for

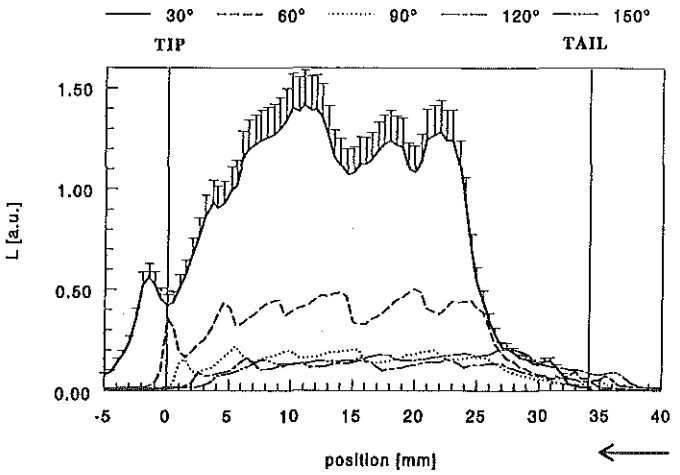

Figure 3.4: *Radiance in 5 directions on the surface of a linear diffuser that is a typical example for commercially available diffusers. The detectors are only calibrated relative to each-other, therefore the radiance units are arbitrary (a.u.). Error bars indicate the standard deviation for 5 measurements with removing and repositioning between measurements, the average SD is in the order of 10 %. For clarity, only the error bars in the 30° direction are indicated. Light is entering the diffuser from the right side (arrow) and the solid vertical lines denote the ends of the diffuser.*

all angles is relatively low. In the region 5 to 25 mm the radiance is more or less constant within one direction. The modulation that is seen on the radiance profiles of all directions and most prominent at 60° and can also be observed with the naked eye. This particular diffuser consists of parts with different concentrations of scattering particles, visible as slightly darker and brighter areas. The 30° radiance also shows a non-zero reading at points beyond the tip of the diffuser. This reading was minimized by using a stop, but there still remains a component which is probably caused by reflections off the end-mirror that most diffuser-designs have at the tip.

The distribution of the fluence rate that was measured at 1 cm distance from this diffuser in air is depicted in figure 5, together with the fluence rate that was predicted by the algorithm described in the methods section. The

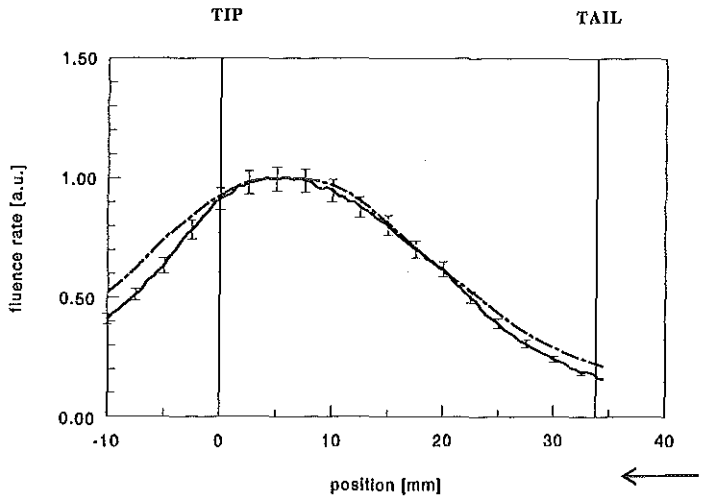

Figure 3.5: *Comparison between measured (solid line) and calculated (dash-dotted line) fluence rate at 1 cm distance from a 3.4 cm linear diffuser. Both curves have been normalised to their maximum value. Solid vertical lines denote the ends of the diffuser. Light enters the diffuser from the right side (arrow).*

distance of 1 cm was taken because this is a typical diameter for a human trachea, a possible area of application for such a diffuser. The figure shows that in both the measurement and the calculation the forward scattering results in a fluence rate pattern with a maximum value at 5.5 mm from the tip. The calculation is not fully in agreement with the measurement, but gives an adequate prediction of the place of the maximum and a good impression of the shape of the curve. The maximum of the fluence rate that was measured in air was 0.44 mWatt/cm^2 with a total diffuser output of 3.4 mWatt (1 mWatt/cm diffuser length).

Figure 6 shows what happens to the fluence rate if both diffuser and detector are immersed in a liquid scattering phantom (Intralipid^T). This setup mimics an extreme case of interstitial treatment. The fluence rate in air is also shown as a reference. The fluence rate increases strongly (by a factor of 5.6) because of the multiple scattering, and the position of the maximum shifts to 18($\pm$1) mm, which is close to the middle of the diffuser at 17 mm.

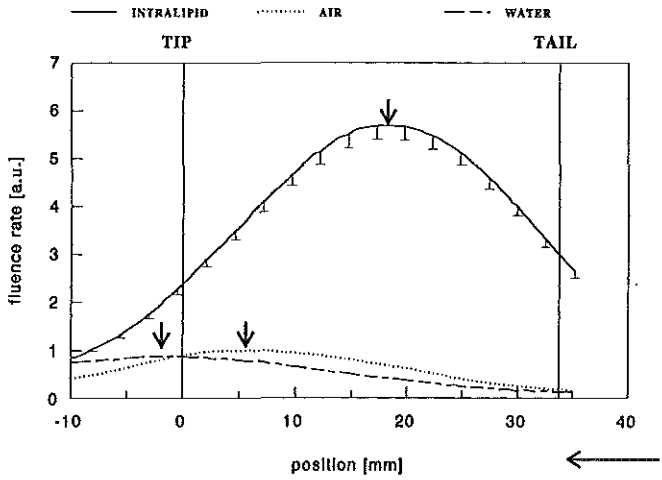

Figure 3.6: *Fluence rate measurements in the geometry depicted in figure 3. Both diffuser and detector are immersed in the same medium, air, water and an Intralipid^T solution, respectively. The standard deviation in measurement for repeated measurements is 5% (n=5). Arrows indicate the spot of maximum fluence rate at 1 cm perpendicular distance from the diffuser with an error of ±1.0 mm. The fluence rate in all curves is normalized to the maximum fluence rate in air, which is located at 5.5 mm. For the Intralipid^T the maximum is at 18 mm with a relative value of 5.7. In water the maximum is located at -2 mm with a relative value of 0.9. Light enters the diffuser from the right side (arrow). Solid vertical lines denote the ends of the diffuser.*

The fluence rate profile is now almost symmetric relative to the bisecting plane of the diffuser. When the diffuser and detector are immersed in water then the maximum fluence rate can be found even further forward than in air, at -2(±1) mm with a relative value of 0.9.

Finally, the fluence rate in the mucosa of a dissected pig trachea (diameter 19(±1) mm) was measured as shown in figure 3. The output of the diffuser was 3.4 mWatt (i.e.1 mWatt/cm diffuser length). The maximum in fluence rate is 2.8 mWatt/cm^2 at 8.0 mm, which is a factor of ≈7 higher than the maximum found in air. When figure 5 and 7 are compared, the shape of

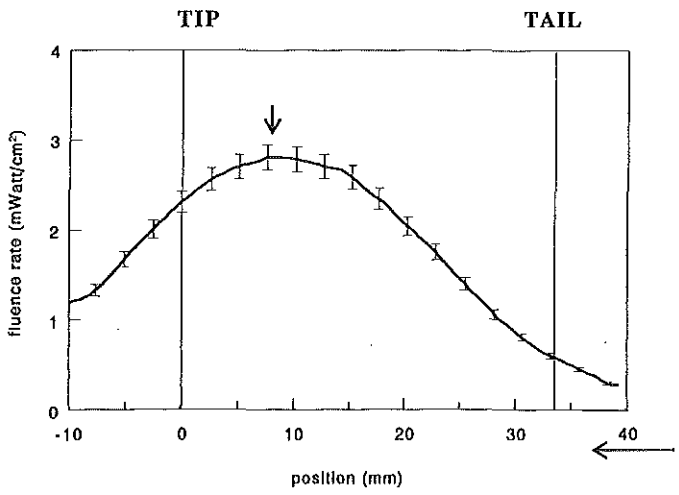

Figure 3.7: *Fluence rate measurement in the mucosa of a pig trachea, geometry as depicted in figure 3. The diameter of the trachea is 19(±1)mm, the length is 70(±1) mm. Output of the diffuser is 3.4 mWatt, equivalent to 1 mWatt/cm diffuser length. Light enters the diffuser from the right side (arrow), solid vertical lines denote the ends of the diffuser. The small arrow indicates the maximum of 2.8 mWatt/cm^2 at 8 mm from the tip.*

the curve in the trachea stays almost the same compared to the curve in air. For example, the fluence rate at 0 mm is 91% of the maximum in air and 82% of the maximum in the trachea. At 34 mm this is 16% and 20%, respectively.

Discussion

We have presented a device that tests the quality of a linear diffuser by measuring the angular distribution of the radiance at each point of the diffuser surface. The radiance in all the diffusers we tested was strongly forward directed, a feature that is not generally known, but was also reported by Spigulis *et al* (1994) who only investigated the light emitted by the distal end of a linear diffuser. In the case that manufacturers supply a proof of quality it is a 90^o measurement. The latter procedure measures the

radiance distribution within one direction along the length of the diffuser, which can be constant and might give the impression that the diffuser has a good performance. The procedure fails to measure in other directions, which might have a different distribution of emitted power as a function of position on the diffuser surface, and more importantly a very different magnitude. We found no depence of the radiance on rotation around the axis of the fibre. Diffusers that employ end-mirrors tend to have peaks in radiance near that mirror. We only tested small diameter (0.5 - 2.5 mm) linear diffusers which can be used with an endoscope or interstitially. The small diameter limits the amount of scattering bulk, and therefore the number of scattering events before the light leaves the diffuser. The limited scattering might be insufficient to deflect the incoming light to larger angles.

The consequence of the forward scattering for treatment in a cavity such as the trachea is that the maximum of the fluence rate on the cavity wall is found more near the tip of the diffuser than at the middle, as would be expected from symmetry arguments. This phenomenon was reported earlier by Feather *et al* (1994) for measurements in air. In previous work we already observed the asymmetry in the fluence rate pattern on the trachea wall (Murrer *et al* 1995). During treatment, the light source should be positioned near a lesion with this phenomenon in mind. The algorithm we presented to predict the fluence rate distribution in air from the results of the radiance measurement also gives a good qualitative impression of the fluence rate distribution in a cavity in a practical situation (trachea). If an absolute value for the fluence rate is required, one measurement of the fluence rate on a fixed distance from the diffuser can be used to scale the fluence rate distribution calculated with the algorithm. This in spite of the fact that the algorithm does not account for the presence of scattering tissue. The presence of the tissue increases the fluence rate (Murrer *et al* 1995), but appears not to alter the shape of the distribution.

Snell's law predicts a more isotropic emission of the light when the refractive index outside the diffuser increases (from $n_{air} = 1$ to $n_{water} = 1.33$). This is because for a fixed entrance angle inside the diffuser, the exiting ray will be deflected more towards the normal (assuming $n_{diffuser} \approx 1.5$), resulting in less forwardly scattered light. In water, however, the maximum in fluence rate moves even further forward, implying more forward scattering. This can be explained by the fact that according to Fresnel's law the reflection coefficient decreases (as the difference between the refractive indexes drops between diffuser bulk and surrounding medium). On average, the light will exit the diffuser after fewer reflections and therefore fewer scattering

events, resulting in more forwardly scattered light. This effect turns out to be dominant in this case.

The experiment in the liquid tissue phantom shows that the scattering by tissue can eliminate the shift in maximum value of the fluence rate caused by the forward scattering of the diffuser and the refractive index effect described above ($n_{tissue} \approx n_{water}$). The fluence rate shows a symmetric pattern, with a maximum near the middle of the diffuser. The influence of added absorber has to be investigated to evaluate the fluence rate distribution in real tissue. For interstitial treatment it seems most important that the light exits the diffuser homogeneously along the length of the diffuser, irrespective of the angular distribution.

Acknowledgments

The authors wish to thank Jerry van der Ploeg for the development and maintenance of the dosimetry equipment. They also wish to thank Ivo Limpens and Jolanda van Helvoirt for making the diffuser-tester operational and Gerd Beck for helpful advice. This work was supported by the Dutch Cancer Society, grant DDHK 93-615.

References

1. Abramowitz M, Stegun I A. (1970) Handbook of mathematical functions, page 878. *Dover*

2. Cairnduff F,Roberts D J H, Dixon B, Brown S B. (1995) Response of a rodent fibrosarcoma to photodynamic therapy using 5-aminolaevulinic acid or polyhaematoporphyrin. *Int. J. Radiat. Biol.* **67** *93-99*

3. Feather J W, King P R, Driver I, Dawson J B. (1994) A method for the construction of cylindrical diffusing fibre optic tips for use in photodynamic therapy. *Lasers Med. Sci.* **4** *229-235*

4. Ji Ying, Walstadt D, Brown J T, Powers S K. (1992) Interstitial photoradiation injury of normal brain. *Lasers Surg. Med.* **12** *425-431*

5. Marijnissen J P A, Star W M. (1987) Quantitative light dosimetry *in vitro* and *in vivo*. *Lasers Med. Sci.* **2** *235-242*

6. Marijnissen J P A, Baas P, Beek J F,van Moll J H, van Zandwijk N, Star W M. (1993) Pilot study on light dosimetry for endobronchial photodynamic therapy. *Photochem. Photobiol.* **58** *92-98*

7. Marijnissen J P A, Star W M. (1996) Calibration of isotropic light dosimetry detectors based on scattering bulbs in clear media. *Phys. Med. Biol.* **41** *1191-1208*

8. Murrer L H P, Marijnissen J P A, Star W M. (1995) *Ex vivo* light dosimetry and Monte Carlo simulations for endobronchial photodynamic therapy. *Phys. Med. Biol.* **40** *1807-1817.*

9. Overholt B F, Panjehpour M, Denovo R C, Petersen M G. (1994) Photodynamic therapy for esophageal cancer using a 180° windowed esophageal balloon. *Lasers Surg. Med.* **14** *27-33*

10. Spigulis J, Pfafrods D, Stafeckis M. (1994) Optical diffusive fiber tip designs for medical laser-lightguide delivery systems *in Croitoru* et al *(eds) Biomedical Optoelectronic Devices and Systems II Proc. SPIE* **2328** *69-75*

11. van Staveren H J, Moes C J M, van Marle J, Prahl S A. (1991) Light scattering in intralipid-10% in the wavelength region of 400-1100 nm. *Appl. Opt.* **30** *4507-4514*

12. van Staveren H J, Marijnissen J P A, Aalders M C G and Star W M. (1995) Construction, quality control and calibration of spherical isotropic fibre-optic light diffusers. *Lasers Med. Sci.* **10** *137-147*

Chapter 4

Note: Improvements in the design of linear diffusers for Photodynamic Therapy

(1997) Phys. Med. Biol. **42** *1461-1464*

L.H.P. Murrer, J.P.A. Marijnissen, W.M. Star

Abstract

The angular radiance distribution of several linear diffusers used for PhotoDynamic Therapy (PDT) was measured. The forward scattering found previously was not observed in these designs. The improved isotropy leads to a better agreement between intended treatment site and actual maximum of the fluence rate profile when the linear diffuser is used in a hollow, cylindrical, organ.

Introduction

Linear (or cylindrical) diffusers are commonly employed for PhotoDynamic Therapy (PDT), either for interstitial treatment or for intracavitary illumination of hollow organs such as the trachea or the oesophagus.

In a previous publication we reported (Murrer *et al* 1996) that commercially available linear diffusers often show a strongly forward directed radiation pattern. When employed in hollow organs, this causes a forward shift of the maximum fluence rate (parallel to the diffuser) on the organ wall. This might result in underdosage of the target area. This problem was not generally recognised, because the appropriate measuring methods were not available and the diffusers were designed predominantly for interstitial (or '*contact*') use in tissue. During interstitial use the directional distribution of the radiance is not important, because the diffuser surface is in direct contact with the tissue. The highly scattering nature of the tissue cancels the anisotropy of the radiance (Murrer *et al* 1996).

New designs of linear diffusers have become available since. This note presents radiance scans of these designs, focusing on the improved isotropy of the radiance.

Materials and Methods

The device we used to measure the radiance at each point of the linear diffuser surface is described in Murrer *et al* (1996). The device is presented in figure 1. It measures the radiance in 5 directions, viz. at 30^o, 60^o, 90^o 120^o and 150^o angle with the direction of the incoming light from the supplying fibre. The detectors consist of a small lens (diameter = 2 mm) mounted on a fixed distance from a cleaved, bare fibre. The radiance of

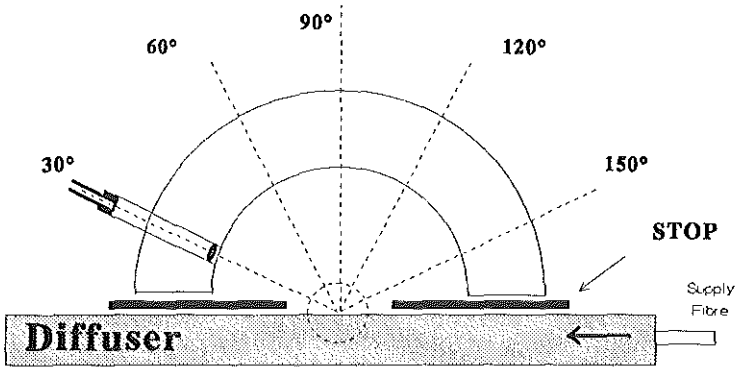

Figure 4.1: *Schematic representation of the measurement device. The light enters the diffuser from the right side (arrow) through a supply fibre. One section of the diffusing surface is sampled from 5 angles (30°..150°) by 5 lenses. The measuring head can be moved parallel to the diffuser. The stop reduces scattered light from other parts of the diffuser surface. The dashed circle indicates the position of the isotropic spherical diffuser for calibration.*

the diffuser surface is measured by forming an image of an element of the diffuser surface on the fibre surface. The entire diffuser surface is scanned by moving the measuring head parallel to the diffuser. The detectors are calibrated relative to each other by measuring the radiance of an isotropic spherical diffuser, which should yield the same reading for all detectors (see figure 1).

Diffusers of 3 manufacturers were tested using 5 mWatt of red light (632.8 nm) from a HeNe laser. The diffusers were kindly provided by Patrick Thielen Microtechnique (PTM, Geneva, Switzerland), Rare Earth Medical (REM, West-Yarmouth MA, USA) and Pioneer (through QLT PhotoTherapeutics Inc, Vancouver, Canada). The dimensions of the diffusers are summarized in table I, together with their flexibility. The REM diffuser is a modified diffuser for interstitial use. For use in hollow organs an additional layer of scattering material (white tubing) is used to make the radiance

Manufacturer	Length diffuser (mm)	Outer diameter (mm)	Flexibility
Patrick Thielen Microtechnique	30	1.0	Flexible
Rare Earth Medical	15	0.6	Flexible
QLT/Pioneer	25	1.7	Rigid

Table 4.1: *Length, outer diameter and indication of flexibility of diffusing part of the linear diffusers*

isotropic. This addition increased the diameter of the diffuser from 0.5 to 0.6 mm.

Results and Discussion

The radiance measurements of the three tested linear diffusers are presented in figure 2. In general, the diffusers presented here show a fairly isotropic radiance of light emitted from the diffuser surface. The highly forward scattering radiance we reported earlier (Murrer *et al* 1996) ,i.e. relatively high 30^o and 60^o radiances, is absent in these diffuser designs. The isotropy of the radiance can be checked roughly with the naked eye, as the observed brightness of the diffuser should not vary with the angle under which it is observed. Both REM and PTM provide a total output versus position plot with each diffuser, that agrees with the average profile measured at 5 different angles within the error of measurement. Both REM and PTM diffusers are flexible and thin (table I), which makes them fit for many applications.

The overall output of the PTM diffuser shows a decrease from the proximal to distal end, which is consistent for all directions. The radiance profiles for the individual angles show a gradual overall decrease of magnitude from forward (30^o) to backward (150^o) scattering, with the latter still at an acceptable level (eg. $\approx$ 80 % of the 30^o level at 20 mm).

The REM diffuser has a better ratio of proximal to distal output, but shows some leakage of light outside the intended diffusing area. Some small peaks

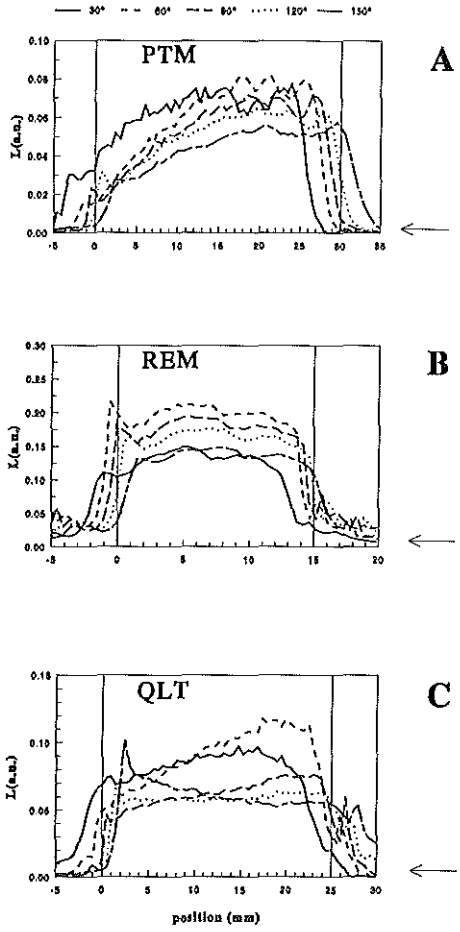

Figure 4.2: *Radiance in 5 directions on the surface of three makes of linear diffusers. The detectors are only calibrated relative to each-other, therefore the radiance units are arbitrary (a.u.). The standard deviation in the measurements is 10 %. For the sake of clarity error bars have not been indicated. The light enters the diffuser from the right side (arrows) and the solid vertical lines denote the ends of the diffuser. The dimensions of the diffusers are indicated in table I. (A) Patrick Thielen Microtechnique [PTM] (B) Rare Earth Medical [REM] (C) QLT/Pioneer [QLT]*

can be observed at the distal end, probably cause by reflections off the end mirror. The additional layer of scattering material on the REM diffuser functions well to make the radiance of the forward scattering diffuser isotropic. The radiance at shallow angles (ie. 30^o and 150^o) has a lower magnitude compared to the other 3 angles that are more perpendicular to the diffuser surface (eg. the 30^o radiance is about 80% of the 90^o radiance at 5mm). This leads to a narrower distribution of incident light on the organ wall compared to an isotropic diffuser.

The QLT/Pioneer diffuser is less consistent in the proximal to distal output ratio for different directions (cf. 60^o and 150^o). Also, the ratio between the radiances at different angles is less favourable (eg. the 150^o radiance is $\approx$ 50 % of the 60^o radiance at 20 mm). The fact that this diffuser is rigid and relatively thick makes it perhaps less versatile for other applications than the ones it is used for now (in the bronchial tree).

The good isotropy of the diffusers presented here will benefit the dosimetric evaluation of treatment in hollow, cylindrical, organs because the maximum of the fluence rate will now be located on the wall of the organ opposite the middle of the diffuser, where it is expected to be. There is no longer a shift of the location of the maximum parallel to the diffuser caused by forward scattering of the diffuser.

Acknowledgments

The authors wish to thank Jerry van der Ploeg for the development and maintenance of the dosimetry equipment. This work was supported by the Dutch Cancer Society, grant DDHK 93-615.

References

1. Murrer L H P, Marijnissen J P A, Star W M. (1996) Light distribution by linear diffusing sources for photodynamic therapy. *Phys. Med. Biol.* **41** *951-961*

Chapter 5

Applicator for light delivery and in situ light dosimetry during endobronchial Photodynamic Therapy: first measurements in humans

(1997) Lasers Med. Sci. **12** *253-259*

L.H.P. Murrer, J.P.A. Marijnissen, P. Baas †, N. van Zandwijk †, W.M. Star

†The Netherlands Cancer Institute, Dept. of Medical Oncology

Abstract

A design of an applicator for light delivery and light dosimetry during EndoBronchial PhotoDynamic Therapy (EB-PDT) is presented. The design incorporates a linear diffuser that is fixed in the centre of the lumen by a steel spring basket that does not block the air flow. An isotropic light detector is a part of the design, to measure the light fluence actually delivered to the bronchial mucosa surface. The applicator is designed for use with common bronchoscopy equipment, and can be used with bronchoscopes with a large biopsy channel ($\approx$ 3 mm). The first clinical measurements were performed and caused no additional discomfort to the (non-photosensitized) patients. The data showed a considerable inter-patient variability of the light fluence rate measured as a result of a fixed output power of the diffuser. This fact and the expected strong dependence of the fluence rate on the lumen diameter stress the importance of *in situ* fluence rate measurement for a proper evaluation of the relationship between light fluence and biological response of EB-PDT.

Introduction

To date, light dosimetry in endobronchial PhotoDynamic Therapy (EB-PDT) has been limited to specifying the total output of the linear diffusing light source or an estimate of the incident irradiation (in some cases also a micro-lens is used). This limits the possibility of interpreting fluence-response data because the true light dose in the tissue is not known. The fluence rate in tissue during EB-PDT depends on the diameter of the lumen and on the optical properties of the mucosa and underlying cartilage which are generally unknown. It is therefore essential to measure the fluence rate during treatment. Few studies on the dosimetric aspects of EB-PDT have been published (Murrer *et al* 1995, Marijnissen *et al* 1993).

In clinical EB-PDT the light source is introduced through a bronchoscope and the position during treatment is monitored and adjusted by either direct or video mediated visual inspection. It is difficult to avoid movement of the light source due to, e.g., coughing and the intense laser light reduces visibility. Fixation of the light source in the treated lumen is therefore required, and central placement in the lumen will ensure homogeneous illumination on the circumference. Non-central illumination induces uncontrollable variations in the light fluence received by the mucosa (Murrer *et*

al 1995).

For application in the oesophagus, applicators have been developed based on a balloon for position fixation of the linear diffusing light source and unfolding of the mucosa (Panjehpour *et al* 1992). A design based on a rigid cylinder has been published by Van den Bergh *et al* (1995). These authors also developed a balloon method for application in the bronchial tree. A drawback of the latter construction is that the air flow is (partly) blocked, which is undesirable for use in patients that already have a reduced respiratory capacity.

This paper presents a design for an applicator that incorporates a linear diffusing light source, a fixation system that does not block the air flow and an isotropic probe that allows for on-line measurement of the true delivered fluence rate and resulting total fluence. The first experiences and dosimetry results in humans and animals are presented.

Materials and Methods

The design of the applicator is presented in figure 1. It is based on a basket made out of four flat steel springs (A), that unfold when moved out of a catheter (D). The width of the steel springs is 0.3 mm and the thickness is 0.1 mm. The applicator is unfolded by retracting the catheter from the basket at the handpiece. The outer diameter of the catheter (2.6 mm) is such that it can be introduced through most flexible bronchoscopes with a large biopsy channel (so-called *treatment scope*). This way the positioning of the applicator can be performed under visual control. The baskets (MTW Fujinon Medical Holland) are normally used to e.g. fix kidney-stones to vaporize them with intense laser light. The basket construction offers the possibility to have a linear diffuser (B) at the centre of the basket, that will then be fixed in the centre of the lumen in which the basket is unfolded. A fibre-optic isotropic light detector is also part of the applicator (C).

The basket

The advantage of the basket construction is that it does not block the air flow in the lumen. Variable diameters of the unfolded basket are available to fit to the various lumen diameters that can be encountered. The springs can easily adjust to the local shape of the lumen, and the fixation force is spread over the entire length of the spring, thereby avoiding local high-pressure points on the mucosa. This is of importance, because the diseased

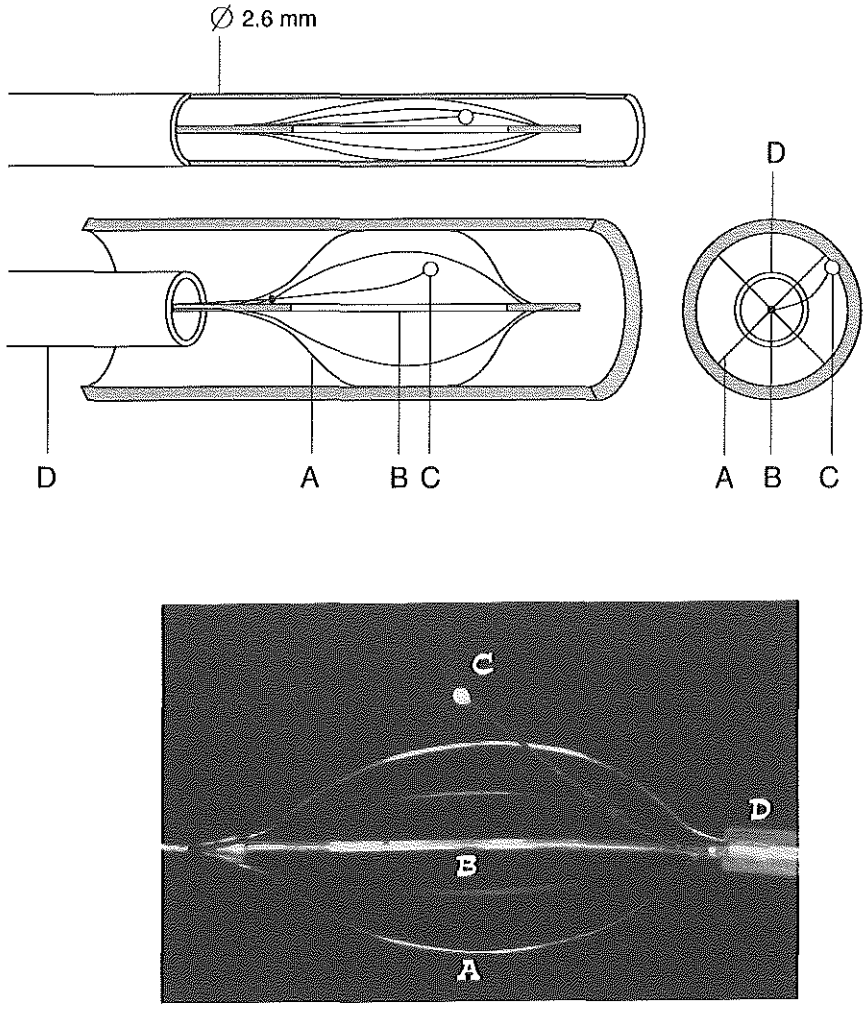

Figure 5.1: *Applicator for light delivery and light dosimetry in the bronchial tree. (top) Schematic drawing of the folded applicator in the catheter, and of the applicator unfolded in a cylindrical lumen. The cross-section shows the position of the detector bulb that is pressed against the wall. (bottom) Photograph of the unfolded applicator. Clearly visible are the light-diffusing fiber at the centre (B) the white bulb of the isotropic detector (C) and the steel springs of the fixation basket (A). The outer diameter of the nylon tubing (D) that contains the folded applicator is 2.6 mm. The black dot shown near the proximal end of the applicator indicates where the detector fibre is attached to the steel spring.*

tissue tends to bleed easily. Bleeding introduces dark spots that absorb light that is then lost for therapy in the target tissue, and generally causes the light distribution to be less homogeneous. The width of the steel springs is such, that the light from the source is minimally shadowed. Also, the light scattering by the tissue will even out the shadowing, because the surface spread of the light is approximately equivalent to the penetration depth of the light in the tissue. The penetration depth is given by $1/\mu_{eff}$ and is in the order of several millimeters for bronchial mucosa at a wavelength of 630 nm (Murrer *et al* 1995) , which is larger than the width of the springs. ($\mu_{eff} = \sqrt{3\mu_a(\mu_a + \mu_s(1-g))}$, with μ_a the absorption coefficient [cm^{-1}], μ_s the scattering coefficient [cm^{-1}], and g the anisotropy factor [-]). The $1/\mu_{eff}$ for green light (514 nm) in bronchial mucosa is in the order of 1 mm (unpublished data), which is also larger than the spring width.

The linear diffuser

We used a thin linear diffuser (outer diameter 0.5 mm, fibre core diameter 200 μm, Rare Earth Medical, West Yarmouth MA, USA), with a diffusing length of 16 mm. The small diameter is necessary to fit the applicator in the catheter. Diffusers with different lengths (e.g. 20 or 25 mm) are available.

The isotropic detector

The detector is attached to one of the springs of the basket. When the basket is unfolded the detector is pressed against the mucosa of the treated lumen, positioned between two springs to avoid erratic readings from reflections off the springs. The detector is mounted in such a way that the bulb is pressed against the mucosa at the location where the maximum fluence rate is to be expected. Because the detector fibre extends beyond the lumen radius, a lateral bend is introduced in the fibre during unfolding. This bend acts as a spring and presses the detector against the mucosa. The maximum can be predicted by measuring the fluence rate in air along the diffuser at a radial distance equal to the radius of the lumen that is to be treated (before assembly of the applicator), and the position of the maximum depends on the lumen diameter and the output characteristics of the linear diffuser (Murrer *et al* 1996). The detector bulb is placed on the lesion to be treated, serving as a reference for positioning of the applicator. The detector bulb will not introduce a shadowing effect, as the material of which the bulb is made has a very low absorption. Also, the penetration depth for red (630 nm) and green (514 nm) light will be sufficient to overcome possible shadowing, as argued above in the case of the springs of the

basket.

The detectors in this study are home made, constructed with a bulb (diameter 0.9 mm) of scattering material (Helioseal^T Vivadent, Schaan, Liechtenstein) mounted on a 100 μm diameter quartz core fibre. This small core diameter has the disadvantages of being fragile and having a relatively low light output. The reason we chose this fibre was twofold. The first was to have as little friction as possible in the catheter (length 1 m), to allow smooth unfolding of the applicator. Secondly, the isotropy of the probe improves with a smaller ratio of the bulb diameter to the fibre core diameter. So in order to minimize the bulb diameter, a small core diameter is required.

The manufacturing procedure of the detectors is patented by Henderson (1991) (European Patent, applications no. 90302852.0 and 90309797.0). Their isotropy is checked by measuring the response to a parallel beam coming from different directions (-160 to 160 degrees angle from forward incidence). The normalized response of the detector has to be within 15% deviation from mean van Staveren *et al* 1995) to be able to measure with an accuracy of 15%. A force of 2.5 N (250 gr.) is applied axially to the bulb to check the bulb-to-fibre connection (van Staveren *et al* 1995, Hudson *et al* 1993).

The light output of the isotropic detector fibre is coupled to a photodiode (Photop UDT-455, Graseby Electronics, Orlando FL USA), and the signal is pre-amplified, A-D converted and stored on a PC. This enables us to do real-time monitoring of the fluence rate and the total light fluence delivered to the mucosa.

Calibration

The output of the linear diffuser is measured in an integrating sphere, by inserting and unfolding the applicator in the sphere. Typical output powers used are 400 mWatt per cm diffuser length (Photofrin, λ =630 nm). The integrating sphere has built-in laserdiodes, that provide a diffuse calibration field for the isotropic detector of the applicator (6.4 mWatt/cm^2 for λ = 630 nm, (van Staveren *et al* 1995)). The calibration voltages are stored on the PC for the real-time conversion from photodiode voltage to fluence rate. The dosimetry-software is also able to switch the laser on and off, by opening and closing a valve that is placed in the resonator of the dye-laser (Spectra Physics 373).

For the measurement with the detector pressed against the mucosa a correction factor of 1.07 ($\pm$2%) for change of refractive index from air to mucosa

has to be introduced (Murrer *et al* 1995, Marijnissen *et al* 1996). Note that this correction factor increases to 1.7 (±2%) in the case that the probe is fully in the tissue (Murrer *et al* 1995, Marijnissen *et al* 1996). With this correction, the detector measures the fluence rate in the top layer of the mucosa with an accuracy of ± 15% (Marijnissen *et al* 1996). Because the refractive index mismatch causes a jump in the fluence rate going from air to tissue, it is very important that the probe is in good contact with the tissue.

If the probe is fully covered with liquid (mucus), the above mentioned correction factor of 1.7 must be used, because the liquid has a refractive index close to that of tissue. In case of doubt it is preferable that the applicator is retracted, cleaned and inserted again. With the bronchoscope still in place this is a simple and fast procedure. Also in the presence of blood, the applicator (and the lesion) must be cleaned, either by rinsing it through the bronchoscope or retracting, rinsing and inserting. The presence of blood will influence the light distribution negatively by creating local dark spots (especially with green light) and reducing the total amount of backscattered light.

Measurements

Measurements with light with a wavelength of 630 nm were performed in three (non-photosensitized) volunteers, during a routine bronchoscopy in parts with normal, healthy tissue (Laser System: Spectra Physics Argon-Dye System 171/373). Informed consent was obtained from all volunteers before the experiment. An additional measurement was performed in normal, healthy tissue of a live pig, to relate the previously published *ex-vivo* results (Murrer *et al* 1995) to measurements in the presence of an intact blood-circulation, as this might cause additional absorption of the light. The animal experiment was approved by the University Animal Experiments Ethical Committee (DEC : protocol 605-93-03).

A useful measure for the increase of the fluence rate in the mucosa due to multiple scattering is the ratio of the measured fluence rate (ϕ_{true}) and the fluence rate at the same position relative to the diffuser in the absence of tissue (ϕ_0), which we called the backscatter factor β_{max} (Murrer *et al* 1995).

$$\beta_{max} = \frac{\phi_{true}}{\phi_0} \tag{5.1}$$

The fluence rate in the absence of tissue is approximated by (Murrer *et al*

1995):

$$\phi_0 = \frac{P_{out}}{2\ \pi\ R_{lumen}\ L_{diffuser}} \tag{5.2}$$

where P_{out} is the output of the linear diffuser (mWatt), $L_{diffuser}$ the length of the diffuser (cm) and R_{lumen} the radius of the lumen (cm).

Results

Use of the applicator

The applicator was introduced and unfolded in the bronchus of human volunteers on four occasions, on three of which the laser was connected and a measurement was made. The applicator was unfolded in the trachea, the bronchi and the sub-bronchi, the main target areas for this device. The unfolding went smoothly and was not hampered by the bends in the flexible bronchoscope.

The patients were only anaesthetized locally, and experienced no additional discomfort from the procedure. The procedure could be entirely controlled from one PC, which made it fast and simple to perform a measurement. The linear diffuser was fixed well in the lumen of one of the bronchi, and no bleeding was observed as a result of manipulations with the applicator. During positioning of the applicator, care was taken to keep the detector well in touch with the tissue, which was checked visually through the bronchoscope. A picture of the unfolded applicator in a bronchus of a volunteer is presented in figure 2.

First dosimetry results

The dosimetry results for the volunteers are presented in table 1. The measurements are made in the bronchus, which has an average diameter of 1.2 cm, which we use for calculation of ϕ_0. The resulting fluence rates show a considerable variation. β_{max} values range from 2.7 to 7.1 with an average value of 4.7 (sd 2.2).

The dosimetry results for the animal experiment are presented in table 2. In these experiments, the placement and measurement were repeated on the same location, and the standard deviation of the measured values was 15%. The measurements were made in the trachea of a pig, with light of 630 nm and 652 nm. These wavelengths are used for PDT with Photofrin^T

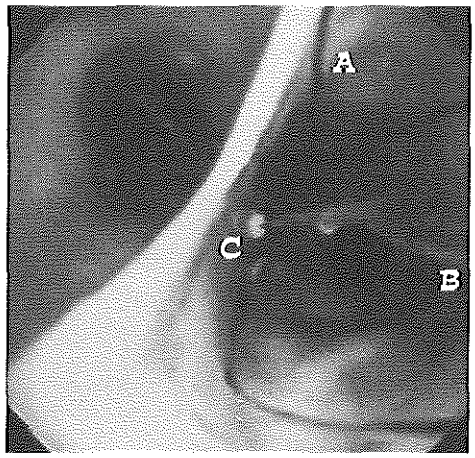

Figure 5.2: *Unfolded applicator during measurement in the bronchus of a (non-photosensitized) volunteer. (A) springs of the fixation basket (B) linear diffuser (C) detector.*

Volunteers

Subject nr.	P_{out} (mWatt) ±5%	ϕ_{true} (mWatt/cm^2) ±15%	ϕ_0 (mWatt/cm^2) ±10%	β_{max} (-) ±20%
1	242	117	43	2.7
2	241	304	43	7.1
3	239	183	42	4.3

Table 5.1: *Output of the diffuser P_{out}, measured fluence rate ϕ_{true}, fluence rate in air ϕ_0 and backscatter factor β_{max} for 3 volunteers. Wavelength = 630 nm. The radius of the treated lumen (bronchus) R_{lumen} is 6 mm. The length of the diffuser $L_{diffuser}$ = 1.6 cm. Indicated are the estimated errors in the measurements.*

Pig Experiment

Wavelength (nm)	P_{out} (mWatt) ±5%	ϕ_{true} (mWatt/cm^2) ±15%	ϕ_0 (mWatt/cm^2) ±10%	β_{max} (-) ±20%
630	210	61.0	20.9	2.9
652	179	46.0	17.8	2.6

Table 5.2: *Output of the diffuser P_{out}, measured fluence rate ϕ_{true}, fluence rate in air ϕ_0 and backscatter factor β_{max} for the trachea of a pig, for wavelengths 630 and 652 nm. The radius R_{lumen} for the trachea is 10 mm. The length of the diffuser $L_{diffuser}$ = 1.6 cm. Indicated are the estimated errors in the measurements.*

and m-THPC^T, respectively. The trachea was excised after the experiment, and the diameter was then measured with calipers.

The measured β_{max} values are lower than the average found in human volunteers, but these values are not readily comparable because they were found at different lumen diameters. In the pig, there is no significant difference in the β_{max} values found for 630 and 652 nm. The trachea was excised after the experiment, and the diameter was then measured with calipers.

The total output of the diffuser used in the experiments ranges from 179 to 242 mWatt, which is in the same order of magnitude as e.g. the Photofrin^T protocol (QLT/Lederle P 503/504) for a 16 mm diffuser (output 400 mW/cm x 1.6 cm = 640 mWatt).

Discussion

We have presented a design that improves the method of light delivery and light dosimetry during endo-bronchial PhotoDynamic Therapy (EB-PDT), suited for use for the treatment of early stage (non-obstructing) cancer. For (partially) obstructive cancer and treatment of segments below the sub-bronchi an interstitial illumination or an illumination with a balloon method seems more appropriate. The current protocols for EB-PDT have

paid very limited attention to complicating factors like the influence of optical properties, the lumen diameter and positioning of the linear diffuser in the lumen that is treated. Currently, the dosimetry in EB-PDT is only defined by the output of the light source.

D'Hallewin *et al* (1992) and Marijnissen *et al* (1993) have shown that considerable variations in diffuse light backscatter factors can be found in whole bladder wall PDT with light of 630 nm wavelength. Hudson *et al* (1994) showed the similar variations in backscattering from skin lesions at the same wavelength. They observed that whitish lesions, as often observed in early-stage bronchial carcinoma showed a significantly increased backscatter factor. Our first results also show considerable variations in the backscatter factor β_{max}. These variations are mainly caused by variations in the optical properties of the (normal) mucosa, perhaps caused by differences in blood contents. Errors in the estimation of R_{lumen} and therefore ϕ_0 also have an influence. Small variations in the tissue absorption can have a large influence on the tissue backscatter factors, as we previously showed with the help of Monte-Carlo simulations of the light distribution of an *ex vivo* pig trachea (Murrer *et al* 1995).

The position of the isotropic probe should be monitored, to make sure it is in contact with the tissue. If mucus is present, the probe should be cleaned or an appropriate correction factor should be used. It is important to keep the illuminated area free from bleeding, to avoid underilluminated spots and to profit maximally from the enhancement of the fluence rate through backscattering. Care must also be taken to keep the probe free from blood, to avoid faulty (too low) readings of the fluence rate.

The diameter of the lumen that is treated is also an important factor for the total light dose in the tissue. The magnitude of the incident light dose is roughly proportional to the inverse of the lumen diameter, and that factor alone causes a considerable variation (67%) when moving from eg. the trachea (Diameter = 20 mm) to the bronchus (Diameter = 12 mm). Furthermore we have shown that the positioning of the linear diffuser in the lumen (on- or off-axis) is crucial for the resulting light fluence (Murrer *et al* 1995).

All these factors taken together prove that it is difficult to perform a well-defined fluence-response study without *in-situ* measurement of the fluence rate. The design we present here offers a possibility to do so, albeit with only one measurement site. For an applicator design that can be used with standard bronchoscopy equipment this seems the maximum achievable.

The EB-PDT applicator published by Van den Bergh *et al* (1995) has the advantage of homogenizing the light by the scattering material at the surface of the fixation balloon. A disadvantage of this method is that the air flow in the treated lumen is blocked, so that it cannot be used in, e.g. the trachea. Fritz *et al* (1991) published a design that was intended for use in brachytherapy which employs a catheter for feeding the iridium wire with a larger concentric second catheter with slits at the distal end that unfold when pushed up at the proximal end. This design might prove a useful concept also if e.g. an isotropic detector would be incorporated. The data from the pig experiment show a lower β_{max}-value for 630 nm illumination of the trachea *in-vivo* (2.9) than found during a series of *ex-vivo* measurements (average 4.9, sd 1.7)) (Murrer *et al* 1995). This may well be attributed to the additional absorption introduced by the blood flow that is absent in the *ex-vivo* material.

Acknowledgments

The authors wish to thank Jerry van der Ploeg and Wieger Renkema for assisting in the development of the applicator. We also wish to thank Paula Hamm, Erik-Jan Bakker, Rob Slingerland and Bert van Geel (Daniel Den Hoed Cancer Centre Rotterdam) and Joos Heisterkamp and Enno Collij at the department of experimental surgery for assisting in the *in vivo* testing of the applicator, and Hans Kneefel for the artwork. This work was supported by the Dutch Cancer Society, grant DDHK 93-615.

References

1. D'Hallewin M A, Baert L, Marijnissen J P A, Star W M. (1992) Whole bladder wall photodynamic therapy with *in situ* light dosimetry for carcinoma *in situ* of the bladder. *Urol.* **148** *1152-1155*

2. Fritz P, Schraube P, Becker H D, Löffler E, Wannenmacher M, Pastyr O. (1991) A new applicator, positionable to the center of tracheobronchial lumen for hdr-ir-192-afterloading of tracheobronchial tumors. *Int. J. Radiation Oncology Biol. Phys.* **20** *1061-1066*

3. Henderson B. (1991) An isotropic dosimetry probe for monitoring light in tissue, theoretical and experimental assessment. *PhD Thesis, Heriot Watt University Edinburgh UK*

4. Hudson E J, Stringer M R, Van Staveren H J, Smith M A. (1993) The development of radio-opaque, isotropic, fibre-optic probes for light dosimetry studies in photodynamic therapy. *Phys. Med. Biol.* **38** *1529-1536*

5. Hudson E J, Stringer M R, Cairnduff F, Ash D V, Smith M A. (1994) The optical properties of skin tumours measured during superficial photodynamic therapy. *Lasers Med. Sci.* **9** *99-103*

6. Marijnissen J P A, Baas P, Beek J F,van Moll J H, van Zandwijk N, Star W M. (1993) Pilot study on light dosimetry for endobronchial photodynamic therapy. *Photochem. Photobiol.* **58** *92-98*

7. Marijnissen J P A, Star W M, In 't Zandt H J A, D'Hallewin M A , Baert L (1993a) *In situ* light dosimetry during whole bladder wall photodynamic therapy: clinical results and experimental verification. *Phys. Med. Biol.* **38** *567-582*

8. Marijnissen J P A, Star W M. (1996) Calibration of isotropic light dosimetry detectors based on scattering bulbs in clear media. *Phys. Med. Biol.* **41** *1191-1208*

9. Murrer L H P, Marijnissen J P A, Star W M. (1995) Ex vivo light dosimetry and Monte Carlo simulations for endobronchial photodynamic therapy. *Phys. Med. Biol.* **40** *1807-1817*

10. Murrer L H P, Marijnissen J P A, Star W M. (1996) Light distribution by linear diffusing sources for photodynamic therapy. *Phys. Med. Biol.* **41** *951-961*

11. Panjehpour M, Overholt B F, Denovo RC, Sneed R E, Petersen M G. (1992) Centering balloon to improve esophageal photodynamic therapy. *Lasers Surg. Med* **12** *631-638*

12. Van den Bergh H, Mizeret J, Theumann J F, Woodtli A, Bays R, Robert D, Thielen P, Philippoz J M, Braichotte D, Forrer M, Savary J F, Monnier PH, Wagnieres G. (1994) Light distributors for Photodynamic Therapy *in Croitoru N I, Miyagi M, Orellana G, Scheggi A V, Sterenborg H J M C (eds) Medical and fiber optic sensors and delivery systems Proc. SPIE* **2631** *173-198*

13. Van Staveren H J, Marijnissen J P A, Aalders M C G and Star W M. (1995) Construction, quality control and calibration of spherical isotropic fibre-optic light diffusers. *Lasers Med. Sci.* **10** *137-147*

Chapter 6

Monte Carlo simulations for EndoBronchial PhotoDynamic Therapy: The influence of variations in optical and geometrical properties and of realistic and eccentric light sources.

Accepted for publication in Lasers Surg. Med.

L.H.P. Murrer, J.P.A. Marijnissen, W.M. Star

Abstract

A Monte Carlo model is presented for the illumination of a cylindrical cavity by a linear diffuser, which is employed to compute the fluence rate distribution during endo-bronchial PhotoDynamic Therapy. The influence of geometrical parameters such as the diameter of the treated lumen, the length of the linear diffuser and the possible off-axis position of the diffuser on the fluence rate have been investigated, as well as the consequences of varying output characteristics of the diffusers. For on-axis isotropic diffusers some simple practical rules are derived to estimate the fluence rate profile on the wall for varying diffuser length and lumen diameter. With linear diffusers that can be modelled as a row of isotropic point sources, a constant fluence rate build-up factor can be employed for varying diffuser lengths and lumen diameters. Extreme off-axis placement of the diffuser causes a highly variable, considerable increase in the maximum fluence rate as well as a highly asymmetrical fluence rate profile on the circumference of the illuminated lumen. The measured radiance profiles of real diffusers can be implemented in the model, which provides a means of evaluating the fluence rate distribution resulting from realistic (non-ideal) light sources. The influence of the optical properties of the bronchial mucosa on the fluence rate build-up factor was also investigated. The changes in fluence rate could be accounted for by diffusion theory.

Introduction

Few studies have been published on the light dosimetry during EndoBronchial Photodynamic Therapy (EB-PDT) (Murrer *et al* 1995, 1997a, Marijnissen *et al* 1993). These studies show that the light dosimetry in the upper respiratory tract strongly depends on light source positioning, optical properties of the tissue and the diameter of the lumen that is illuminated. We showed that the fluence rate distribution calculated with Monte Carlo simulations provides accurate absolute values for the fluence rate as measured *ex vivo* in a pig trachea (Murrer *et al* 1995).

Monte Carlo simulations offer the possibility to vary the geometry and optical properties (Saponaro *et al* 1996) to asses the influence of those parameters on the fluence rate distribution. Especially in complex geometries where analytical radiative transport calculations are not feasible the Monte Carlo simulations prove particularly useful to achieve more insight

(qualitatively as well as quantitatively) in the role of geometry and optical properties.

The present paper seeks to describe the fluence rate distributions as a result of different illumination conditions and to inter-relate the different conditions by rules-of-thumb. The issues that will be addressed are the influence of the length and emission profile of the light source, the on- or off-axis positioning of the light source, the diameter of the treated lumen and the influence of the optical properties on the fluence rate build-up.

Methods

Monte Carlo Model

The Monte Carlo code was adapted from the Pascal code used to simulate whole bladder wall illumination (Keijzer *et al* 1991, Van Staveren *et al* 1995). The simulations were run on a Pentium PC. The geometry of the experiment was modelled as a cylinder of air (diameter D) embedded in a cylindrically symmetric semi-infinite medium (thickness T, outer radius $r \rightarrow \infty$) (figure 1). T was chosen 5 cm, which was the length of the trachea specimens used in previous experiments (Murrer *et al* 1995). Making the slab thicker generally resulted in no significant changes in light distribution and for the sake of spatial resolution the slab thickness was kept limited. The air in the cylinder has negligible absorption and scattering, and the index of refraction is 1.

The semi-infinite medium has the optical properties of the mucosa layer at the inner side of the trachea at the chosen wavelength ($\lambda = 630$ or 514 nm). The optical properties $\mu_a(cm^{-1})$ the absorption coefficient, $\mu_s(cm^{-1})$ the scattering coefficient and $g\,(-)$ the anisotropy coefficient for the mucosa of pig tracheas were measured *ex vivo* with a double-integrating sphere setup combined with an Inverse Adding Doubling (IAD) algorithm (Pickering *et al* 1993) The average values (630 nm (n=6), 514 nm (n=4)) as well as the value for one individual trachea (630 nm) that were used in the simulations are shown in table 1. The refractive index of the mucosa is 1.37 ($\pm$ 0.01) for the wavelengths used (Murrer *et al* 1995).

The linear light source with a length L is modelled as a continuous distribution of isotropic and equally strong point sources or with strength varying with position and anisotropic radiance (see below). The quality of linear diffusers available now is such that they can be accurately described

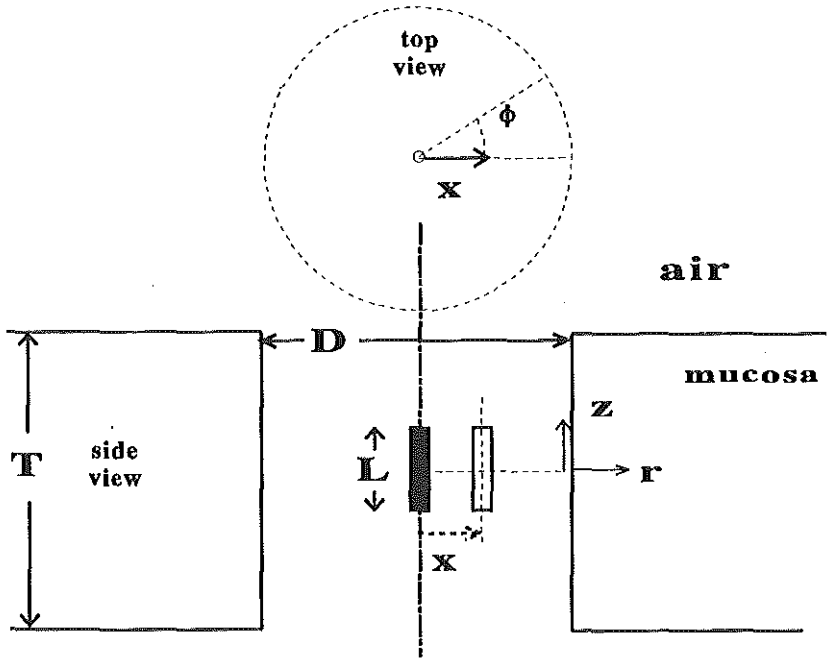

Figure 6.1: *Monte Carlo model geometry, with L the length of the diffuser, D the diameter of the cavity, T the thickness of the slab, x the eccentricity of the light source, r the depth in the tissue and z the height, ϕ azimuthal angle*

with isotropic point sources (Murrer *et al* 1997). The diffusers simulated in this paper will consist of equally strong and isotropic point sources, unless otherwise stated. The light source was placed either on the central axis or eccentrically with a distance x from the central axis. In the case of central placement of the light source a 2-dimensional grid was employed to store the data. In the case of off-axis placement of the light source the cylindrical symmetry is violated and a 3-dimensional grid was employed. In the 3D case, more photons (N $\approx$ 250.000) were needed to obtain a good signal-to-noise ratio, as opposed to the 2D case where only one tenth of this number (N $\approx$ 25.000) was required. Several runs were performed (N = 3..5) to calculate the standard deviations on the simulated values for the fluence rate. The resolution in the z, r and ϕ direction was 1 mm, 0.2 mm and 6 degrees, respectively.

Wavelength (nm)	absorption μ_a (cm^{-1})	scattering μ_s (cm^{-1})	anisotropy g (-)	remark
630	0.22 (0.17)	113 (19)	0.80 (0.06)	n=6
630	0.15 (0.02)	81.2 (0.9)	0.77 (0.01)	single trachea
514	1.83 (1.01)	119 (19)	0.77 (0.08)	n=4

Table 6.1: **Optical properties of bronchial mucosa.** *Measured* ex vivo *with a double-integrating sphere setup. The data on 630 nm were published before (Murrer* et al *1995), the 514 nm data are similar to those found by Van Staveren* et al *(1995) for bladder mucosa. (Standard deviations between parentheses).*

Theoretical Considerations for cylindrical symmetry

The geometry parameter Q is defined as:

$$Q = L/D \tag{6.1}$$

With L (cm) the length of the diffuser and D (cm) the diameter of the lumen. The incident fluence rate (mW/cm^2) at a certain point is defined as the fluence rate in air at that point as a result of the light emitted by the diffuser, without contributions of backscattering by the tissue. The incident fluence rate on the wall of the cavity calculated from a radially emitting (perpendicularly to the diffuser's axis) line source is:

$$\phi_{inc,radial}(z) = \begin{cases} P/(\pi LD) & \leftarrow \ |z| \leq L/2 \\ 0 & \leftarrow \ |z| > L/2 \end{cases} \tag{6.2}$$

with P (mW) the total output power of the diffuser and z (cm) the position on the wall relative to the middle of the diffuser (figure 1). This source function does not describe the actual situation, but is sometimes used as a rough estimate by dividing the output of the diffuser by the estimated area of illumination (the surface area of a cylinder with radius D and length L).

If, more realistically, a superposition of isotropic point sources is considered as a model for the linear diffuser, the incident fluence rate on the wall (mW/cm^2) is described by:

$$\phi_{inc,isotropic}(z) = \frac{P}{\pi LD}\ \frac{1}{2}(\arctan[\frac{L-2z}{D}] + \arctan[\frac{L+2z}{D}]) \qquad (6.3)$$

which is equation 6.2 corrected by a factor describing the geometry.

In the case of isotropic point sources, the ratio R between the incident fluence rate at z=0 and z=$\pm L/2$ (opposite middle and endings of the diffuser, respectively) yields:

$$R = \frac{\phi_{inc}(z = \pm L/2)}{\phi_{inc}(z = 0)} = \frac{\arctan[2Q]}{2\arctan[Q]} \qquad (6.4)$$

The fluence rate build-up factor β is defined as the ratio of the incident fluence rate on the cavity wall at z=0 divided by the measured (or simulated) fluence rate at that position ($\phi_{true}(z = 0)$) in the case of on-axis position of the diffuser (Murrer *et al* 1995).

$$\beta = \frac{\phi_{true}}{\phi_{inc}(z = 0)} \qquad (6.5)$$

For the two different source terms (radial and diffuse) β is:

$$\beta_{radial} = \frac{\pi LD}{P}\ \phi_{true,radial}(z = 0) \qquad (6.6)$$

and

$$\beta_{isotropic} = \frac{\pi LD}{P}\ \frac{\phi_{true,isotropic}(z = 0)}{\arctan[Q]} \qquad (6.7)$$

The expression for β derived from diffusion theory (Star 1995) for an infinitely long, radially radiating, diffuser in an infinitely long cylindrical (air)cavity in an infinite medium yields:

$$\beta_{diff.th.} = \frac{\mu_{eff}}{\mu_a} - 2 \qquad (6.8)$$

with μ_{eff} (cm^{-1}) the effective attenuation coefficient, defined as: $\mu_{eff} = \sqrt{3\mu_a(\mu_a + (1-g)\mu_s)}$.

Realistic light sources

Using a uniformly distributed random variable, the distribution of the site and elevation angle of emission θ of the photons from the linear diffuser is generated for Monte Carlo simulations (See Appendix). The azimuthal

angle ϕ is taken randomly from the interval [0,2π]. The distribution of the place of emission is described by the total probability of light emission at each position of the diffuser, estimated by summing the radiance in all directions at that position. The measurement of these profiles was described in detail by Murrer *et al* (1996). Furthermore, the angular distribution of the light emitted from the diffuser at a particular position on the diffuser is generated. Here the distribution of the emission angle of the photon is described by a 6^{th} degree interpolation polynomial as described by Murrer *et al* (1996). The diffuser used as an example in (Murrer *et al* 1996) is used again in the present paper.

In figure 2, a comparison is made between the original distribution and the random number generator counts when the above procedure is applied. An example for both the place and the angle of emission are shown. The power distribution of this particular diffuser shows a peak near the end, which is caused by reflections off the end-mirror in this diffuser. The angular distribution of the radiance shows a forward directed pattern (maximum at 30^o). The angle indicated is the angle between the direction of the light entering the diffuser and the light emitted by the diffuser. Because of the cylindrical symmetry around the diffuser axis a 2-dimensional simulation can be applied.

Results

Radial versus Isotropic source terms

Figure 3 presents the fluence rate profiles generated by an on-axis linear diffuser that consists of either radially or isotropically radiating elements. A 2 cm diffuser in a cavity of 2 cm diameter was simulated and the average optical properties for 630 nm (table 1) for the mucosa were used. The resulting fluence rates at z=0 and r=0 are 680(12) [1] mW/cm^2 (radial) and 487(16) mW/cm^2 (isotropic). The calculated incident fluence rates (see methods) are 79.6 (radial) and 62.5 mW/cm^2 (isotropic), corresponding with β values of 8.5(0.2) and 7.8(0.3), respectively. The depth profiles at z=0 differ only a by constant factor of 1.47(0.02) (average of all depths), and both reach the level of the incident fluence rate at 5 mm depth. The rectangular radial incident fluence rate pattern as indicated in figure 3 causes a fluence rate pattern on the cavity wall that is much narrower than the profile caused by the bell-shaped incident fluence rate profile of the isotropic source. The

[1] standard deviations between parentheses

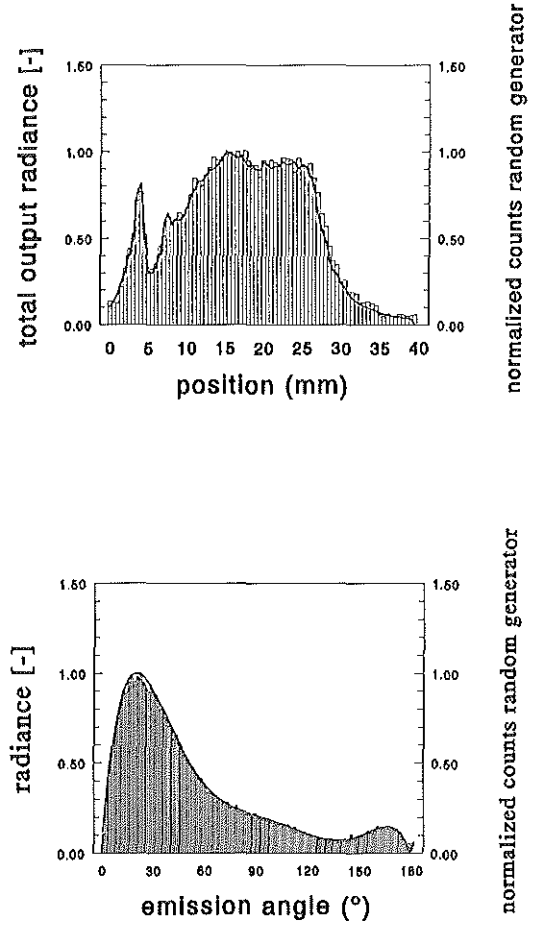

Figure 6.2: *Random number distributions describing the probability distribution of the site of emission (top) and the elevation angle θ of emission (bottom) (on position 15 mm) of the linear diffuser. The bars represent the counts of the random number generator per bin, the solid lines represent the measured distributions*

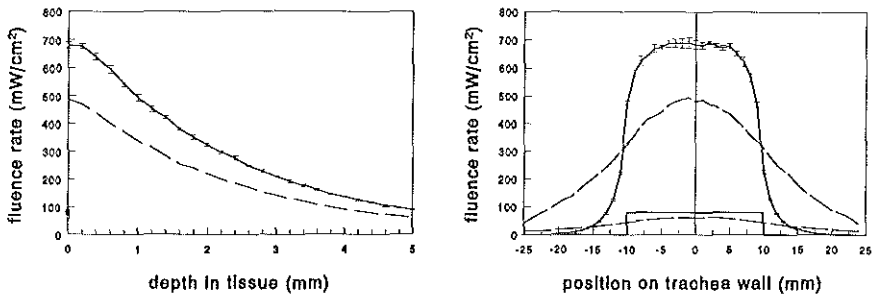

Figure 6.3: *Fluence rate profiles resulting from illumination by a 2 cm diffuser (total output of 1000 mW) with both radial (solid lines) and isotropic (dashed lines) emission patterns. Diameter of the cavity is 2 cm, optical properties: average values for 630 nm (table 1). Error bars calculated from 5 simulations of 25000 photons each. For clarity, error bars only on radial curves. Left: fluence rate in tissue at z=0. Incident fluence rate for radial and isotropic source function indicated by solid and open square, respectively. Right: fluence rate at the wall (r=0). Incident fluence rate profiles for both source terms are also indicated on the bottom of the graph (solid and dashed lines for radial and isotropic emission patterns, respectively).*

resulting radial profile reaches 10% of the maximum value at 13 mm from the center, while the isotropic profile reaches this level at 24 mm from the center.

Non-ideal light source

In figure 4, the fluence rate profile on the wall of the trachea as simulated with the measured source characteristics (see methods) placed on-axis is compared with the profile measured in an *ex vivo* pig trachea with unknown optical properties. For the simulations the average optical properties for λ=630 nm are used (table 1). Although the profiles for measurement and simulation do not coincide, the figure shows that the position of the maximum of the fluence rate on the wall is the same (within measurement and simulation accuracy) for both curves.

The calculated (2.1 mW/cm^2) and measured (2.8 mW/cm^2) fluence rates at the maximum are of the same order of magnitude, but do not agree wit-

hin error ranges. This is to be expected, because the simulation uses optical properties different from those of the measured trachea. However, the distinct asymmetry in the measured profile is reproduced in the simulation.

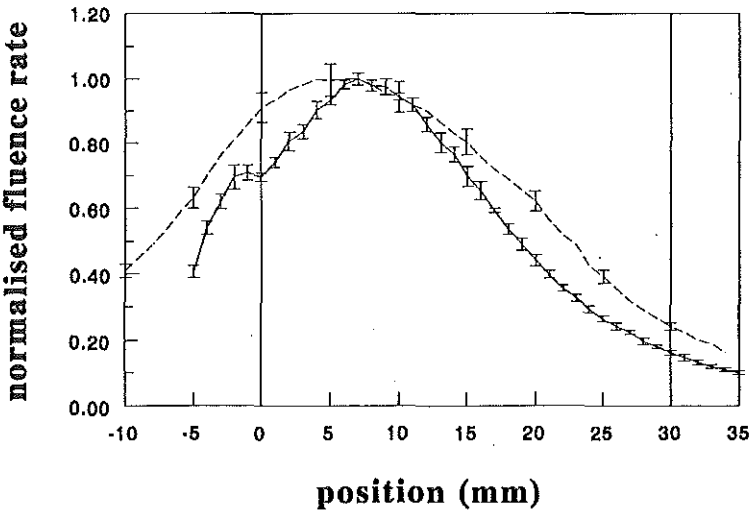

Figure 6.4: *Fluence rate profile on the wall of an* ex vivo *pig trachea with a diameter of 19 mm. The length of the diffuser is 3.4 cm, the total output power is 3.4 mWatt. Vertical lines denote the beginning and ending of the diffusing part. Dashed line: as measured with an isotopic probe (taken from Murrer* et al *1995), solid line: Monte Carlo simulation, average of 5 runs of 25000 photons each, average optical properties at 630 nm, see table 1 . Both curves are normalised to the maximum value, located at 8 mm for the measurement (2.8 mW/cm^2) and at 7 mm for the simulation (2.1 mW/cm^2).*

Variations in L and D: the geometry parameter

In figure 5, the $\beta_{radial-estimate}$ and $\beta_{isotropic}$ values are shown, calculated from the simulated value for ϕ_{true}, using both the incorrect, estimated radial source function $\phi_{inc,radial}$ and the correct isotropic $\phi_{inc,isotropic}$ source function. The relationship $\beta_{isotropic} = \beta_{radial-estimate}/\arctan[Q]$ connects

the two β-values. The β-values are plotted as a function of the geometry parameter Q for both 630 and 514 nm light.

The values of L and D were varied from 1 to 5 cm in steps of 1 cm. The figure shows that the geometry parameter is useful to describe β in different geometries. In the left part of the figure the β values calculated with the incorrect(roughly estimated) radial source function show a one-to-one correspondence between β and the geometry parameter. When the correct source term is used to calculate the β value (right part) β is almost constant with a slow decrease with increasing values of Q. A linear curve-fit yields: $\beta_{630}(Q) = 8.36 - 0.34Q$ $(r = 0.78)$ and $\beta_{514}(Q) = 3.32 - 0.15Q$ $(r = 0.83)$ in which r is the correlation coefficient. A first-order estimate of β for all geometries can be made by taking the average value of β for all values of the geometry parameter, which is 7.7(± 11%) for 630 nm and 3.0(± 11%) for 514 nm. The slow decrease of β with increasing Q is probably caused by the finite length of the cylindrical cavity. High Q values occur for long diffusers (4 and 5 cm) in the set of L and D values that were simulated. These diffusers lose relatively much light out of the ends of the cavity because their lengths are close to the thickness of the slab (T = 5 cm).

The fluence rate at z=±L/2 and r=0 (opposite the ends of the diffuser) can be estimated roughly using eq. (6.4), assuming that the shape of the total fluence rate profile does not differ too much from the incident profile. The fluence rate is then estimated by taking the fluence rate at z=0, and multiplying it by the factor of eq. (6.4). The simulated fluence rate is 86%(22) of the value estimated for 630 nm and 90%(16) for 514 nm. This indicates that, on average, the total fluence rate profile is somewhat narrower than the incident profile.

Varying lumen diameter

In figure 6 the fluence rate at z=0 and r=0, 2 and 5 mm is plotted for varying lumen diameter. The light source is 2 cm long, on-axis and consisting of isotropic point sources with a total output of 1000 mW. The average optical properties for 630 nm are used (table 1).

The curves for 0, 2 and 5 mm differ only by a constant factor, which means that the penetration depth (when related to the fluence rate at 0 mm) is the same for all lumen diameters. The fluence rate at 2 and 5 mm is 41(2)% and 11(1)% of the fluence rate at 0 mm. The average β value for all lumen diameters is 7.2(0.5), in agreement with figure 5 (same optical properties). The regression line is given by: $\beta_{630}(Q) = 8.21 - 0.53Q$ $(r = 0.94)$.

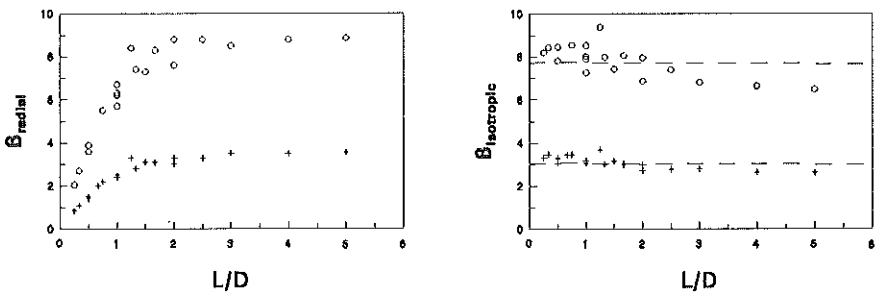

Figure 6.5: *Monte Carlo simulations of β for varying diffuser lenghts and lumen diameters plotted against the geometry parameter. Optical properties are the average for 630 nm (table1). Each point is calculated by one run of 25.000 photons, the statistical standard deviation of these values is $\approx$ 7%. Left: $\beta_{radial-estimate}$ for (incorrect) assumption of radially emitting source, Right: $\beta_{isotropic}$ for correct light source consisting of isotropic point sources. +: λ = 514 nm, o: λ = 630 nm. The dashed lines indicate the average values of $\beta_{isotropic}$, 7.7 (sd 0.8) and 3.0 (sd 0.3) for 630 and 514 nm, respectively.*

Variation in optical properties: Relation with diffusion theory

When the optical properties for the individual trachea (table 1) are used the value for $\beta_{diff.th.}$ is 17.3. A Monte Carlo simulation that uses these optical properties and an (isotropic) diffuser of 2 cm (on-axis) in a lumen with a diameter of 2 cm yields a $\beta_{m.c.}$ of 8.4 ($\pm$5%). The reason for this difference is that the diffusion theory formula is derived for a different geometry (see methods). In order to investigate if the diffusion theory formula can qualitatively describe the dependence of β on the optical properties, the value for both $\beta_{m.c.}$ and $\beta_{diff.th.}$ were normalised by setting them at unity at this set of optical properties. From there, the value for both μ_a and μ_s were varied in the Monte Carlo simulations and the diffusion theory formula. The results are presented in figure 7.

The normalised β values for varying scattering found for both Monte Carlo and diffusion theory agree well (mean deviation 2%). For varying absorption (μ_a) the agreement is less good. For increasing μ_a the agreement is still acceptable (mean deviation 15%), but for decreasing μ_a the discrepancy increases (mean deviation 32%), as is clear from the figure.

The Monte Carlo data show less increase in β with decreasing absorption

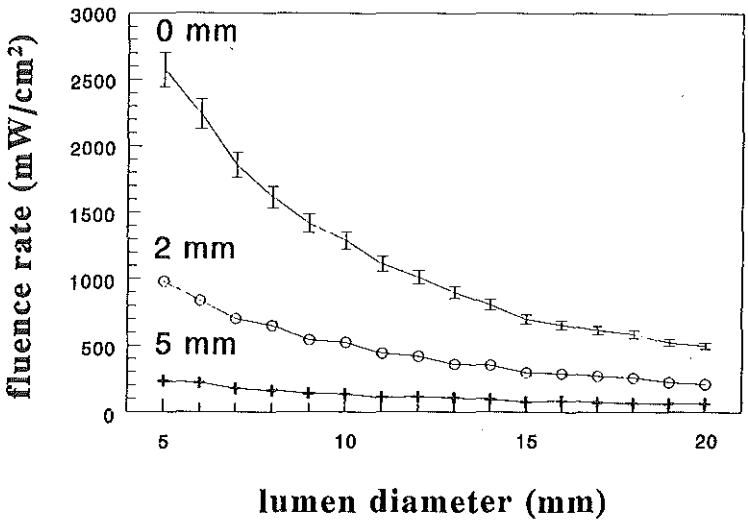

Figure 6.6: *Fluence rate at z=0 mm and r=0, 2 and 5 mm depth in tissue for varying lumen diameter. The simulated (on-axis) diffuser has a length of 2 cm, and a total output power of 1000 mW. Optical properties are the average values for 630 nm (see table 1). Mean values and error bars calculated from 5 runs of 25000 photons each.*

than diffusion theory. With lower absorption the photons travel along optical paths that penetrate deeper in the tissue. Because of the finite length of the simulated cavity, photons escape and cause less build up of fluence rate compared with the infinitely extended diffusion theory geometry.

The variations in μ_s cause changes in β from a decrease of 34% at 40 cm^{-1} to an increase of 26% at 120 cm^{-1}. When μ_a is decreased to 0.05 cm^{-1} the β value increases by 65%. Increasing the μ_a to 0.30 cm^{-1} decreases β by 30%. Variations in μ_a may be expected when the blood content of the tissue changes.

The β values found for 514 and 630 nm light in the section about the geometry parameter can be inter-related with diffusion theory in the above manner. The ratio of $\beta_{diff.th.,630}(= 15.6)$ and $\beta_{diff.th.,514}(= 4.92)$ is 3.2, while this ratio for $\beta_{m.c.,630}$ and $\beta_{m.c.,514}$ is 2.6 (0.6). These ratios agree

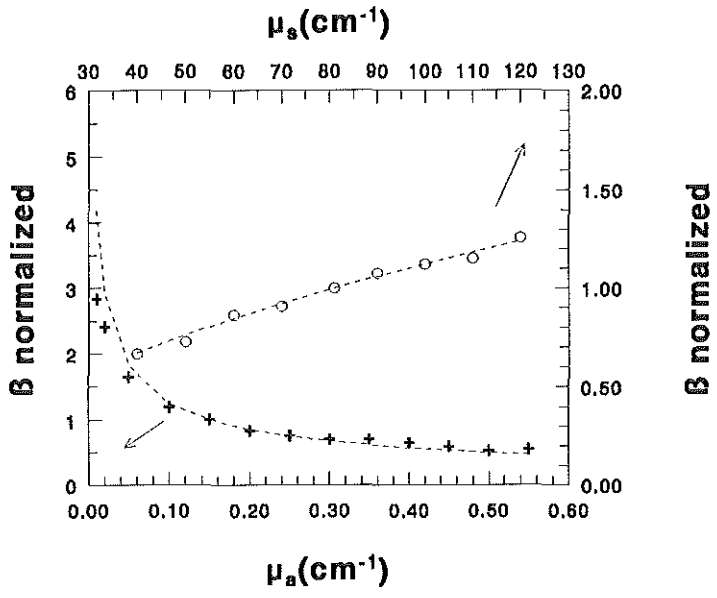

Figure 6.7: *Variations in β values from diffusion theory (dashed lines) and Monte Carlo simulations (symbols) when μ_a (+, bottom x-axis and left y-axis)) or μ_s (○, top x-axis and right y-axis) are varied. The β values are normalised to the β values for diffusion theory and Monte Carlo at mu_a = 0.15 cm^{-1}, μ_s = 81 cm^{-1} and g = 0.77. Statistical variations on the Monte Carlo data: $\approx$ 7%.*

within simulation error.

Also, the above procedure can be used to estimate the unknown absorption coefficient of the pig trachea in which the fluence rate profile resulting from a realistic light source was measured. The simulation with μ_a=0.22 cm^{-1} resulted in a maximum fluence rate that was 75% of the measured value. Assuming constant scattering properties, the above procedure yields a μ_a of 0.13 cm^{-1} for the trachea, which is a realistic value, considering the average value in table 1.

Eccentric light sources

The optical properties of the single trachea (table 1) were used to investigate the influence of the off-axis placement of the light source. A trachea with

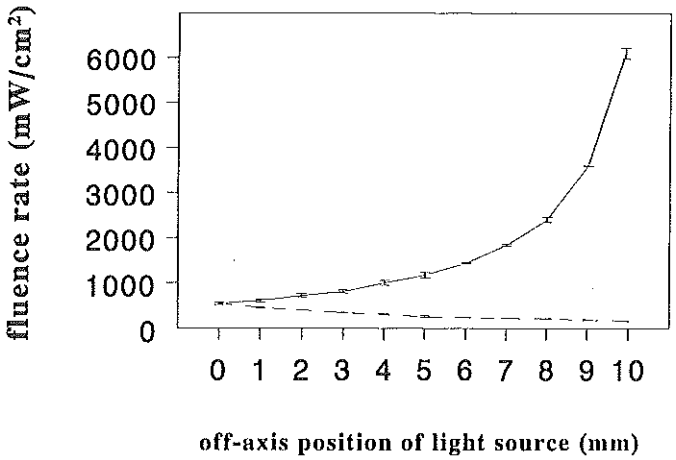

Figure 6.8: *Fluence rate on z=0 and r=0 resulting from illumination of a cavity (D = 2 cm) with an off-axis isotropic diffuser of 2 cm length, optical properties of single trachea (table 1). Total output power of the diffuser is 1000 mW. Solide line indicates the fluence rate at $\phi = 0^o$, dashed line indicates the fluence rate at the opposite side (ϕ=180°). Mean values and error bars calculated of 3 runs of 250000 photons each.*

D = 2 cm with a diffuser (output 1000 mW) of 2 cm length was simulated. The resulting fluence rate at z=0, r=0 and ϕ=0° and 180° is shown in figure 8. When the diffuser is placed on-axis, the fluence rate is 548(27) mW/cm^2, corresponding to a β of 8.8(0.4). Moving the diffuser away from the center to the wall increases the fluence rate to 1174(57) mW/cm^2 at 5 mm and 6110(130) mW/cm^2 at 9.9 mm off-axis, which is a 2- and 11-fold increase of the fluence rate, respectively.

The positioning of the diffuser close to the wall is critical for the fluence rate. Moving the diffuser to 9 mm off-axis decreases the fluence rate by 41% to 3602 mW/cm^2. Moving the diffuser 1 mm off-axis to either side causes a 10% change in the fluence rate. The fluence rate at 180° gradually decreases with increasing off-axis position to a value of 169(10) mW/cm^2 at 9.9 mm off-axis placement. This is 31% of the on-axis level, and 3% of the level at 0°.

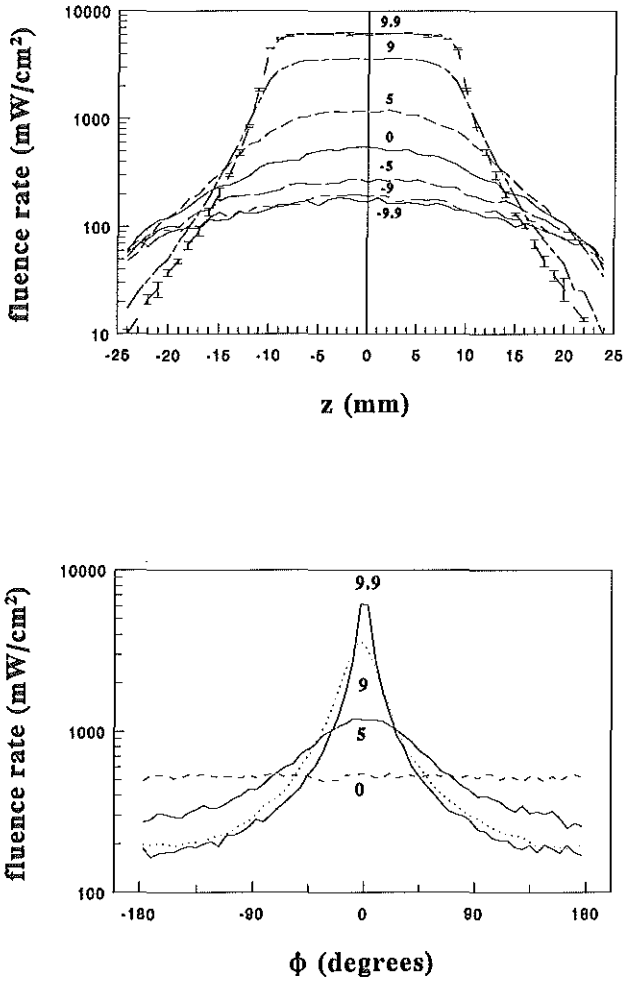

Figure 6.9: *Fluence rate profiles on the wall (r=0) of a cavity (D = 2 cm) resulting from illumination with a 2 cm isotropic diffuser, optical properties for a single trachea at 630 nm (table 1). Numbers indicate the off-axis position (mm) of the diffuser. Positive and negative numbers indicate that the diffuser is moved towards and away from the site, respectively. Top: Fluence rate profiles at ϕ=0°, for varying off-axis positions. Bottom: Fluence rate profiles at z=0, for varying off-axis positions. For clarity, error bars are only indicated once in the top graph. Mean values and error bars calculated of 3 runs of 250000 photons each.*

Figure 9 presents the fluence rate profiles on the wall of the cavity (r=0) in the z- and the ϕ-direction. The closer the light source is positioned to the wall, the narrower the profile in the z-direction (top) becomes, which is a consequence of the fact that the incident fluence rate pattern is also narrower, because the diffuse light has less distance to expand before hitting the wall.

The figure shows that the relative increase between different off-axis positions is larger for positions close to the surface (cf. 9 and 9.9 mm) as compared to those far away from the surface (cf. -9 and -9.9 mm). This indicates that the fluence rate for off-axis light source positions close to the surface is relatively sensitive to small displacements of the light source.

The profiles in the ϕ direction (bottom) show that profiles narrow considerably for extreme off-axis positions. In the ϕ direction we define the area of treatment for different off-axis positions as that area with a fluence rate of more than 50% (arbitrary) of the maximum. For 5, 9 and 9.9 mm off-axis this area is 23.0, 6.2 and 3.1 mm, respectively.

Discussion

The Monte Carlo Model

Although the model of the trachea is simple, we showed previously (Murrer *et al* 1995) that it is suitable to simulate absolute values of the fluence rate in the bronchial mucosa (thickness $\approx$ 1 mm) and to a certain extent in the cartilage ($\approx$ 3 mm) by use of the optical properties of the mucosa only. This is because the absorption and reduced scattering of the cartilage (Murrer *et al* 1995) are very similar to those of the mucosa at 630 nm. With the use of green light the penetration depth is such, that in practice only the mucosa layer needs to be considered in the model. The incorporation of realistic light sources in the model facilitates the interpretation of the consequences of the use of light sources with varying output characteristics. In the future we hope to expand the model with a multi-layer structure to incorporate the cartilage and with local spots of different optical properties to simulate lesions.

Source term

In practice often a first estimate of the fluence rate on the wall is made by dividing the total output of the diffuser by the surface of the cylinder with the radius of the lumen and the length of the diffuser. This incident

fluence rate can not be used for inter-patient comparison, as the fluence rate build-up is highly variable between patients. An other aspect of the above estimate is the underlying assumption of a radially emitting diffuser. The incident fluence rate profile of a real (isotropic) diffuser is not rectangular but bell-shaped. Therefore a larger margin around the lesion should be illuminated to ensure proper treatment of the tumour and the tumour bed.

Influence of optical properties

The analogy between the β values calculated with diffusion theory and those found with Monte Carlo can be used to estimate the variations in β that can be expected when the inter-specimen variations in the average optical properties for 630 nm in table 1 are taken into account. The largest change in β occurs when μ_a and g are lowered by one standard deviation and μ_s increased by one standard deviation (maximum reduced scattering). The β for the average optical properties (7.7 figure 5) then increases by a factor of 2.8 to 21.3. The lowest β is 4.0 (52%), for maximum absorption and minimal reduced scattering. This shows that considerable inter-patient variations can occur in the applied fluence rate due to variations in optical properties as reported previously by Marijnissen *et al* (1993a) for bladder and Hudson *et al* (1994) for skin at 630 nm.

The influence of blood content of the mucosa can be directly estimated from figure 7. Changes in the order of 1 total volume percent introduce changes in the order of the average absorption at 630 nm (Cheong *et al* 1990), an increase in absorption of 0.15 cm^{-1} introduces a decrease of 30% in the fluence rate, and a decrease of the absorption causes even larger increases in the fluence rate. The latter may occur when vascular shutdown occurs, one of the possible effects of Photodynamic Therapy.

Practical use

Several rules of thumb can be derived for use in clinical practice, provided that diffusers with good characteristics are used (Murrer *et al* 1997). For practical use, the β value can be assumed the same for all lumina in one patient, and then the maximum fluence rate on the wall for on-axis illumination can be calculated according to $\phi = \beta \cdot P^*/(\pi D) \cdot \arctan(L/D)$. This relation can be used to estimate that the maximum fluence rate increases by a factor of 2.2 when going from the trachea (D=20 mm) to a bronchus (D=12 mm) with a 2 cm diffuser. A protocol written to cover different areas in the bronchi should incorporate these large difference in dosimetry.

For on-axis isotropic diffusers, as a first-order estimate the fluence rate

profile on the wall can be described as the incident fluence rate pattern enhanced by a factor β, like we observed with an *ex vivo* measurement in a pig trachea (Murrer *et al* 1996).

The geometry parameter in humans can vary between 0.25 and 7.5 because of the length of the applied diffuser (0.5 to 3 cm) and the diameter of the treated lumen (20 to 4 mm). The corresponding term correcting for the geometry ($\arctan(Q)$) then varies from 0.24 for L = 0.5 cm and D = 2 cm (Q = 0.25) to 1.44 for L = 3 cm and D = 0.4 cm (Q = 7.5). The illumination of even smaller lumina or obstructing tumours becomes comparable to interstitial treatment and is beyond the scope of this paper.

The fluence rate opposite the ends of the diffuser is 95% of the maximum in the case of the smallest Q (0.25) and 52% for the largest Q (7.5), as can be estimated with the help of eq.6.4. This is important to know when choosing a diffuser length for treatment of a lesion of a certain length. For treatment with a large Q it may be wise to use a diffuser that is longer than the lesion to avoid under-illumination of the edges of the tumour. The length of the diffuser can be chosen such that the incident fluence rate (eq.6.3) on the lesion perimeter is eg. $\gtrsim$ 80% of the fluence rate at z=0.

Penetration depth

The data in figure 7 show that, for varying lumen diameter and constant optical properties, the penetration depth is a constant. The definition of penetration depth is somewhat arbitrary. If the penetration depth is defined as the depth at which the fluence rate has decreased to a certain percentage of the fluence rate at the wall, then the penetration depth is indeed constant. This, however, implies knowledge of the fluence rate at the wall of the lumen through either calculation or preferably measurement.

Another definition of penetration depth is the maximum depth at which the fluence rate exceeds a certain threshold value needed for the photosensitiser to induce tissue damage. When this definition is used, the penetration depth can be interpreted as depth of necrosis or treatment depth. With the latter definition the penetration depth increases with decreasing lumen diameter. This is not a practical definition, because it requires knowledge of the fluence rate in depth. In practical use, only a measurement at the surface is possible and therefore the first definition seems more appropriate.

Eccentric illumination

When the diffuser is placed off-axis in the lumen, large dose variations can occur. Slight deviations from the on-axis position produce only minor

variations in the fluence rate at the wall, but positions close to the wall cause an increase in dose rate at the wall of several orders of magnitude, which is very sensitive to small displacements, as we reported earlier in *ex vivo* measurements (Murrer *et al* 1995). The fluence rate at the wall opposite the site toward which the diffuser is moved decreases to one third of the on-axis value. A very narrow region (3 mm for total 9.9 mm eccentricity in a 2 cm diameter lumen) receives the same (within 50%) fluence, which in general is smaller than the lesion plus a margin of surrounding tissue. In case of unknown extension of pre-malignant tissue we advocate uniform illumination (Murrer *et al* 1995) as in the bladder (Marijnissen *et al* 1989) to make sure a large enough margin is treated. Therefore we strongly advise to always use an on-axis illumination if possible.

General conclusion

The data shown here clearly demonstrate the considerable variations in the fluence rate levels and patterns as a consequence of varying geometries and optical properties. Protocols for Photodynamic Therapy in the bronchi should therefore be designed with special attention to the dosimetry in order to achieve reproducible results.

The relationships derived above to estimate the fluence rate should be related to an *in vivo* measurement of the fluence rate (Murrer *et al* 1997a). From this measurement a value for β can be calculated, and then the dosimetry in another lumen can be based on this β value and the knowledge of the lumen diameter and diffuser length. This, however, assumes the same optical properties in every lumen. In the case of a clearly visible lesion, an *in situ* measurement should be attempted. If possible, an *in situ* measurement of the optical properties might be performed (Bays *et al* 1996) which could then be compared with an extended set of Monte Carlo simulations with varying optical properties to estimate the fluence rate distribution.

Combination of light dosimetry and a measurement of the fluorescence of the sensitiser present in the tissue (Braichotte *et al* 1996) might prove a useful tool for optimising the treatment parameters. Monte Carlo simulations can be very useful in investigating the excitation and escape of fluorescence from the tissue.

Acknowledgements

The authors wish to thank Marleen Keijzer for supplying the basic code for the Monte Carlo simulations. The Laser Centre at the Amsterdam Medical Centre kindly provided access to the double-integrating-sphere setup. This work was supported by the Dutch Cancer Society, grant DDHK 93-615.

References

1. Bays R, Wagnières G, Robert D, Braichotte D, Savary J-F, Monnier P, van den Bergh H. (1996) Clinical determination of tissue optical properties by endoscopic spatially resolved reflectometry. *Appl. Opt.* **35** *1756-1766*

2. Braichotte D, Savary J F, Glanzmann T, Monnier P, Wagniéres G, van den Bergh H. (1996) Optimizing light dosimetry in photodynamic therapy of the bronchi by fluorescence spectroscopy. *Lasers Med. Sci.* **11** *247-254*

3. Cheong W F, Prahl S A, Welch A J. (1990) A review of optical properties of biological tissues. *IEEE J. Quantum Electron.* **26(12)** *2166-2185*

4. Hudson E J, Stringer M R, Cairnduff F, Ash D V, Smith M A. (1994) The optical properties of skin tumours measured during superficial photodynamic therapy. *Lasers Med. Sci.* **9** *99-103*

5. Keijzer M, Pickering J W and van Gemert M J C. (1991) Laser beam diameter for port wine stain treatment. *Lasers Surg. Med.* **11** *601-605*

6. Lux I and Koblinger L. (1991) Monte Carlo particle transport methods: Neutron and photon calculations. *CRC Press: Boca Raton Fl*

7. Marijnissen J P A, Jansen H, Star W M. (1989) Treatment system for whole bladder wall photodynamic therapy with *in vivo* monitoring and control of light dose rate and dose. *J. Urol.* **142** *1351-1355*

8. Marijnissen J P A, Baas P, Beek J F, van Moll J H, van Zandwijk N, Star W M. (1993) Pilot study on light dosimetry for endobronchial photodynamic therapy. *Photochem. Photobiol.* **58** *92-98*

9. Marijnissen J P A, Star W M, In 't Zandt H J A, D'Hallewin M A, Baert L. (1993a) *In situ* light dosimetry during whole bladder wall photodynamic therapy: clinical results and experimental verification. *Phys. Med. Biol.* **38** *567-582*

10. Murrer L H P, Marijnissen J P A, Star W M. (1995) *Ex vivo* light dosimetry and Monte Carlo simulations for endobronchial photodynamic therapy. *Phys. Med. Biol.* **40** *1807-1817.*

11. Murrer L H P, Marijnissen J P A, Star W M. (1996) Light distribution by linear diffusing sources for photodynamic therapy. *Phys. Med. Biol.* **41** *951-961*

12. Murrer L H P, Marijnissen J P A, Star W M. (1997) Improvements in the design of linear diffusers for photodynamic therapy *Phys. Med. Biol.* **42** *1461-1464*

13. Murrer L H P, Marijnissen J P A, Baas P, van Zandwijk N, Star W M. (1997a) Applicator for light delivery and in situ light dosimetry during endobronchial Photodynamic Therapy: first measurements in humans. *Lasers Med. Sci.* **12** *253-259*

14. Pickering J W, Prahl S A, van Wieringen N, Beek J F and van Gemert M J C. (1993) Double-integrating-sphere system for measuring the optical properties of tissue. *Appl. Opt.* **32** *399-410*

15. Press W H, Flannery B P, Teukolsky S A, Vetterling W T. (1989) Numerical Recipes in Pascal: The art of scientific computing. *Cambridge University Press*

16. Saponaro S, Farina B, Murrer L H P, Pignoli E, Rizzo R, Star W M, Tomatis S, Marchesini R. (1996) Endoluminal photodynamic therapy: influence of optical properties on light fluence in the cylindrical diffusing fibre geometry. *Proc. SPIE* **2923** *86-95*

17. Star W M. (1995) Diffusion theory of light transport. *In: 'Optical-thermal response of laser-irradiated tissue', chapter 6, ed. Welch A J, van Gemert M J C (Plenum: New York :131-206)*

18. Van Staveren H J, Beek JF, Keijzer M and Star W M. (1995) Integrating sphere effect in whole bladder wall photodynamic therapy: II The influence of urine at 458, 488, 514 and 630 nm optical irradiation. *Phys. Med. Biol.* **40** *1307-1315*

Appendix

Construction of a non-uniformly distributed random variable

ξ is a random variable, uniformly distributed between 0 and 1 ($p_u(s) = 1$ for $0 \leq s \leq 1$, and 0 otherwise). We used Ran3 from Numerical Recipes (Press *et al* 1989).

To generate a random variable distributed according to $p(s)$ using the uniform distribution $p_u(s)$, a function f(s) has to be found such that the following condition is obeyed (Lux and Koblinger 1991):

$$\int_0^{\xi} p_u(s)ds = \xi = \frac{\int_0^{s_1} p(s)ds}{\int_0^{\infty} p(s)ds} = f(s_1) \tag{6.9}$$

The integral in the denominator normalizes the distribution which is necessary because the distributions used are often obtained from (generally not normalized) measurements. The random variable s_1 is sampled through

$$s_1 = f^{-1}(\xi) \tag{6.10}$$

Here we have a p(s) that is either no analytical function (measurement of output power versus position), or a function (6^{th} degree polynomial) that has no analytical inverse function f^{-1}. Therefore, a discrete description of the functions is used, viz. a series of N x and y values (y_i, x_i). The x-values are equally spaced by Δx. Equation 6.9 is rewritten as:

$$\xi = \frac{\sum_{n=1}^{n1} y_n(x_n)\Delta x}{\sum_{n=1}^{N} y_n(x_n)\Delta x} = f(x_{n1}) \tag{6.11}$$

The function is normalised such that $f(x_N) = 1$. For each x_{n1} value a ξ_{n1} value is calculated. The inverse function

$$x_{n1} = f^{-1}(\xi) \tag{6.12}$$

is obtained by linear interpolation between the x_{n1} values paired to the two ξ_{n1} values that are closest to the ξ value generated by the uniform random number generator.

Chapter 7

Short- and long-term normal tissue damage with Photodynamic therapy in pig trachea: A fluence-response study comparing Photofrin and mTHPC

Submitted to: Br. J. Cancer

L.H.P. Murrer, K.M. Hebeda †, J.P.A. Marijnissen, W.M. Star

†Department of Pathology, St. Radboud University Hospital Nijmegen, The Netherlands.

Abstract

The damage to normal pig bronchial mucosa caused by PhotoDynamic Therapy (PDT) using mTHPC and Photofrin as photosensitisers was evaluated. An endobronchial applicator was used to deliver the light with a linear diffuser and to measure the light fluence *in situ*. The applied fluences were varied, based on existing clinical protocols. A fluence finding experiment with short-term (1-2 days) response as an endpoint showed considerable damage to the mucosa with the use of Photofrin (fluences 50-275 J/cm^2, drug dose 2 mg/kg) with oedema and blood vessel damage as most important features. In the short-term mTHPC experiment the damage found was slight (fluences 12.5-50 J/cm^2, drug dose 0.15 mg/kg). For both sensitisers atrophy and acute inflammation of the epithelium and the submucosal glands was observed. The damage was confined to the mucosa and submucosa leaving the cartilage intact. A long-term response experiment showed that fluences of 50 J/cm^2 for mTHPC and 65 J/cm^2 for Photofrin treated animals caused damage that recovered within 14 days, with sporadic slight fibrosis and occasional inflammation of the submucosal glands. Limited data on the pharmacokinetics of mTHPC show that drug levels in the trachea are similar at 6 and 20 days post injection, indicating a broad time window for treatment. The importance of *in situ* light dosimetry was stressed by the inter-animal variations in fluence rate for comparable illumination conditions.

Introduction

PhotoDynamic Therapy (PDT) for treatment of lung cancer has been investigated extensively with the use of Photofrin as a photosensitiser (McCaughan *et al* 1988, Hayata *et al* 1996, Lam 1994) for palliation, as well as with curative intent for treatment of early-stage lung cancer. Cortese *et al* (1997) showed that PDT with hematoporphyrin derivative (HpD) can be an alternative to surgery. Currently also the use of meta-TetraHydroxyPhenyl Chlorin (mTHPC) as a photosensitising agent is evaluated experimentally and clinically for the treatment of cancer of the lungs, oesophagus and larynx (Grosjean *et al* 1996, Lofgren *et al* 1994, Abramson *et al* 1994).

The common method of light delivery in this application of PDT is the use of a linear (or cylindrical) diffuser, which is suited to illuminate hollow, cylindrical organs such as the trachea or the bronchi. The light dosimetry

of this treatment consists of a measurement of the total output of the linear diffuser only, and the applied 'light dose' is defined as the total amount of light energy emitted per unit of length of the diffuser (J/cm). Little is known about other important factors that determine the light fluence rate (and fluence) distribution in the tissue, which is the appropriate 'light dose' to evaluate PDT effects.

In previous work we showed that the *in situ* fluence rate resulting from illumination of the bronchi with identical diffusers and output can vary considerably between individuals (Murrer *et al* 1997). This is related to the inter-individual variations in optical properties of the bronchial mucosa. Similar variations in fluence rate caused by variations in optical properties (with red light of 630 nm) are found in the bladder (D'Hallewin *et al* 1992) and in the skin (Hudson *et al* 1994). Also the positioning of the diffuser in the lumen (Marijnissen *et al* 1993, Murrer *et al* 1995) and the output characteristics of the linear diffuser used (Murrer *et al* 1996) have great influence on the fluence rate distribution in the tissue.

Because so many, sometimes unknown, parameters can influence the fluence rate in the mucosa, it is necessary to perform an *in situ* measurement of the fluence rate to quantify the applied fluence. An applicator which makes it possible to perform such a measurement together with a controlled way of light delivery has been developed in our group (Murrer *et al* 1997). With the help of this applicator, the present study seeks to find a relationship between the applied fluence (true 'light dose') and the short-term (1-2 days) damage found in the normal (healthy) tracheal mucosa resulting from PDT with Photofrin and mTHPC. Consequently, the long-term damage resulting from an applied fluence that results in potentially recoverable short-term damage is investigated to determine the tolerance of normal tissue to PDT.

Methods

General Protocol

The study was performed in two parts. In the first (acute) part the normal tissue damage of the bronchial mucosa caused by PhotoDynamic Therapy in the trachea of healthy pigs was assessed visually as well as histologically 24 and 48 hours after illumination. Both mTHPC and Photofrin were used. The photosensitiser dose was kept the same in all experiments and the total light fluence was varied (with constant fluence rate) in three areas in the

trachea of each pig. This part served as a fluence-finding experiment for the second part. In the second part one single total light fluence was applied and the bronchial mucosa damage was followed visually during the 2 weeks follow-up period and histologically after termination of the experiment. The total light fluence applied in the second part is the fluence that showed potentially recoverable damage in the first part for each drug applied. The experimental protocol (nr. 604-96-02) adhered to rules laid down in the Dutch Animal Experimentation Act and was approved by the Committee on Animal Research of the Erasmus University Rotterdam.

Animals and anesthesia

The animals used in this study were female pigs of a crossbreed of Danish Landrace and Yorkshire pigs (≈30 kg). The animals were kept on a standard diet. The day before treatment as well as the day before follow-up bronchoscopy they were kept fasted. For all procedures the animals were sedated with Ketamine (im, 10 mg/kg), and intubated. They were ventilated artificially with a mixture of nitrous oxide : oxygen (1:2 V:V) and 1.5% isoflurane. During ventilation, anesthesia was maintained with pancorium (iv, 4 mg) and fentanyl (iv, 0.1 mg). After the experimental procedures the animals were hand-ventilated until independent breathing was restored. During the treatment the artificial ventilation duration never exceeded 45 minutes, during drug delivery and follow-up bronchoscopies the duration was less then 15 minutes. During drug delivery the animals were ventilated with a mask only and received no additional iv. anesthesia. The animals were sacrificed with a bolus injection of pentobarbital (iv).

Drug delivery

In both the acute and follow-up part 6 animals were used. In each part 2 animals received Photofrin^{TM} and 4 animals received mTHPC^{TM} (meta-tetrahydroxyphenyl chlorin). The Photofrin was kindly provided by Quadra Logic Technologies (Vancouver, Canada) and the mTHPC was kindly provided by Scotia Quantanova (Guildford, Great Brittain).

The Photofrin was dissolved in a 5% dextrose solution and administered intraveneously by a slow-push injection 48 hours before treatment according to the Lederle/QLT protocol (P 503/504) for endobronchial PDT. The applied dose was 2 mg per kg bodyweight. The mTHPC was dissolved in a mixture of ethanol, polyethylene glycol and water that was supplied with

the drug, and injected intraveneously by a slow-push injection 96 hours before treatment. This drug delivery-illumination interval is also used by other groups for mTHPC-PDT (eg Grosjean *et al* 1996). The applied dose was 0.15 mg per kg bodyweight. The animals were housed separately in subdued light conditions during the entire study.

Light delivery and dosimetry

The light was delivered using an applicator that was specifically developed for endobronchial PDT. The applicator incorporates a linear diffuser for light delivery, a fixation system that ensures the central positioning of the diffuser in the trachea and an isotropic probe for *in situ* measurement of the fluence rate on the trachea wall (Murrer *et al* 1997).

The design has been improved with a 1.5 cm diffuser with isotropic instead of forward scattering properties (Murrer *et al* 1997a) manufactured by Rare Earth Medical (West Yarmouth MA, USA). The isotropy of the diffuser causes the maximum of the fluence rate to be located on the trachea wall opposite the middle of the diffuser. The isotropic probe measures the fluence rate at this maximum.

With the aid of a Monte Carlo model for the geometry of a linear diffuser in a trachea (Murrer *et al* 1995) we estimated an overlap of less than 5% of the maximum fluence rate between separate fields when a diffuser of 1.5 cm is used with an inter-lesion spacing of 5 cm. This is possible in the pig's trachea which is generally longer than the 15 cm (3 times 5 cm) needed for the experiment.

The diameter of the isotropic probe fibre core has been increased by a factor of two compared to our first design, which causes a higher light output of the isotropic probe, enabling a more sensitive measurement. The isotropic probe (bulb diameter 0.8 mm) mounted on a 200 μm quartz core fibre was produced by Rare Earth Medical (West Yarmouth MA, USA).

The light source used was a KTP/Nd:YAG laser with a dye unit (KTP/YAG 832 and Dye module series 600, Laserscope, San Jose CA, USA) that was tuned to a wavelength of 652 or 630 nm for mTHPC or Photofrin, respectively. The output of the linear diffuser is measured with an integrating sphere. The applicator is inserted in the sphere and unfolded and the laser is switched on. The voltage reading of a built-in photodiode is converted to the total output in mW with appropriate calibration factors for the two wavelengths used. The same integrating sphere is used to calibrate the iso-

tropic probe in air (van Staveren *et al* 1995). Built-in laser diodes provide a stable diffuse light field, which is calibrated with the same photodiode that is used for the output measurement. The output voltage of the photodiode is multiplied by an appropriate calibration factor to calculate the diffuse light field in the sphere for both wavelengths used.

When in contact with tissue, the reading of the isotropic probe calibrated in air has to be corrected because of the difference of refractive index (n) between air (n=1) and tissue (n=1.37). When the probe is pressed against the mucosa, the reading of the probe calibrated in air has to be multiplied by a factor 1.07 (± 2%) (Murrer *et al* 1995, Marijnissen and Star 1996). It is important that the isotropic probe is kept free of mucus and blood to ensure correct calibration. This can be checked through the bronchoscope and if necessary the probe must be rinsed through the bronchoscope or the applicator must be retracted, cleaned and inserted again (Murrer *et al* 1997). The light output of the isotropic probe is coupled to a photodiode inside a home-built dosimetry device, that displays the fluence rate as well as the integrated fluence rate in time (total fluence). The dosimeter is calibrated by inserting and unfolding the applicator in the sphere with the laserdiodes switched on.

Applied Fluences

The fluence rates and the total fluences that were applied for the different sensitisers in the acute experiment were derived from either an existing protocol (Photofrin) or from protocols for eg. skin or ENT application (mTHPC) in humans.

The mTHPC-treatment fluence and fluence rate was derived from the incident fluences and fluence rates in protocols for eg. skin, where an incident fluence rate of 100 mW/cm^2 is used to a total incident fluence of 10 J/cm^2. In a pilot experiment on rats, we observed that the incident fluence rate on a shaved spot of skin (2 cm diameter) increased to 250% by backscattering. This factor serves as an approximation of the translation between the measurement of the incident fluence (irradiance) with a flat detector and the actual fluence rate measured with an isotropic probe touching the skin. Therefore we decided to take 2.5 times 10 J/cm^2 (flat detector) = 25 J/cm^2 (isotropic probe) as the central fluence and half and twice that fluence (12.5 and 50 J/cm^2) for the other 2 illumination fields. The highest total fluence was used on the field most distal to the animal's head, and the fluence decreased with more proximal location, thereby ensuring minimal

relative overlap between illumination fields.

To rule out fluence rate effects, the fluence rate was kept constant and the illumination time was varied to achieve different total fluences. The fluence rate was set at 400 mW/cm^2 as measured on the isotropic probe because this is the fluence rate we expected to find in the Photofrin treatment, based on *ex vivo* measurements (Murrer *et al* 1995). Using the 2.5 times build-up factor described above, this fluence rate is equivalent to an incident collimated irradiance of about 160 mW/cm^2, comparable to incident fluence rates commonly used in mTHPC and Photofrin protocols. Treatment times were 62.5, 125 and 250 seconds for the three fields.

The protocol for Photofrin (QLT/Lederle P 503/504) prescribes a light output of 400 mW per cm diffuser length used for a duration of 500 seconds, yielding a total of 200 J per cm diffuser length. In the acute experiment we applied this protocol in one of the three fields illuminated. The other two fields were illuminated with half and twice this energy viz. 100 and 400 J per cm diffuser length with the same output in mW of the diffuser. The variation in energy applied was achieved by varying the time of exposure, leading to treatment times of 250, 500 and 1000 seconds.

Again the field with the highest total fluence was chosen most distally to the head of the animal and the resulting fluence rate and total fluence on the probe were recorded. The measured total fluence was used to determine a total fluence for the follow-up part of the experiment. In the follow-up part, the fluence rate on the probe was set at $\approx$ 400 mW/cm^2 (the same as the mTHPC experiment) and then the illumination was continued until the desired total fluence was reached.

Build-up factor

Because of the scattering properties of the illuminated tissue, the fluence rate resulting from the illumination with the diffuser will be higher than the the incident fluence rate on the mucosa. For diffusers with good isotropic properties (as used in our applicator) the maximum incident fluence rate for central placement in the lumen ϕ_0 (mW/cm^2) can be calculated from (Murrer *et al* 1995):

$$\phi_0 = \frac{P}{\pi LD} \arctan(L/D) \tag{7.1}$$

with P the total output power of the diffuser (mW), L the length of the

diffuser (cm) and D the diameter of the trachea (cm). The build-up factor β is defined as the ratio of the measured fluence rate ϕ_{true} and the incident fluence rate,

$$\beta = \frac{\phi_{true}}{\phi_0} \tag{7.2}$$

and depends on the optical properties of the mucosa.

Treatment

The respiration tube (diameter 9 mm) was fixed just below the larynx to leave a maximum length of trachea exposed to be used for illumination. A fibre bronchoscope with a large working channel (diameter 2.8 mm, Fujinon Medical Holland) was introduced through the tube, and the applicator was fed through the working channel. During this procedure the artificial ventilation was maintained through the open space between the bronchoscope and the tube. After unfolding of the applicator the positioning of the detector was checked through the bronchoscope to ensure good contact with the mucosa and to ensure that there was no blood or mucus on the probe. The relative position of the applicator in the trachea was measured by the markings on the bronchoscope relative to the teeth of the animal. The larynx served as a reference for the zero position.

The applicator was fixed in the trachea such that the most proximal position was not too close to the tube to avoid reflections off the tube. In the case of the acute Photofrin treatment, the output of the diffuser was preset to a fixed output of 600 mW defined by the Photofrin protocol (1.5 cm diffuser x 400 mW/cm) and the time of exposure was measured. The resulting fluence rate and total fluence were recorded. In the other cases the laser was switched on and the output was adjusted such that the probe reading was 400 mW/cm^2, and kept at that level by adjusting the output if necessary. The treatment was halted when the desired total fluence was achieved. After the treatment the output of the applicator was measured, and the calibration of the probe was checked.

In the acute experiment half of the animals (1 Photofrin, 2 mTHPC) were sacrificed at 24 and the other half at 48 hours. In the follow-up experiment the animals were sacrificed after 14 days. On day 1, 3, 7, 10 and 14 the animals' tracheas were examined by bronchoscopy. In the case of excessive damage, the experiment was to be terminated earlier.

Precautions

Several precautions were taken to avoid damage related to non-treatment light. During transport to and from the operating theatre the animals were shielded from light with dark cloth. In the operating theatre only necessary lights were left on, and those were not directed at the animals. Also here the animals were covered with dark cloth. The bronchoscope's light source was operated on the lowest setting allowing good visual control of the situation. During treatment the light source was switched off entirely. The duration of of bronchoscopy with the light source on was kept to a minimum (1-2 minutes). During recovery after the experiments the animals were kept warm by cloth instead of using an infrared lamp.

Tissue damage assessment

The damage to the normal mucosa was inspected both visually and histologically. The appearance of the mucosa was either photographed or recorded on videotape in the live animal. Images of the mucosa before treatment were made to serve as a reference. In the acute experiment, images were made after 24 or 48 hours. Images were taken during each bronchoscopy in the follow-up experiment. The damage was scored according to: none/normal = 0, some/slightly increased = 1, much = 2.

After the experiment, the tracheas were excised and fixed in buffered formaldehyde (4%). After fixation, the material was cut and Heamatoxylin Eosin (HE) stained for histological analysis. Longitudinal strips of the whole trachea as well as rings from the centre of the treated areas were examined. The histological effects of the treatment were judged partly qualitatively (for example the nature of the inflammatory cells) and partly quantitatively (for example the number of inflammatory cells and the number of mucus producing cells in the epithelium). The damage was scored for a panel of histological characteristics according to no/none = 0, light/few = 1, severe/much = 2. Of these, the most relevant are discussed in the results.

mTHPC tissue level determination

Tissue samples were taken from the mTHPC treated animals after they were sacrificed at 6 and 20 days after injection (2 and 14 days after treatment). Samples were taken from the skin, trachea (cartilage and mucosa in one

sample) and oesophagus and were snap-frozen in liquid nitrogen for further processing. The method of determining the mTHPC tissue levels with High Performance Liquid Chromatography (HPLC) is described by Wang *et al* (1993).

Results

In table 1 an overview is given of the treatment parameters. The treatment sites are coded dist (distal) mid (middle) and prox (proximal) indicating their position relative to the larynx of the animal. For each animal the output of the applicator's diffuser is specified as well as the measured fluence rate and the total fluence as measured by the isotropic probe.

General Comments

The treatment and follow-up in the acute part of the experiment was conducted as planned without problems. In the follow-up experiment one animal (nr. 3) was excluded from the study because of technical problems during the illumination that led to uncertainty about the actual light dose delivered. Furthermore, animal 2 from the follow-up group had to be sacrificed earlier (day 10) because of damage to the skin of the belly of the animal. To the best of our knowledge, this damage was not PDT related because 3 other animals with the same drug dose that were housed and treated under exactly the same conditions showed no signs of this skin damage. Moreover, the mTHPC tissue levels of damaged and undamaged skin samples were not excessively high (10-50 ng/g, see section on mTHPC levels). Probably the animal was accidentally exposed to concentrated, alkaline detergent. Except for this incident, the general condition of all animals was good during the experiments.

Dosimetry

In the case of the acute Photofrin experiment the diffuser output was fixed and the fluence rate was measured and found to be stable within 5%, indicating good fixation of the diffuser and the isotropic probe. The output of the diffuser was checked afterwards and was found to be stable within 5%.

In the other situations were the output was varied to achieve a fluence rate of ≈ 400 mW/cm^2 the output of the diffuser could be adjusted within

nr	site	sensitizer	interval injection-treatment (days)	sacrificed on day	fluence rate (mW cm^{-2}) (± 15%)	output applicator (mW) (± 5%)	total fluence (J cm^{-2}) (± 15%)	diameter trachea (cm) (± 5%)	β (± 20%)
acute									
	dist	mTHPC	4	1	400	796	50	1.0	2.6
1	mid	mTHPC	4	1	400	796	25	1.0	2.6
	prox	mTHPC	4	1	400	507	12.4	1.3	5.4
	dist	mTHPC	4	1	400	859	50	0.9	2.0
2	mid	mTHPC	4	1	400	979	25	1.0	2.1
	prox	mTHPC	4	1	400	919	12.7	1.0	2.1
	dist	Photofrin	2	1	270	600	274	1.0	2.1
3	mid	Photofrin	2	1	257	600	133	0.8	1.6
	prox	Photofrin	2	1	330	600	79	0.9	2.4
	dist	mTHPC	4	2	400	1350	51	1.2	1.8
4	mid	mTHPC	4	2	400	1480	25	1.0	1.3
	prox	mTHPC	4	2	400	1220	12.6	1.2	2.0
	dist	mTHPC	4	2	400	1474	50	1.2	1.6
5	mid	mTHPC	4	2	400	1288	25	1.2	1.8
	prox	mTHPC	4	2	400	1165	12.7	1.2	2.0
	dist	Photofrin	2	2	188	600	190	1.2	2.0
6	mid	Photofrin	2	2	178	600	90	1.0	1.4
	prox	Photofrin	2	2	195	600	50	0.9	1.4
follow-up									
1		mTHPC	4	14	400	584	50	1.2	4.1
2		mTHPC	4	10†	400	605	50	1.1	3.7
3		Photofrin	2	-‡	-	-	-	-	-
4		mTHPC	4	14	400	468	50	1.1	4.7
5		mTHPC	4	14	400	620	50	1.2	4.1
6		Photofrin	2	14	375	450	65	1.0	3.9

Table 7.1: *Summary of the treatment parameters and light dosimetry. mTHPC dose was 0.15 mg/kg bodyweight, Photofrin dose 2 mg/kg bodyweight. †Sacrificed earlier because of non-PDT skin damage. ‡Excluded from the experiment because of uncertainty of the light dose applied. For further explanation see text.*

seconds after the start of the illumination to reach the desired level. Once this level was reached, only minor adjustments of the output ($\leq 5\%$) were needed to have a stable (within 5%) reading on the isotropic probe.

The diameters of the tracheas were measured in the microscopic slides and corrected for the 10% shrinkage due to fixation. The diameters were used to calculate the incident fluence rate and the build-up factor for every field illuminated. The average trachea diameter in the acute experiment was 1.06 (0.14[1]) cm and in the follow-up experiment the average diameter was 1.12 (0.08) cm, which is not significantly different despite the 12 or 13 days age difference between the two groups of animals.

There was no clear difference in β values between 630 ($\beta = 2.1(0.9)$) and 652 nm ($\beta = 2.6(1.2)$). There was a pronounced difference, however, in β values between the acute ($\beta = 2.1(0.9)$) and the follow-up group ($\beta = 4.1$ (0.4)), which also existed for the two separate wavelengths. The overall average β value found was 2.5(1.2) for all animals and wavelengths.

Visual damage score

During each bronchoscopy, an image of the treated areas was taken and the damage was described qualitatively by specifying the amount of red and white discoloration, oedema and increase of mucus formation on the mucosa. The scores indicated in table 2 give an indication of the entire field treated.

In the acute experiment, the most pronounced damage is found in the animals treated with Photofrin (3 and 6). All three fields illuminated showed redness and oedema in both animals, with slightly less damage at the proximal site were the lowest fluence was applied. There was no clear difference between the damage observed after 24 and after 48 hours. The mTHPC-treated animals (1,2,4 and 5) showed very little effect in all animals with all applied fluences. Some whitish discoloration of the tissue was found after 48 hours (animal 4 and 5), which was not seen at 24 hours. In animal 1 (after 24 hours) some mucus was observed.

In figure 1 bronchoscope images are shown of the areas treated with the highest fluences for both sensitisers, taken 24 hours after treatment. In the image taken in the Photofrin treated animal the red discoloration (hemorrhage, see histology), swelling (oedema) and some excess mucus formation are clearly visible (fluence 274 J/cm^2). The image of the mTHPC trea-

[1]standard deviation in parentheses

acute

sacrificed after	1 day									2 days								
animal	**1**			**2**			**3**			**4**			**5**			**6**		
sensitiser	mTHPC			mTHPC			Photofrin			mTHPC			mTHPC			Photofrin		
site	D	M	P	D	M	P	D	M	P	D	M	P	D	M	P	D	M	P
redness	0	0	0	0	0	0	2	2	1	0	0	0	0	0	0	2	2	1
whiteness	0	0	0	0	0	0	0	0	0	1	1	1	1	1	1	0	0	0
oedema	0	0	0	0	0	0	2	2	1	0	0	0	0	0	0	2	2	1
mucus	1	1	1	0	0	0	1	1	1	0	0	0	0	0	0	1	1	1

follow-up

animal	**1**					**2†**					**3‡**				
sensitiser	mTHPC					mTHPC					Photofrin				
day	1	3	7	10	14	1	3	7	10	14	1	3	7	10	14
redness	0	0	0	0	0	0	1	0	0	-	-	-	-	-	-
whiteness	0	0	0	1	0	0	0	0	0	-	-	-	-	-	-
oedema	0	0	0	0	0	0	0	0	0	-	-	-	-	-	-
mucus	0	0	1	1	0	0	0	1	0	-	-	-	-	-	-
animal	**4**					**5**					**6**				
sensitiser	mTHPC					mTHPC					Photofrin				
day	1	3	7	10	14	1	3	7	10	14	1	3	7	10	14
redness	1	0	0	0	0	0	0	0	1	0	0	1	0	0	0
whiteness	0	0	0	0	0	0	0	0	0	0	0	0	0	0	0
oedema	0	1	0	0	0	0	1	0	1	0	0	0	1	0	0
mucus	0	1	0	0	0	0	1	0	0	0	0	1	0	0	1

Table 7.2: *Visual damage score for acute and follow-up experiment. 0 = none/normal, 1 = some/slight increase, 2 = much, – = not available. D = distal, M = middle, P = proximal. †Sacrificed on day 10 because of (non-PDT) skin damage. ‡Excluded from experiment because of unreliable dosimetry.*

ted animal (fluence 50 J/cm^2) shows mucosa with the same appearance as before treatment.

An overview of the tracheas treated with three fluences and excised and fixed 48 hours after treatment is presented in figure 2. The Photofrin treated trachea shows three bands of dark discolouration, indicating areas were hemorrhage has occurred. The width of the dark areas is (left to right) 2.5, 2 and 1.5 cm for fluences of 190, 90 and 50 J/cm^2, respectively. The trachea of the Photofrin treated animal that was sacrificed after 24

Photofrin

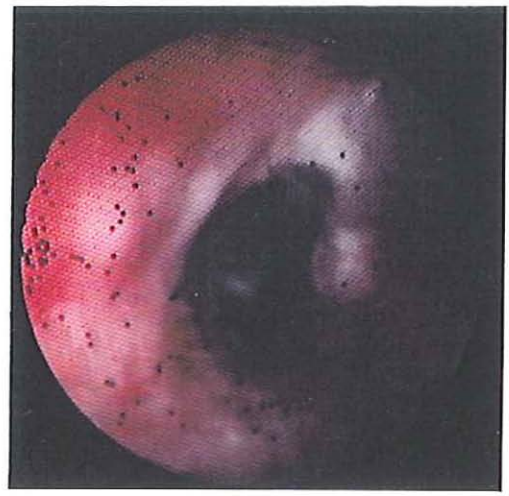

mTHPC

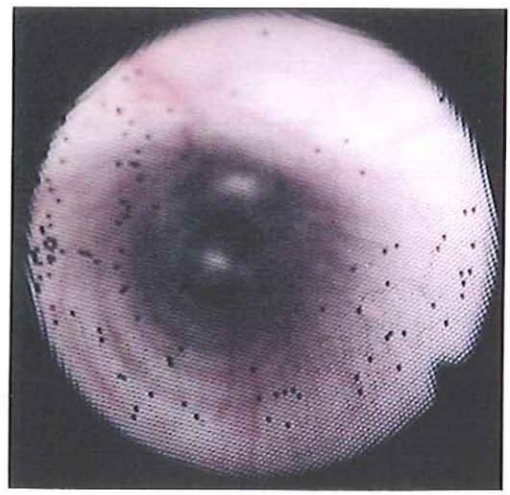

Figure 7.1: *Bronchoscope image of the part of the trachea illuminated with the highest fluence for both sensitisers taken 24 hours after treatment. Top: Photofrin treatment with 274 J/cm^2 (630 nm). Bottom: mTHPC treatment with 50 J/cm^2 (652 nm). The black dots in both pictures are bronchoscope imaging artefacts.*

hours also showed dark discolourated areas for the middle (133 J/cm^2) and high (271 J/cm^2) fluences, although not as sharply demarcated as in the animal sacrificed after 48 hours. No clear region of damage was observed for the lowest fluence (79 J/cm^2). The mTHPC treated tracheas showed no macroscopical treatment effects, the appearance is quite comparable to that of a normal, untreated trachea (see figure 2).

In the follow-up experiment the overall damage observed visually was mild (as intended). The mTHPC-treated animals showed some whitish discoloration and mucus on different days of the follow-up varying from day 3 to day 10. On day 14 the situation was normal again. The Photofrin-treated animal showed some redness on day 3 and some oedema on day 7 (probably non-specific because of the long time span after illumination). On day 14 the situation had returned to normal, apart from some mucus formation.

Histology

The major changes in histology are summarised in table 3, and some examples of the histology are shown in figure 3. No systematic inter-animal variations were observed. A slight chronic inflammation was present directly beneath the epithelium (lamina propria) in all animals and was considered as non-specific. For all experiments the changes were limited to the trachea lining epithelium (lamina propria) and the submucosa. The cartilage or deeper tissues were not affected in any of the groups, except for fluence independent circumscript mononuclear infiltrates that were found in the oesophageal glands in 2 of 3 mTHPC and 0 of 1 Photofrin treated animals in the acute experiment (of 1 mTHPC and 1 Photofrin animal no oesophageal tissue was available in the acute part). In the long-term study oesophageal glands of 0 of 4 mTHPC and 2 of 2 Photofrin animals were found to contain these infiltrates.

Changes of the respiratory epithelium of the trachea consisted of increasing seriousness of loss of mucus producing cells, diminishing number of nuclear rows, flattening of the cells, loss of cilia and denudation and influx of PolyMorphoNuclear(PMN) cells. The seromucinous submucosal glands lining the trachea were also involved in therapy related damage. They showed an increase of infiltrating mononuclear cells and, immediately after treatment, of PMN cells. Loss of mainly mucinous cells, flattening of the epithelial cells and widening of acini is referred to as atrophy of submucosal glands. Mainly the deep submucosal blood vessels (near the cartilage) showed hyperemia. Damage of blood vessels in the lamina propria and submucosa

Photofrin

mTHPC

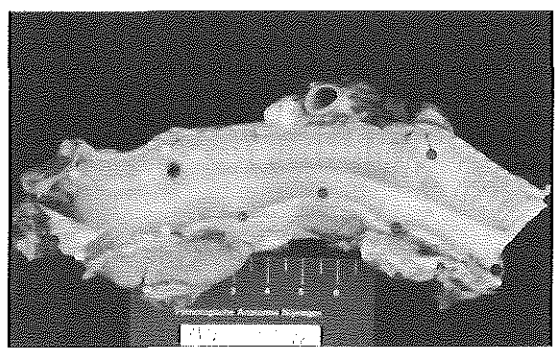

Figure 7.2: *Overview picture of the dissected and fixed tracheas of animals sacrificed 48 hours after treatment. The tracheas were cut lengthwise and opened. The larynx was located at the right side. Top: Photofrin treatment with (left to right) 190, 90 and 50 J/cm^2 (630 nm). Bottom: mTHPC treatment with (left to right) 50, 25 and 12.4 J/cm^2 (652 nm).*

sensitiser	mTHPC								Photofrin							
sacrificed after (days)	1			2			14		1			2			14	
total fluence (J/cm^2)	50	25	12.5	50	25	12.5	50	c	274	133	79	190	90	50	65	c
epithelium																
reduction of mucus producing cells	0/1	1/1	1/2	2/0	2/1	2/2	0/1/1/1	0/0/0/0	2	2	2	2	2	2	1	0
acute inflammation	0/0	0/0	0/1	1/0	1/1	1/1	2/0/1/1	1/0/0/1	1	1	2	0	1	1	0	0
submucosa																
acute inflammation	1/1	1/2	2/2	1/0	1/1	1/1	1/1/1/1	0/0/0/0	1	1	2	2	2	2	0	0
oedema	1/1	2/1	2/0	1/1	2/1	1/1	1/1/0/0	0/0/0/1	2	2	1	2	2	1	0	0
hyperemia	0/0	0/0	0/0	0/0	0/0	0/0	0/2/0/1	1/0/0/1	2	2	0	2	2	1	1	2
damage of blood vessels	1/0	1/0	0/0	0/0	0/0	0/0	0/1/0/0	0/0/0/0	2	2	1	2	2	0	0	0
atrophy of submucosal glands	1/0	1/1	0/2	1/1	2/1	2/1	0/2/0/1	0/0/0/0	2	2	2	1	1	2	1	1
acute inflammation of submucosal glands	0/1	0/1	1/2	1/0	2/1	2/1	0/0/0/0	0/0/0/0	1	0	2	1	1	2	0	0
fibrosis	0/0	0/0	0/0	0/0	0/0	0/0	0/1/0/1	0/0/0/0	0	0	0	0	0	0	1	0

Table 7.3: *Histological damage scores for acute and follow-up experiment. no/none = 0, light/few = 1, severe/much = 2. Control values c are taken from sites in a treated trachea which received little or no light (distance from illumated area $\geq$ 10 cm).*

Photofrin, 190 J/cm^2, Acute

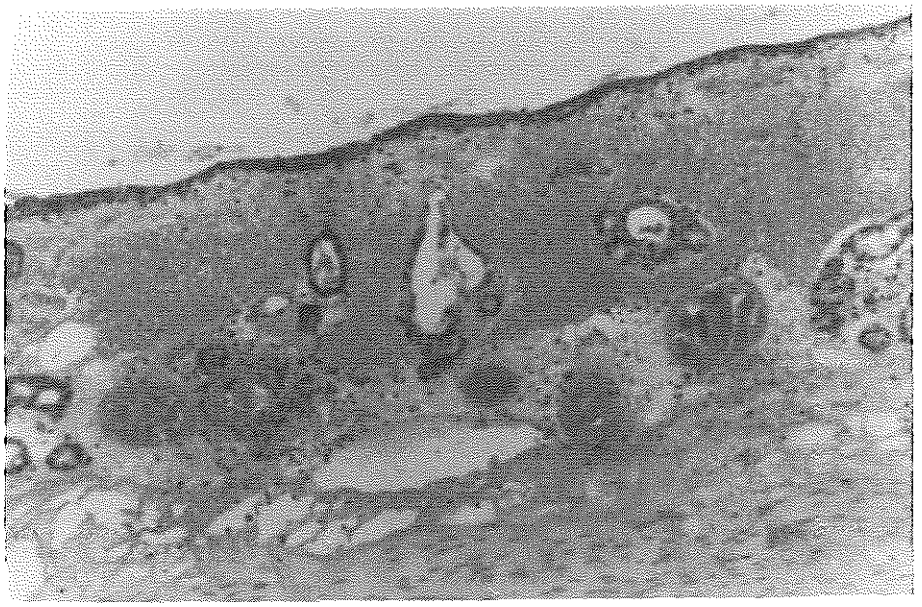

mTHPC, 25 J/cm^2, Acute

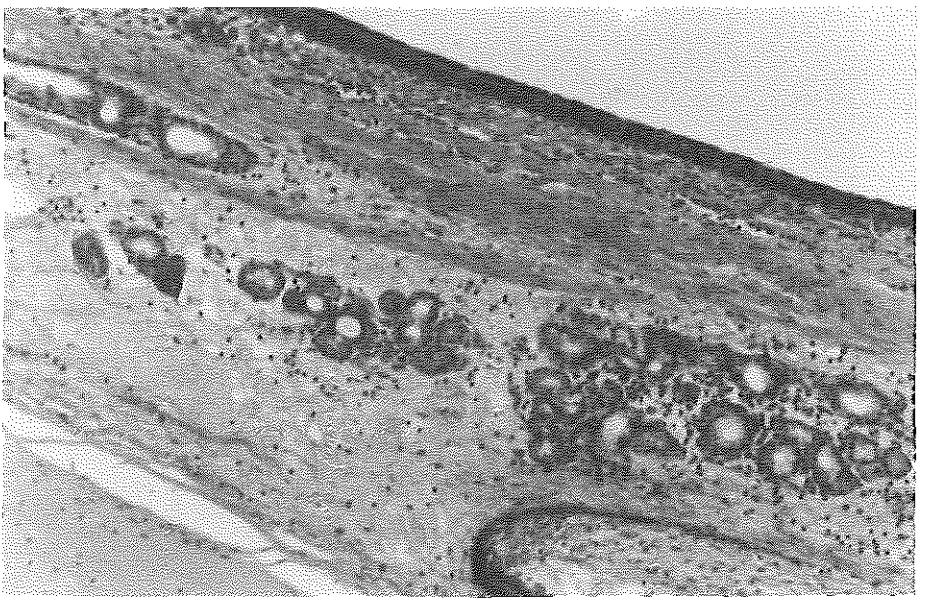

mTHPC, 50 J/cm^2, Follow-up

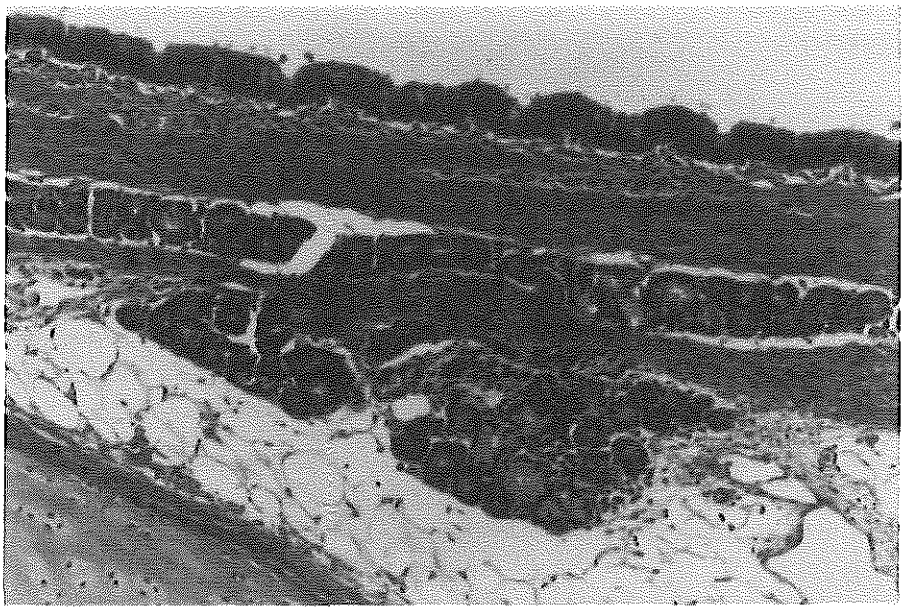

Figure 7.3: *Histological slides of the acute and the follow-up experiment (HE stained).* **Top***: Damage to the trachea 48 hours after illumination of a Photofrin injected animal with a fluence of 190 J/cm^2. The epithelium is atrophic. The submucosal glands and blood vessels are damaged and surrounded by oedema. PMN cells are absent, only sporadic mononuclear cells are seen. (Magn. 25x)* **Middle***:Damage 48 hours after illumination (mTHPC, 25 J/cm^2). The epithelium shows loss of mucus producing cells. In the submucosa some oedema and a slight diffuse infiltration of mononuclear cells is seen. The glands show slight atrophic changes. (Magn. 100x)* **Bottom***: Damage 2 weeks after illumination (mTHPC, 50 J/cm^2). The trachea appears normal, with epithelium containing mucus producing cells, seromucinous glands without atrophy and only slight focal infiltration with mononuclear cells as is seen in the control tissues. Fibrosis is lacking.(Magn. 100x)*

consisted of frank destruction of endothelium (nuclear debris and disappearance of endothelium without inflammatory reaction) and stasis. Only very small areas with accumulation of coarse collagen bundles were seen occasionally near the submucosa at 2 weeks after irradiation.

mTHPC

In the dose finding experiment no clear correlation between the applied fluence and severity of changes was observed in the mTHPC group. A quite intense inflammatory reaction with oedema and infiltrating PMN cells was seen in the lamina propria and submucosa for all fluences at day 1 after treatment, while the epithelium showed a slight or focal decrease of mucus producing cells without signs of acute inflammation. In one animal the submucosal blood vessels showed very slight damage. At 2 days after treatment, inflammation and oedema were less while mucus producing cells were almost lacking in the epithelium.

In the follow-up experiment the changes in the treated part of the trachea compared to the untreated (table 3) part were only slight and could be found only in some animals. The changes consisted only of minor loss of mucus producing cells in the epithelium and submucosal glands combined with slight acute inflammation with some oedema of the submucosa and some hyperemia. Small areas of fibrosis were found in the submucosa of 2 of 4 animals.

Photofrin

All treated areas in the Photofrin treated animals showed an immediate severe denudation of the epithelium and loss of mucus producing cells that persisted during the second day of treatment. At both 1 and 2 days after treatment the high fluences caused severe vascular damage in the lamina propria and submucosa with stasis, fragmentation of endothelial nuclei, karyolysis and severe oedema. These severe vascular changes were not observed in mTHPC treated animals. One day after treatment a surprisingly slight infiltration of PMN cells was seen in the Photofrin treated animals. Only at day 2 the acute inflammation was severe in all irradiated fields. Two weeks after the treatment with 65 J/cm^2 little difference was seen between the irradiated spot and the control area. (The control spot of the Photofrin treated animal that was excluded from the experiment showed the same characteristics). A slight loss of submucosal glands and a small

area of fibrosis were found in the submucosa of the treated spot.

Applied fluences for the follow-up experiment

The fluences used in the follow-up experiment were 50 J/cm^2 and 65 J/cm^2 for mTHPC and Photofrin, respectively. The fluences with potentially recoverable damage were chosen based on the effects observed in the acute experiment, with the observed visual and histological damage as a guideline.

For the mTHPC treatment the highest applied fluence of the acute experiment was used, because both visually and histologically no severe effects (such as blood vessel damage) were observed. The Photofrin fluence was chosen as an average of the lowest dose applied in both animals in the acute experiment. In this fluence range severe effects started to show as a dark band of hemorrhage with 79 J/cm^2 in the first and no such area in the second animal with a fluence of 50 J/cm^2. Histologically these dark bands are the result of hyperemia, severe damage to blood vessels and oedema.

mTHPC tissue levels

The levels of mTHPC were determined in trachea, oesophagus and belly skin samples, the data are shown in figure 4. The trachea sample (ring height: 5 mm) was taken from a distal part that received little or no light, and included cartilage as well as mucosa. The oesophagus sample was taken from the same region (section of 5 mm). The average value for the mTHPC level in the trachea is 44 ng/g (n=2) at 6 days and remains at a level of 46 ng/g (n=3) at 20 days after injection. The oesophagus level decreases from 46 ng/g (n=2) at 6 days to 20 ng/g (n=3) at 20 days. The skin drug level at 6 days was highly variable with a value of 358 and 44 ng/g for two different animals. The level at 14 days is more consistent at 18 ng/g (n=3), comparable to the oesophagus level.

Discussion

Normal tissue damage with Photofrin and mTHPC

During the acute experiment we observed a distinct difference in normal tissue damage between the Photofrin and mTHPC treatment. The fluences

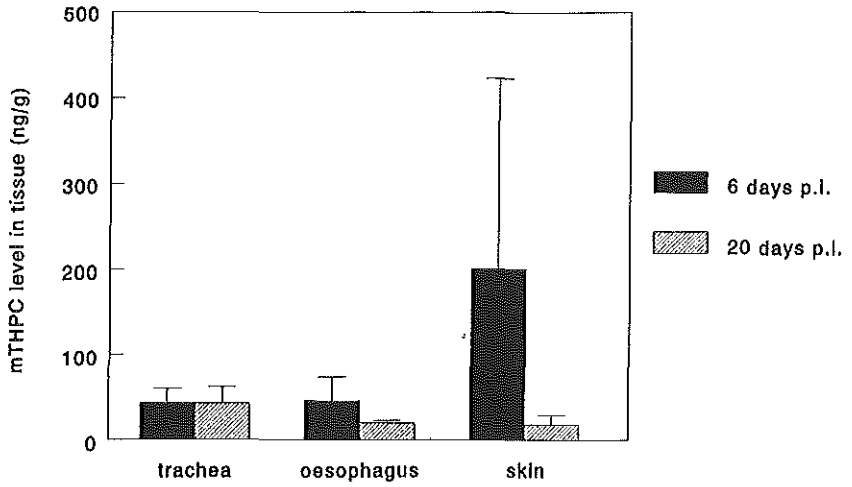

tissue type mTHPC concentration	trachea (ng/g)	oesophagus (ng/g)	skin (ng/g)
6 days after injection	55/33	26/66	358/44
20 days after injection	63/26/39	20/17/22	9/14/30

Figure 7.4: *mTHPC levels of pig tissues, taken from animals sacrificed 2 days (animals acute 4 and 5) and 14 days after treatment (animals follow-up 1, 4 and 5).*

used where based on values used for treatment of tumours in clinical practice were excessive normal tissue damage is to be avoided. Therefore such a distinct difference was not expected. It must be noted that the fluence used in the clinical QLT/Lederle Photofrin protocol was poorly defined because it only specifies the output of the linear diffuser irrespective of the lumen diameter and the optical properties of the mucosa. The mTHPC total flu-

ences chosen in this study were comparable to those employed by Savary *et al* (1994), who used fluences up to 16 J/cm^2 of *incident* light, roughly comparable with the 50 J/cm^2 *total* fluence we used (with the conversion factor 2.5, see methods). Photofrin protocols for the treatment of skin lesions use total irradiances (*incident* fluences) of 50-100 J/cm^2 or higher (Wilson *et al* 1992) with acceptable normal tissue response. With the conversion factor of 2.5 this indicates a fluence range of 125-250 J/cm^2. These fluences are somewhat higher than the total fluences we measured for the illuminated fields treated according to the QLT/Lederle protocol , viz. 133 and 90 J/cm^2 (mid sections in the acute animals 3 and 6). In these fields considerable normal tissue damage was observed at fluences that induce no severe side-effects in the treatment of skin lesions. Obviously, the light dosimetric conversion is just one aspect to take into account when adapting a protocol written for a specific target for use in an other organ.

In the mTHPC fluence finding experiment no clear correlation between the applied fluence and the normal tissue damage was observed. The fluence range that was investigated might be below threshold for the induction of significant effects. Abramson *et al* (1994) observed an such illumination threshold for the induction of oedema and erythema in the canine larynx. Unfortunately, the absolute fluence levels of Abramson's study and the present work cannot be compared because the former only specifies the diffuser output.

The fluences applied in the follow-up experiment did not induce severe long-term effects (14 days) as could be observed visually as well as histologically. This result suggests that, while treating a lesion in the trachea, the normal (sub)mucosa of the trachea of the pig can withstand a fluence of $\approx$ 50 J/cm^2 for both sensitisers for the drug dose and interval between injection and treatment used here. The maximum tolerable fluence for mTHPC might be even higher, as we tested the highest fluence from the acute experiment in the follow-up experiment. 50 J/cm^2 fluence can be compared (with the reservations noted above) to an incident irradiation of $\approx$ 20 J/cm^2, which is already a relatively high 'light dose' for skin treatments.

One has to bear in mind, however, that the presence of (pre-)malignant tissue can alter the pharmacokinetics locally and alter the sensitivity of the surrounding tissue to PDT. The pharamacokinetics could be monitored *in vivo* by a fluorescence measurement to evaluate the influence of the presence of malignant tissue (Braichotte *et al* 1996, Monnier *et al* 1990). A pig tumour model in the trachea could give more insight in this matter, possibly the technique used by Hayata *et al* (1983) to induce an invasive squamous

cell carcinoma in a canine model could be used in the pig also.

For both sensitisers and all fluences employed, the damage was limited to the mucosa and the submucosa and did not extend into or beyond the cartilage. The cartilage structure contains little blood and has therefore a low oxygen and photosensitiser content (Lofgren *et al* 1994), and is relatively insensitive to photodynamic therapy. Lofgren observed a concentration of 10 ng/g of mTHPC in the cartilage as opposed to 80 ng/g in the mucosa of the canine larynx, 6 days after injection of 0.3 mg/kg mTHPC.

Vascular effects

Irreversible vascular damage was observed in the acute Photofrin experiment. This damage may explain the fact that the influx of PMN cells (acute inflammation) seems delayed for the highest fluence rates used. At day 1, only for the lowest fluence applied an extensive influx of PMN cells is seen, while for the areas treated with higher fluences severe inflammation only occurs at day 2 (Table 3).

Also with mTHPC vascular effects have been reported (Lofgren *et al* 1994). In our study, vascular effects seem slight and reversible. Contrary to the Photofrin findings, PMN cell infiltration was at its maximum on day 1 and reduced on day 2. This suggests vascular spasm instead of destruction of the vasculature as seen in the Photofrin animals.

Fluorescence imaging after injection of mTHPC shows that the drug content of vascular endothelium reaches a peak at 96 hours and then decreases again (Savary *et al* 1997, Andrejevic *et al* 1996). However, Menezes da Silva *et al* (1995) showed that most extensive vascular occlusion after illumination occurred at 11 hours after mTHPC injection, independently of the blood serum level (peak at 3 hours). Their explanation is that vascular damage must result from damage to other cells than endothelial cells. Our illuminations were performed much later (96 hours) than this time point of maximum vascular sensitivity to mTHPC-PDT, thus possibly explaining the lacking of irreversible vascular damage in our study.

mTHPC tissue levels

The level of mTHPC in the trachea was determined from samples containing both the mucosa and the cartilage. From the fact that the cartilage contains little mTHPC (Lofgren *et al* 1994) it can be concluded that the levels in

the mucosa only, are higher than those indicated in figure 4. The fact that the mTHPC level in the trachea stays at the same level between 6 and 20 days after injection indicates that the day of treatment can be chosen over a long period of time (assuming that the ratio of the cartilage/mucosa levels does not change).

Dosimetry: the build-up factor β

The β-values found in the experiment are lower than the values found in previous *ex vivo* experiments (Murrer *et al* 1995), and this can be attributed to the absence of blood in the *ex vivo* experiment. The blood in the mucosa in the *in vivo* situation increases the absorption of the treatment light, thereby lowering the build-up factor. The β-values found in this experiment agree with those reported in earlier *in vivo* experiments on pigs , while β values in human volunteers are higher (average 4.7, sd 2.2, n=3)(Murrer *et al* 1997).

The β-values show large inter-animal variations (average 2.5, standard deviation 1.2), as was also observed in measurements in humans (Murrer *et al* 1997). This shows the necessity of *in situ* fluence rate measurements to assure equal illumination conditions. The presence of tumour tissue in the trachea may alter the dosimetry. Lesions often present as a region of whitish discoloration, representing areas with relatively low absorption of light, causing a locally higher build-up factor. Hemorrhages (or blood vessels located near the mucosa surface) induce locally increased absorption and consequently a lower build-up factor. These influences of local 'colour' are reflected in the intra-animal variations in β (table 1).

The difference in β between the acute and the follow-up group (for both wavelengths) may be caused by variations in the oxygenation of the blood of the animals. The absorption of the light by the blood depends on the oxygenation of the blood (Cheong *et al* 1990), which is influenced by the anaesthesia. The anesthesia during the two parts of the experiments was conducted by different operators, which may explain the variations.

Acknowledgments

The authors wish to thank Joos Heisterkamp, Enno Collij, Rob Meijer, Henk Bronk and Roy Spruyt at the Laboratory of Experimental Surgery as well as Otto Speelman, Dennis Francois and Ronald van Loon for support

during the experiments. Scotia Quantanova and QLT are acknowledged for generously supplying the photosensitisers (mTHPC and Photofrin, respectively). Jerry van der Ploeg and Edward Donkersloot are greatly acknowledged for the construction of the bronchus applicators. The histological sections were prepared at the department of pathology of he St. Radboud University Hospital Nijmegen. The mTHPC tissue levels were determined at the lab of Dr. Lim of the MRC Toxocology Unit, University of Leicester (UK). This work was supported by the Dutch Cancer Society, grant DDHK 93-615.

References

1. Abramson A L, Lofgren L A, Ronn A M, Nouri M, Steinberg B M. (1994) Treatment effects of *meta*-tetra-(hydroxyphebyl)chlorin on the larynx. *New approaches to cancer treatment: unsaturated lipids and photodynamic therapy 142-147 Ed. D.F. Horrobin, Churchill Communications Europe, London*

2. Andrejevic S, Savary J-F, Monnier P, Fontolliet C, Braichotte D, Wagnières G, van den Bergh H. (1996) Measurements by fluorescence spectroscopy of the time-dependent distribution of meso-tetra-hydroxyphenylchlorin in healthy tissues and chemically induced "early" squamous cell carcinoma of the Syrian hamster cheek pouch. *Photochem. Photobiol. B* **36** *143-151*

3. Braichotte D, Savaray J-F, Glanzmann T, Monnier P, Wagnières G, van den Bergh H. (1996) Optimizing light dosimetry in photodynamic therapy of the bronchi by fluorescencè spectroscopy. *Lasers Med. Sci.* 11 *247-254*

4. Cheong W F, Prahl S A, Welch A J. (1990) A review of optical properties of biological tissues. *IEEE J. Quantum Electron.* **26(12)** *2166-2185*

5. Cortese D A, Edell E S, Kinsey J H. (1997) Photodynamic Therapy for early stage squamous cell carcinoma of the lung. *Mayo Clin. Proc.* **72** *595-602*

6. D'Hallewin M A, Baert L, Marijnissen J P A, Star W M. (1992) Whole bladder wall photodynamic therapy with *in situ* light dosimetry for carcinoma *in situ* of the bladder. *J. Urol.* **148** *1152-1155*

7. (1996) Grosjean P, Savary J-F, Wagnières G, Mizeret J, Woodtli A, Thuemann J-F, Fontolliet C, van den Bergh H, Monnier P. Tetra(m-hydroxyphenyl)chlorin clinical photodynamic therapy of early bronchial and oesophageal cancer. *Lasers Med. Sci.* 11 *227-235*

8. Hayata Y, Kato H, Konaka C, Hayashi N, Tahara M, Saito t, Ono J. (1983) Fiberoptic bronchoscopic photoradiation in experimentally induced canine lung cancer. *Cancer* **51** *50-56*

9. Hayata Y, Kato H, Furuse K, Kusunoki Y, Suzuki S, Mimura S. (1996) Photodynamic therapy of 168 early stage cancers of the lung and oesophagus: a Japanese multi-center study. *Lasers Med. Sci.* **11** *255-259*

10. Hudson E J, Stringer M R, Cairnduff F, Ash D V, Smith M A. (1994) The optical properties of skin tumours measured during superficial photodynamic therapy. *Lasers Med. Sci.* **9** *99-103*

11. Lam S. (1994) Photodynamic therapy of lung cancer. *Seminars in Oncology* **21** *No 6 Suppl 15 15-19*

12. Lofgren L A, Ronn A M, Abramson A L, Shikowitz M J, Nouri M, Lee C J, Batti J, Steinberg B M. (1994) Photodynamic therapy using m-Tetra-(HydroxyPhenyl)Chlorin: an animal model. *Arch. Otolaryngol. Head Neck Surg.* **120** *1355-1362*

13. Marijnissen J P A, Baas P, Beek J F, van Moll J H, van Zandwijk N, Star W M. (1993) Pilot study on light dosimetry for endobronchial photodynamic therapy. *Photochem. Photobiol.* **58** *92-98*

14. Marijnissen J P A, Star W M. (1996) Calibration of isotropic light dosimetry detectors based on scattering bulbs in clear media. *Phys. Med. Biol.* **41** *1191-1208*

15. McCaughan J S, Hawley P C, Bethel B H, Walker J. (1988) photodynamic therapy of endobronchial malignancies. *Cancer* **62** *691-701*

16. Menezes da Silva F A, Newman E L. (1995) Time-dependent photodynamic damage to blood vessels: correlation with serum photosensitizer levels. *Photochem. Photobiol.* **61** *414-416*

17. Monnier P, Savary M, Fontolliet C, Wagnières G, Chatelain A, Cornaz P, Depeursinge C, van den Bergh H. (1990) Photodetection and photodynamic therapy of 'early' squamous cell carcinomas of the pharynx, the oesophagus and the tracheo-bronchial tree. *Lasers Med. Sci.* **5** *149-168*

18. Murrer L H P, Marijnissen J P A, Star W M. (1995) *Ex vivo* light dosimetry and Monte Carlo simulations for endobronchial photodynamic therapy. *Phys. Med. Biol.* **40** *1807-1817*

19. Murrer L H P, Marijnissen J P A, Star W M. (1996) Light distribution by linear diffusing sources for photodynamic therapy. *Phys. Med. Biol.* **41** *951-961*

20. Murrer L H P, Marijnissen J P A, Baas P, van Zandwijk N, Star W M. (1997) Applicator for light delivery and in situ light dosimetry during endobronchial photodynamic therapy: first measurements in humans. *Lasers Med. Sci.* **12** *253-259*

21. Murrer L H P, Marijnissen J P A, Star W M. (1997a) Improvements in the design of linear diffusers for photodynamic therapy *Phys. Med. Biol.* **42** *1461-1464*

22. Savary J-F, Monnier P, Wagnières G, Braichotte D, Fontolliet C, van den Bergh H. (1994) Preliminary clinical studies of photodynamic therapy with mesa-tetrahydroxyphenyl chlorin (m-THPC) as a photosensitising agent for the treatment of early pharyngeal, oesophageal and and bronchial carcinomas. *Proc. Spie* **2078** *330-340*

23. Savary J-F, Monnier P, Fontolliet C, Mizeret J, Wagnières G, Braichotte D, van den Bergh H. (1997) Photodynamic therapy for early squamous cell carcinomas of the esophagus, bronchi, and mouth with m-Tetra(Hydroxyphenyl) Chlorin. *Arch. Otolaryngol. Head Neck Surg.* **123** *162-168*

24. van Staveren H J, Marijnissen J P A, Aalders M C G, Star W M. (1995) Construction, quality control and calibration of spherical isotropic fibre-optic light diffusers. *Lasers Med. Sci.* **10** *137-147*

25. Wang Q, Altermatt H J, Ris H B, Reynolds B, Stewart J C M, Bonnet R, Lim CK. (1993) Determination of 5,10,15,20-tetra-(m-hydroxyphenyl)chlorin in tissues by high performance liquid chromatography. *Biomed. Chromatogr.* **7** *155-157*

26. Wilson B D, Mang T S, Stoll H, Jones C, Cooper M, Dougherty T J. (1992) Photodynamic therapy for the treatment of basal cell carcinoma. *Arch. Dermatol.* **128** *1597-1601*

Chapter 8

Photodynamic Therapy as Adjuvant Therapy in Surgically Treated Pleural Malignancies

(1997) Br. J. Cancer **76** *819-826*

P. Baas[1], L. Murrer, F.A.N. Zoetmulder[2], F.A Stewart[3], H.B. Ris[4], N. van Zandwijk[1], J.L. Peterse[1], E.J.Th Rutgers[2]

The Netherlands Cancer Institute, Dept of Medical Oncology[1], Oncological Surgery[2] and Experimental Therapy[3]. Department of Thoracic Surgery[4], Inselspital, Berne, Switzerland.

Abstract

Five patients with a pleural malignancy (4 malignant mesotheliomas and one localised low grade carcinoid) were treated with maximal surgical resection of the tumour followed by intra-operative adjuvant photodynamic therapy (PDT). The additional photodynamic treatment was performed with light of 652 nm from a high power diode laser, and meta-tetrahydroxy phenylchlorin (mTHPC) as the photosensitiser. The light delivery to the thoracic cavity was monitored by in situ isotropic light detectors. The position of the light delivery fibre was adjusted to achieve optimal light distribution, taking account of reflected and scattered light in this hollow cavity. There was no 30 day postoperative mortality and only one patient suffered from a major complication (diaphragmatic rupture and haematopericardium). The operation time was increased by a maximum of one hour to illuminate the total hemithoracic surface with 10 J/cm^2 (incident and scattered light). The effect of the adjuvant PDT was monitored by examination of biopsies taken 24 hours after surgery under thoracoscopic guidance. Significant damage, including necrosis, was observed in the marker lesions with remaining malignancy, compared to normal tissue samples which showed only an infiltration with PMN cells and oedema of the striated muscles cells. Of the five patients treated, four are alive with no signs of recurrent tumour with a follow-up of 9-11 months. One patient was diagnosed to have a tumour dissemination in the skin around the thoracoscopy scar and died of abdominal tumour spread. Light delivery to large surfaces for adjuvant PDT is feasible in a relatively short period of time (<1 hour). In situ dosimetry ensures optimal light distribution and allows total doses (incident plus scattered light) to be monitored at different positions within the cavity. This combination of light delivery and dosimetry is well suited for adjuvant treatment with PDT in malignant pleural tumours.

Introduction

Pleural tumours, especially malignant mesothelioma (MM) are considered to be incurable since at diagnosis the disease is usually advanced and spreads diffusely in the pleural space. Radical resections can seldom be performed. Macroscopically the resection may appear complete but microscopically tumour cells are often evident (Butchart and Gibbs, 1990). For those cases which are considered surgical candidates, adjuvant treatments have mostly been given in the form of radiation therapy (DaValle *et al* , 1986;

Hilaris *et al* , 1984) and chemotherapy (Rusch *et al* , 1994; Sugarbaker *et al* , 1991). Despite some positive results from these studies, overall survival was not significantly improved, whereas side effects were increased. Irradiation of a large field including organs like the spinal cord, heart, oesophagus and liver makes it difficult for the radiation oncologist to give an adequate radiation dose without exceeding normal tissue tolerance. Chemotherapy has so far shown to be of only limited use in the primary treatment of malignant mesothelioma (Chahinian *et al* , 1982,1993; Sfrensen *et al* 1985; Krarup-Hansen and Hansen, 1991; Ruffie, 1993), but the most active compounds (e.g. doxorubicin) might be of use for the treatment of minimal residual tumour. Postoperative chemotherapy is, however, associated with liver and kidney toxicity and it may be difficult to achieve adequate drug concentration in the areas with reduced perfusion after resection.

Photodynamic therapy (PDT) has been used by several investigators as an adjuvant treatment for MM but in most cases the conditions were not optimal (Pass *et al* , 1994; Lofgren 1991; Takita *et al* , 1994; Ris *et al* , 1991, 1996). Lack of high power lasers and effective photosensitisers with a high singlet oxygen yield, plus a lack of knowledge of the dosimetric aspects of light distribution and scattering in a hollow cavity, limited the general usefulness of this form of treatment. Haematoporphyrin derivatives were used in most studies but the excitation wavelength (630 nm) has only a limited penetration in tissue and the singlet oxygen yield is low for these sensitisers. Ris and colleagues (1996) were the first to publish a study using a second generation photosensitiser, m-THPC (meta-tetrahydroxyphenylchlorin), for the treatment of MM. m-THPC has a longer excitation wavelength (652 nm), resulting in somewhat better tissue penetration, and a much higher singlet oxygen yield than haematoporphyrin derivative sensitisers. One potential problem in this study was that the light was administered sequentially to fields in the thoracic cavity by using a cut-off fibre and microlens. This technique inevitably resulted in overlapping illumination fields. In addition, no account was taken of the contribution of scattered light to the total light dose. The doses quoted, based on incident light alone, will therefore be an underestimate of the light dose to tissues in the illuminated cavity.

In this feasibility study we have tested a new method of light application using a high power diode laser and real time, in situ measurement of light delivery to the tissue in the thoracic cavity after macroscopically complete resection of the tumour.

Material and Methods

Patient selection

In the period of January to June 1996, patients with a histological diagnosis of malignant mesothelioma were asked to participate in this study. In addition to extensive surgical and pulmonary work up they had to fulfil the following criteria: Performance Status <1 (ECOG), age < 75 year, weight loss < 10 % in the preceding three months, adequate cardiac function to accept a pneumonectomy and a calculated pulmonary rest capacity of > 1 l/sec expiration after resection. The surgical work up consisted of a CT scan to exclude possible ingrowth in major organs like the vertebrae, the heart and lymph nodes. All patients had a thoracoscopic examination and mediastinoscopy for optimal diagnosis and staging. The new staging criteria according to the IMIG (International Mesothelioma Interest Group) were used (1995). Patients with positive lymph nodes at mediastinoscopy or distant metastasis were excluded from the study. Details of patient and tumour characteristics are given in table 1.

Surgical procedure

Patients were selectively intubated by a double lumen tube and placed in a lateral decubites position. The previous entrance port of thoracoscopy or thoracotomy was excised and an extra pleural resection was initiated. To reduce the chance of sunburn by the theatre lights, these were out of focus and the normal skin was completely covered by sheets. The pleural tumour was resected extra-pleurally on the side confined to the ribs and mediastinum; resection of tumour from the pericardium and the diaphragm was more difficult. To facilitate the pleural resection and to limit blood loss, a CUSA (Cavitron Ultrasound Surgical Aspirator) was used. In patients with extensive involvement of the visceral pleura a pneumonectomy was performed. The surgical aim was to achieve macroscopic tumour resection, but in areas which were unsuitable for radical resection, tumour reduction to $\leq$ 5 mm thickness was performed. To prevent local tumour spread beyond the thoracic cavity, the normal boundaries (like pericardium and diaphragm) of the thoracic cavity were left intact. An ipsilateral lymph node dissection was part of the pleural pneumonectomy procedure. The bronchial stump was closed by staples (TA 55, Autosuture^R). To obtain histological specimens after the combined treatment, a thoracoport (Thoracoport, Autosuture^R) was inserted in the upper part of the anterior chest wall and covered with sterile adhesive tape. A small marker lesion, easily accessible by thoracoscopy, was left behind and indicated by a suture.

Patient no	age (years)	sex	diagnosis	TNM after resection	side	comments
1	37	M	epitheloid	$T_3N_1M_0$	right	extensive tumour mass on diaphragm and mediastinum, pretreatment with one course of Mitomycin C, Vinblastin and Cisplatin
2	40	M	carcinoid	$T_xN_0M_0$	left	localised tumour in the parietal pleura (9 cm diameter) which was first diagnosed as a MM at thoracoscopy
3	59	M	epitheloid	$T_2N_1M_0$	right	large tumour mass on parietal pleura, diaphragmatic sinuses and in the diaphragm
4	41	F	epitheloid	$T_{1b}N_0M_0$	left	tumour located especially at the diaphragmatic sinuses
5	54	M	epitheloid	$T_3N_0M_0$	right	tumour diffusely located in the thorax with location in the top which was difficult to remove surgically

Table 8.1: *Patient and tumour characteristics.* T_x *: primary tumour cannot be assessed;* T_{1b} *: tumour extending on both visceral and parietal pleura;* T_2 *: tumour with ingrowth of the lung or diaphragm;* T_3 *: tumour encompassing the pericardium;* N_0 *: no lymph nodes;* N_1 *: positive lymph nodes within the visceral pleura;* M_0 *: no distant metastases*

Patients were detubated immediately post-operatively and monitored on the ICU. Oxygen saturation was measured for a few minutes every hour, using a finger clamp (red light). Fluid replacement was administered according to vital signs, blood pressure and urinary output balanced with the anticipated perspiration.

Photodynamic procedure

Patients were injected with 0.1 mg/kg of mTHPC (meta-tetrahydroxyphenyl chlorin, supplied by Scotia Pharmaceuticals, Guilford, England) 4 days before the operation. Twenty milligrams of the drug were dissolved in 5 ml solvent containing ethanol, polyethylene glycol and water and shaken for 5 minutes. The drug was given intravenously as a slow push injection (4 mg/ml). After administration patients were nursed in subdued light for a minimum of 2 weeks.

The thoracic cavity was integrally illuminated with a spherical diffusing fibre (bulb diameter 3 mm, Rare Earth Medical Inc., West Yarmouth MA, USA). If necessary, a micro- lens fibre (PDT inc., Santa Barbara CA, USA) was used for additional local illumination. The fibre was coupled to a diode laser (Applied Optronics, 6W) that provides 6 Watts of light at 652 nanometer. During a pilot experiment, in which we measured the fluence rate distribution in the thoracic cavity of a (non-sensitised) patient after pneumonectomy, we observed that the region near the diaphragm posed a problem for illumination. Due to the absence of the lung mass, the diaphragm folds into the thoracic cavity and forms a region (sinus) where the light is shadowed. A transparent sterile plastic bag (Steri-Drape^{TM}, 3M) was therefore placed in the thoracic cavity and filled with saline (at body temperature) to stretch the diaphragm. This resulted in a better distribution of the light. Before placing and fitting the transparent sterile bag, optimal haemostasis was obtained and the thoracic cavity was cleaned thoroughly to prevent light absorption by blood. The light source was introduced via a sterile tube (Stomach Catheter 18 G) in the centre of the filled bag. The surgical wound was approximated during the illumination to maximise back scattering of light due to reflections in the cavity. This procedure was performed to obtain a uniform light distribution. Before and after illumination the presence of blood pockets was easily verified by visual inspection through the saline in the bag.

The distribution and total dose of the light delivered was monitored with isotropic light detectors (probes) with an accuracy of +/- 15%, (Van Staveren *et al* , 1995), manufactured in the Clinical Physics Department of the

Daniel den Hoed Cancer Centre. The probes (diameter 1 mm) were connected to photodiodes (Photop UDT-455, Graseby Electronics, Orlando FL, USA), whose output was A/D converted and displayed and stored on a PC. This system allowed us to do real-time fluence-rate and integrated fluence measurements. The isotropic probes measure the total light fluence delivered to the tissue, including both direct incident and scattered light from the tissue bulk. The latter is not measured when flat photodiodes are used, as in some previous studies of PDT in malignant mesothelioma (Pass *et al*, 1994). The probes were calibrated in air in an integrating sphere with a well defined diffuse light field (Van Staveren *et al*, 1995). The integrating sphere and the photodiodes are incorporated in one device that can be connected to the printer port of any regular Personal Computer. The probes were then placed in a sterile polyethylene lockable extension tube (inner diameter 1-2 mm, Vygon, Ecouen, France) filled with saline to match the refractive index of the surrounding medium (saline and tissue), resulting in a proper calibration of the isotropic probes. For further details on these calibrations see also Marijnissen and Star, 1996. Four probes were used to monitor the treatment. The probes (in the tubes) were sutured at strategic spots in the thoracic cavity before the sterile bag with saline was placed in position. One probe was always situated in the sinus, and one in the top of the thoracic cavity. The third and the fourth probe were positioned to cover representative areas of the cavity, including critical structures like the oesophagus, the pericardium or the lung surface if only a pleurectomy was performed.

At the start of the treatment, the spherical diffuser was placed in the centre of the cavity and the position of the diffuser was manually adjusted until the fluence-rate readings on all detector probes were approximately equal. If the detectors showed an imbalance in fluence rate during the treatment, the diffuser was manually repositioned to regain the desired distribution. If a region (e.g. the sinuses) received insufficient light, this region was given top up illumination using a micro-lens fibre after removal of the saline filled bag. The four probes were recalibrated (software-wise) for the absence of the saline (which causes a refractive index mismatch), and left in place to measure the scattered light at other than the directly illuminated regions. The illumination was continued until the required total dose of 10 J/cm^2 was reached, averaged over all measured sites. Sometimes an imbalance between the total light dose on the four spots was allowed, for instance when the probe was on a spot with a visible tumour mass. Twenty-four hours after treatment a thoracoscopy was performed (4 patients) through the

thoracoport with a 0^o rigid optic held in a forceps device (Wolf, Germany). Biopsies were taken from apparently normal tissue and from the marked indicator lesions. The tissue was collected in formaldehyde and processed for histology. The thoracoport was replaced by a transparent tube and additional illumination (20 J/cm at 400 mW/cm using a 2 cm cylindrical diffuser) was given to the tract in order to kill any remaining tumour cells.

Results

Five patients were suitable for the combined surgical/PDT treatment. The mediastinoscopy was normal in these patients, there were no contra-indications for a pleuropneumonectomy and written informed consent was obtained. Four of the patients had diffuse mesothelioma (confirmed by an expert panel) for which a pleuropneumonectomy was indicated. The chest X-ray of the first patient is shown in Figure 1.

One patient with a localised lesion was treated with excision of the pleural tumour and was illuminated with the lung in situ. This patient proved to have a carcinoid tumour instead of a malignant mesothelioma when the excised tumour was analysed (Table 1). A sixth patient referred for the adjuvant PDT therapy, proved to be irresectable at operation. The operation was therefore terminated and no additional PDT was given.

The total PDT-treatment time was (maximally) one hour, including placement of the probes and the bag. The integrated cumulative dose (J/cm^2) is shown as a function of time for all patients in Figure 2 a-e and the delivered dose to all sites of measurement is given in Table 2.

In patient 1 the fluence rates on all but one probe were balanced (Figure 2a). The probe in the sinus showed a low fluence rate, indicating that the diaphragm was not properly stretched. The total light dose to the sinus was less than 1 J/cm^2. Two additional illuminations using a micro-lens were therefore given. The bag was removed and the diaphragm stretched manually, leaving the other probes in situ. The probe near the oesophagus registered an additional light dose of 2.5 J/cm^2 as a result of the scattered light from the micro-lens illuminations, the other probes showed an additional dose of 1.5 J/cm^2. The probe located in the sinus was used to measure the additional dose given by the micro-lens. The total dose on the diaphragm, outside the areas which were additionally illuminated, is estimated to be about 1 J/cm^2 higher than the initial dose of 8.6 J/cm^2. The average dose for the entire cavity was 10.1 J/cm^2.

	Light dose (J/cm^2)				
Probe position	Patient 1	Patient 2	Patient 3	Patient 4	Patient 5
top of thoracic cavity	9.8	9.9	8.5	8.5	8.5
lung surface	-	10.5	-	-	-
retro-sternal	10.2	-	-	-	-
oesophagus/mediastinum	11.7	-	7.8	-	-
tumour	-	12.8	-	-	-
pericard	-	-	-	8.5	10.4
thorax surgical entrance	-	-	10.5	9.1	10.2
diaphragmatic sinus	<1.0	9.0	14.4	9.4	8.5
extra sinus illumination					
anterior and posterior	8.6	-	-	-	-
Average	10.1	10.0	10.3	8.9	9.4

Table 8.2: *Total cumulative light doses delivered to various sites in the thoracic cavity*

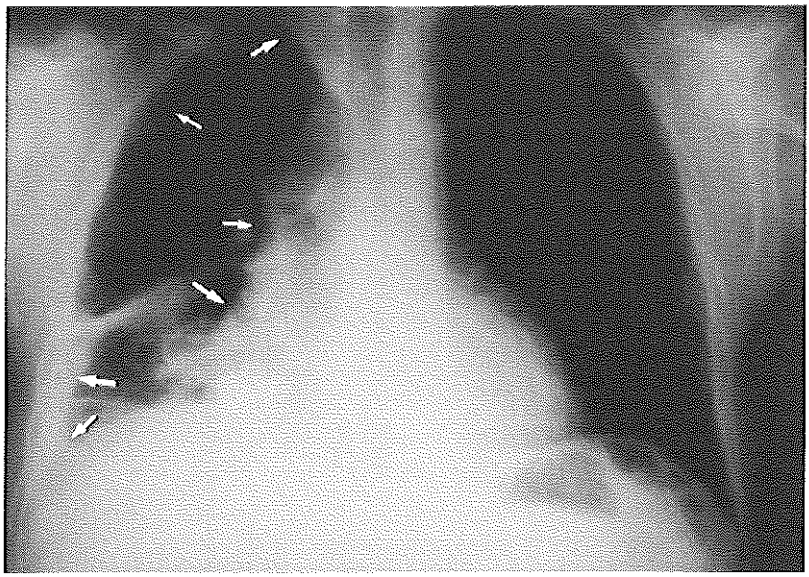

Figure 8.1: *Chest X-ray (postero-anterior view) of this patient before operation. The arrows indicate the contours of the mesothelioma on the right side.*

In patient 2 the (deflated) lung was still present in the thoracic cavity. The dose on the lung surface was monitored to avoid excessive normal tissue damage (Figure 2b). The fluence rate on the probes was balanced, except for the probe on the tumour located on the lateral thoracic wall. The tumour surface was additionally illuminated with a micro-lens. In this situation the scattered light contributed little extra dose to the other sites of measurement. The diaphragm was well-stretched and the light dose in the sinus was sufficient. The tumour received 12.8 J/cm^2, the average for the cavity was 10.6 J/cm^2.

In patient 3 well-balanced fluence-rates were established on all probes (Figure 2c), with, intentionally, a higher fluence rate on the sinus, which received 14.4 J/cm^2 to the remainder of tumour mass on the diaphragm. The average dose delivered was 10.3 J/cm^2.

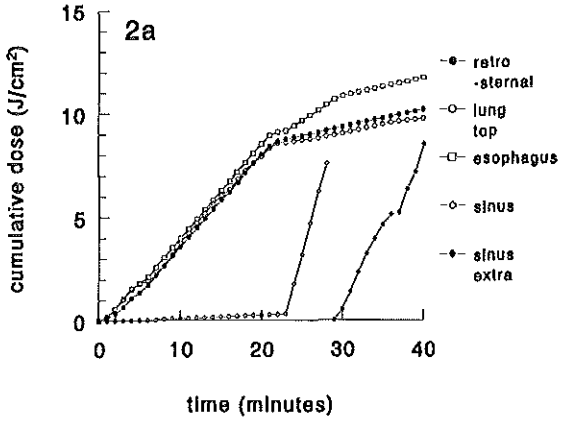
2a
cumulative dose (J/cm²)
15
10
5
0
0
10
20
30
40
time (minutes)
retro -sternal
lung top
esophagus
sinus
sinus extra

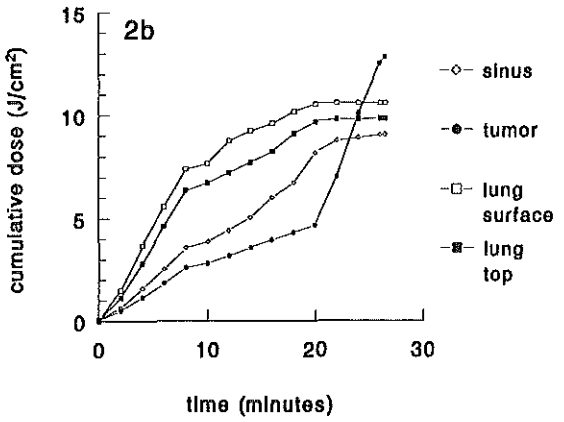
2b
cumulative dose (J/cm²)
15
10
5
0
0
10
20
30
time (minutes)
sinus
tumor
lung surface
lung top

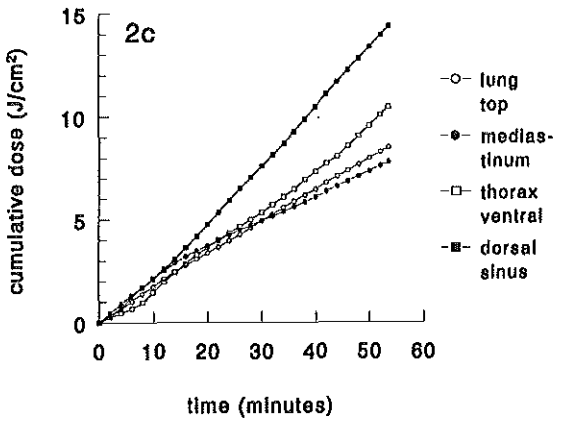
2c
cumulative dose (J/cm²)
15
10
5
0
0
10
20
30
40
50
60
time (minutes)
lung top
mediastinum
thorax ventral
dorsal sinus

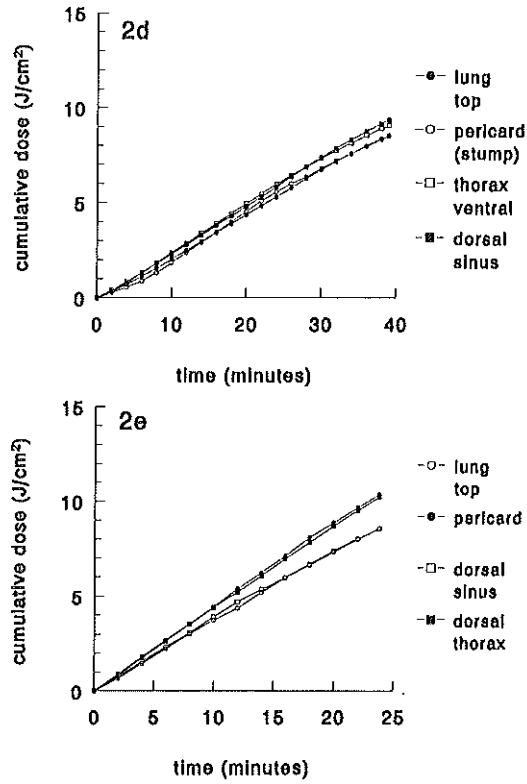

Figure 8.2: *Cumulative light dose (J/cm^2) plotted in time (minutes) for different probes located on different places in the thoracic cavity. The prescribed average light dose on all probes was 10 J/cm^2.* a *Illumination of patient 1. The probe in the sinus received only 1 J/cm^2 in the 25 minutes of illumination. Additional illumination, using a micro-lens, was therefore given to the diaphragm in two successive sessions while the other probes were left* in situ. *During this additional illumination the other probes registered an extra fluence of 1 to 3 J/cm^2.* b *Illumination of patient 2 in whom the lung was left in situ. After removal of the pleural tumour an additional illumination was given to the resected area. In this case minimal additional light dose was recorded on the other probes.* c *Illumination of patient 3 showing that all probes received a constant fluence rate, with preference to the diaphragm where most of the tumour had been resected.* d *and* e *Illumination of patients 4 and 5 showing equal distribution of light throughout the thoracic cavity.*

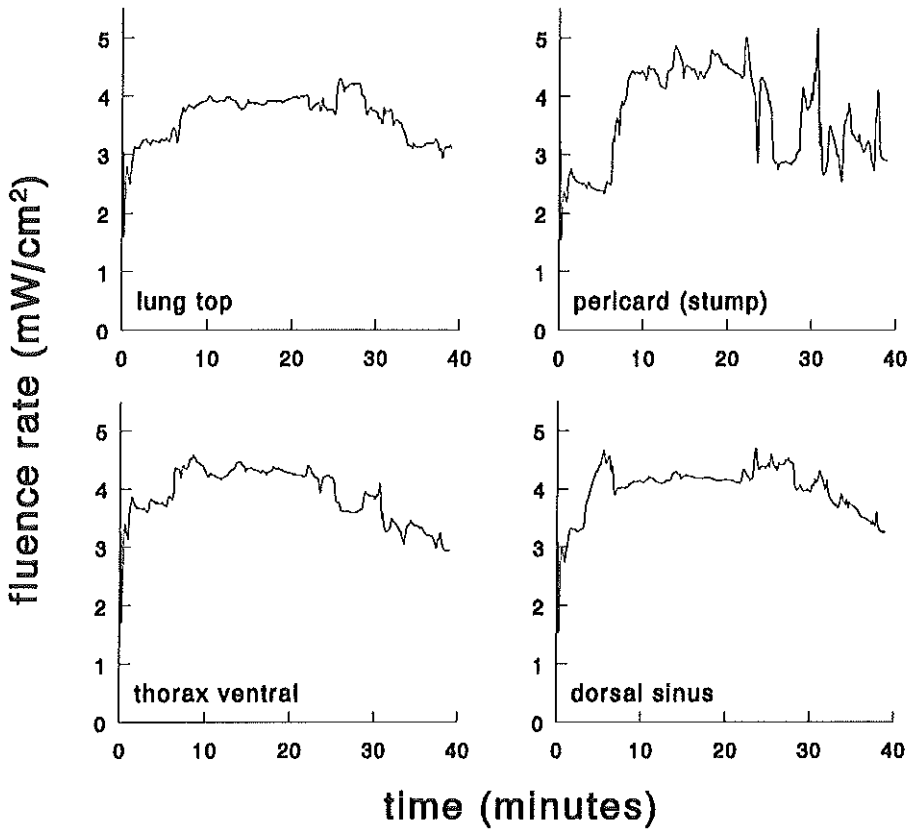

Figure 8.3: *Fluence rate (mW/cm^2) recorded in time (minutes) during the illumination of the thoracic cavity of patient 4. Small changes in fluence rate occur during illumination due to respiration and the manual repositioning of the light source.*

In patients 4 and 5 the fluence rates on all probes were well balanced (Figure 2d and e). Average doses for the cavity were 8.9 and 9.4 J/cm^2, respectively. Changes in fluence rate during the illumination period for patient 4 is illustrated in Figure 3. Apart from the fluctuations caused by the manual repositioning of the spherical diffuser, the fluence rate on all probes was kept stable at 3-4 $mWatts/cm^2$.

Post treatment complications and follow-up

There was no 30 day mortality and the duration of the hospital stay was less than 3 weeks for patients 1,2,3 and 5 (Table 3). In patient 1, skin photosensitivity occured in the intensive care due to monitoring with a pulse-oximeter on the index finger. A small grade 2 sunburn resulted from the measurement (which lasted 4 hours). (Other patients were monitored intermittently for several seconds on different fingers). Eleven months after operation patient 1 was in good clinical condition and had resumed working full time. On CT scanning, there was no evidence of tumour recurrence in the thoracic cavity. Patient 2 had recovered fully from the operation and resumed working part time at 10 months after operation. Physical and radiological examination did not reveal any recurrences and the lung function parameters (spirometry and diffusion) were unchanged. The third patient suffered from constipation related to the post-operative pain medication. Reduction of the opiates and oral and rectal laxatives resolved this complication. Sixteen weeks post-operatively, diffuse tumour spread was diagnosed in the superficial skin vessels originating from the thoracoscopic scar. He died of local and abdominal tumour spread at 7 months after treatment. No post mortem was performed.

In patient 4, the diaphragm was elevated one day after surgery and thoracoscopic examination was difficult. On day 2 signs of a diaphragmatic rupture had become apparent and a rethoracotomy had to be performed to replace the stomach in the abdominal cavity and to close the diaphragmatic rupture. The margins of the rupture were biopsied and a Marlex covering was used to strengthen the diaphragm. Increased fluid production in the thoracic cavity resulted in shifting of the mediastinum to the right, hampering respiration. Repeated punctures (thoracentheses) were necessary to remove the superfluous pleural fluid. Ten days after treatment the patient had increased dyspnea and a pulsus paradoxus was noted. On radiological examination (chest X-ray and ultra sound) a pericardial effusion was noted and 500 cc of haemorrhagic fluid was removed. Cytological examination revealed no tumour cells and the post operatively initiated anticoagulant therapy was withdrawn. Further recovery was uneventful and on day 40 after admission she was discharged. Ten months after treatment she was well with no signs of tumour recurrences on CT scan examination. Patient 5 experienced post-operative pain which could be controlled with analgetics. Nine months after treatment he was still tired but had no other complaints. The radiologic examination did not show any signs of recurrences. None of the patients experienced any generalised sunburn effects after discharge.

Patient no.	hospital stay (days)	complication (post-operative)	follow-up (months)	current tumour status and long term side effects
1	18	grade 2 sunburn on index finger	11,alive	no evidence of tumour recurrence
2	16	no complications	10,alive	no evidence of tumour recurrence fatigue since operation
3	18	constipation on basis of opiates	7,death	diffuse vascular metastasis originating from the thoracoport leading to abdominal metastasis and death
4	41	rupture of diaphragm requiring rethoracotomy, increased effusion in operated cavity treated with multiple thoracentheses, haematopericardium requiring drainage	10,alive	no evidence of tumour recurrence limited exercise tolerability fatigue lower back pain with normal MRI
5	20	grade 2-3 skin burn on a 5 cm area in the surgical scar	9,alive	no evidence of tumour recurrence increased susceptibility for infections

Table 8.3: *Post-surgical complications and follow-up*

Histologic examination

In the 4 patients who underwent pleuropneumonectomy, a thoracoscopy was performed one day after PDT and tissue was taken from apparently normal and indicator lesions. In Table 4 details of the histological specimens are given. In all specimens obtained, an infiltration with poly-morphonuclear cells and oedema was observed. This was more marked in the tumour tissue than in the samples obtained from the chest wall where the tumour had been resected completely. Figure 4a shows an example of vital mesothelioma in the resection specimen of patient number 1. In the biopsies of the target lesion (Figure 4b), sampled 24 hours after the combined treatment, necrotic residual mesothelioma with an increased number of polymorphonuclear cells was found. The patient who was re-operated for the diaphragmatic rupture also had tissue sampling 48 hours after the PDT. Biopsies taken from the diaphragm at the site of rupture showed a thin muscle layer but no evidence of (PDT induced) necrosis was found.

Discussion

From time of diagnosis of MM the mean survival is generally 9-14 months despite agressive treatment. It is well recognised that surgery alone is insufficient for the majority of malignant pleural mesothelioma cases and (adequate) adjuvant therapies are limited by their toxicity and damage to normal tissue or the inability to cover all sites of the resection areas. Various chemotherapeutic regimens containing mitomycin-C, doxorubicin and adriamycin have been investigated but their effectiveness has not clearly been demonstrated. Although some long term survivors have been reported, the overall effect has been disappointing (Krarup-Hansen and Hansen, 1991). The addition of radiotherapy to the operated hemithorax has also failed to demonstrate an increase in survival (DaValle *et al* , 1986; Hilaris *et al* , 1984). One of the major problems is the planning of the radiation field to administer a tumouricidal dose without excessive normal tissue toxicity.

The primary objective of this study was to develop a suitable illumination and dosimetry procedure for intra-thoracic PDT. Photodynamic therapy offers some advantages as a local adjuvant treatment since it has a restricted normal tissue toxicity which is related to the depth of penetration of the light used and the concentration of photosensitiser. For optimal efficacy, the photosenstiser should preferentially concentrate in tumour tissue and/or its vasculature, and its singlet oxygen production should be high

Patient	tumour sample	normal tissue
1	partly necrotic, partly viable tumour cells inflammatory cells and oedema	fat tissue, muscle cells, partly necrotic, oedema
2	no data	no data
3	no tumour cells identifiable inflammatory cells	inflammatory cells and muscle cells
4	no tumour identifiable inflammatory cells, oedema	inflammatory cells and oedema in striated muscle cells
4 at 48 hrs	no tumour cells identifiable	no necrosis of diaphragm biopsies or of chest wall biopsies
5	necrosis of tumour cells inflammation	fat tissue and muscle cells with some necrosis

Table 8.4: *Tumour and normal tissue response to PDT after 24 hours*

(a)

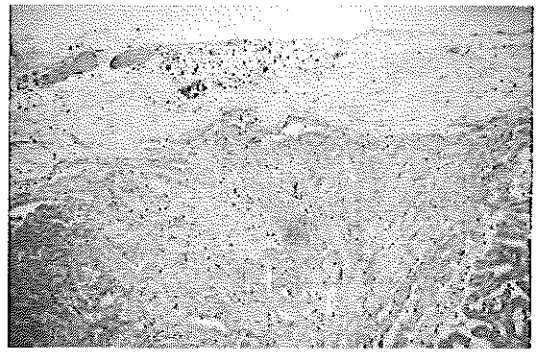

(b)

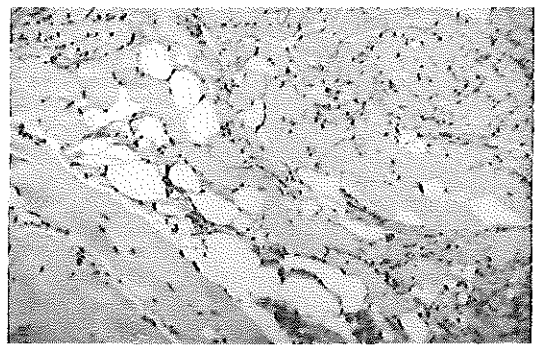

Figure 8.4: *a. Pleural mesothelioma, epithelial type (HE, 10x, pleuropneumonectomy specimen) of patient 1. b. Necrotic mesothelioma, 24 hours after combined treatment (HE, 20x, biopsy of target lesion) of patient 1.*

at illumination. A second important aspect is optimal light delivery and dosimetry, especially when larger areas are treated.

Promising results on the use of PDT in MM have been reported in the literature. In the largest study (Pass *et al* , 1994) 42 patients were treated with haematoporphyrin derivative and illumination in a phase I study, but no increased survival (mean 12.4 months) was observed. The illumination,

2 days after sensitisation, was performed with two Argon dye lasers. The output of each laser at 630 nm was 5 Watt maximally and the average additional time to perform the PDT was 89 minutes (including placement of fibers). The actual laser time was 68 minutes to achieve a total light dose of 25 J/cm^2. Since light dosimetry was performed with flat photodiodes, which do not measure all scattered light, the total light delivery to the tissue was underestimated. Ris *et al* (1996) performed a pilot study in 8 patients using 0.3 mg/kg m-THPC and 10 J/cm^2 after an interval of 48 hours. Seven patients had good local control of their thoracic disease but developed distant metastasis after 4-18 months. One patient died of pulmonary embolism 8 days after resection. Post-mortem examination showed extensive necrosis in the remaining tumour but no damage to normal structures like the heart and the oesophagus.

In all previous studies with PDT its potential has been well recognised, but the lack of understanding of dosimetry and the inability to administer adequate light doses in a short period of time has prevented a more general use of PDT. The development of second generation photosensitisers, with a higher singlet oxygen yield, have made PDT treatment more attractive, especially for larger areas. The higher activity of the photosensitisers and the new types of high power diode lasers now available enables the treatment period to be considerably shortened. We have been able to apply this adjuvant photodynamic treatment in 40 to 60 minutes. The shorter half life or reduced retention in the skin of such photosensitisers also greatly reduces the skin photosensitivity for the patients.

The cumulative light dose (fluence) to the tissues of the thoracic cavity can be measured by isotropic probes in real time. This is independent of the optical properties of the tissues in the cavity, which may vary considerably between patients. These differences are enhanced by multiple reflections in a closed cavity with walls of scattering tissue (Van Staveren *et al* , 1994). The prescribed light dose, based on the use of isotropic probes for in situ dosimetry, will be lower than the same dose specified with the use of flat detectors, because the latter do not detect all the light in the tissue. It is therefore impossible to compare results from different studies on basis of incident light dose alone. To overcome this problem generally accepted methods of light delivery and measurement should be developed for specific clinical settings. The total light dose received by the target tissue should be described by in situ dosimetry measurements. With the simple illumination technique as used in this study, one spherical diffuser occasionally supplemented with a micro-lens illumination, it was possible to achieve a control-

led distribution of the light delivered to the thoracic cavity. The on-line measurement allows for repositioning of the diffuser during the treatment, thereby correcting for asymmetry in the fluence rate distributions and preventing under- or overillumination of some areas. Great care must be taken when illuminating the cavity sequentially with adjoining light-fields, as has been done in several studies (e.g. Ris *et al* , 1996), since the scattered light contributes a considerable amount to the dose received on locations that are not directly illuminated. This could lead to overdosing of some areas, unless this is continually monitored during illumination.

In this study we have shown that the combination of PDT and surgical resection for pleural tumours is feasible and that in situ light dosimetry greatly improves the reproducibility and controllability of this combined treatment. The operation time increased by less than one hour (on an average of 5 hours surgery alone) in the current set-up and the duration of the hospital stay was generally no longer than expected for sugery alone. Larger numbers of patients and longer follow-up will be required to determine whether this type of adjuvant treatment offers a benefit in terms of local control and survival. The absence of tumour recurrence and survival observed in four of five patients so far is promising. In the patient who died with recurrence after 7 months, tumour cells may have been spread from the thoracoscopic entrance. We have therefore abandoned the practice of leaving an indwelling thoracoport for 24 hours biopsy sampling.

Tissue specimens, taken 24 hours after treatment showed extensive damage to the tumour tissue and only minor damage to striated muscle of the chest wall after a light dose of only 10 J/cm^2 . Clearly the light dose and/or the drug dose could be escalated or the time interval between drug administration and illumination could be reduced in an attempt to achieve better results.

The improvements in methods of light administration and dosimetry greatly improves the possibility to safely apply PDT on larger surfaces. Using this information as a starting point we are now planning further dose escalation and phase II studies.

Acknowledgments

We thank dr Willem Star for his comments and advice, Hugo Oppelaar for his technical support and gratefully acknowledge the support of Scotia Pharmaceuticals, Guilford, England.The study was partly supported by the

Dutch Cancer Society project NKI 97-1446

References

1. Butchart E G and Gibbs A R (1990) Pleural Mesothelioma. *Curr. Opin. Oncol.* **2** *352-358*

2. Chahinian A P, Pajak T F, Holland J F, Norton L, Ambinder R M Mandel E M (1982) Diffuse malignant mesothelioma: prospective evaluation of 69 patients. *Ann. Int. Med.* **96** *746-755*

3. Chahinian A P, Antman K, Goustou M, Corson J M, Suzuki Y, Modeas C, Herndon II J E, Aisner J, Ellison R R, Leone L, Vogelzang N J and Green M R (1993) Randomised phase II trial of cisplatin with mitomycin or doxorubicin for malignant mesothelioma by the Cancer and Leukemia Group *B. J. Clin. Oncol.* **11** *1559-1565*

4. DaValle M J, Faber L P, Kittle C F and Jensik R J (1986) Extrapleural pneumonectomy for diffuse Malignant Mesothelioma. *Ann. Thor. Surg.* **42** *612-618*

5. Hilaris B S, Nori D, Kwong E, Kutcher G J and Martini N (1984) Pleurectomy and intraoperative brachytherapy and postoperative radiation in the management of malignant pleural mesothelioma. *Int. J. Radiat. Oncol. Biol. Phys.* **8** *19-25*

6. IMIG (1995) A new staging system for malignant mesothelioma. *Chest* **108** *1122-1126*

7. Krarup-Hansen A and Hansen H H (1991) Chemotherapy in malignant mesothelioma : A review. *Cancer Chemother. Pharmacol.* **2** *391-394*

8. Lofgren L, Larsson M, Thaning L, Hallgren S (1991) Transthoracic endoscopic photodynamic therapy for malignant mesothelioma. *Lancet* **337** *359*

9. Marijnissen J P A and Star W M (1996) Calibration of isotropic light dosimetry detectors based on scattering bulbs in clear media. *Phys. Med. Biol.* **41** *1191-1208*

10. Pass H I, Delaney T, Tochner Z, Smith P E, Temeck B K, Pogrebniak H W, Kranda K C, Russo A, Friauf W S, Cole J W, Mitchell J B and Thomas G (1994) Intrapleural photodynamic therapy: results of a phase I trial. *Ann. Surg. Oncol.* **1** *28-37*

11. Ris H B, Altermatt H J, Inderbitzi R, Hess R, Nachbur B, Stewart J C M, Wang Q, Lim C K, Bonnet R, Berenbaum M C and Althaus U (1991)

Photodynamic therapy with Chlorins for diffuse malignant mesothelioma: initial clinical results. *Br. J. Cancer* **64** *1116-1120*

12. Ris H B, Altermatt H J, Nachbur B, Stewart C M, Wang Q, Lim C K, Bonnet R, Althaus U (1996) Intraoperative photodynamic therapy with mTHPC for chest malignancies. *Las. Surg. Med.* **18** *39-45*

13. Ruffie P (1993) Mesothelioma chemotherapy. *Eur. Respir. Rev.* **3** *11, 199-203*

14. Rusch V W, Saltz L, Venkatraman E, Ginsberg R, McCormack P, Burt M, Markman M Kelsen D (1994) A phase II trial of pleurectomy/decortication followed by intrapleural and systemic chemotherapy for malignant mesothelioma. *J. Clin. Oncol.* **12** *156-1163*

15. Sfrensen P G, Bach F, Bork E, Hansen HH (1985) Randomised trial of doxorubicin versus cyclophosphamide in diffuse malignant mesothelioma. *Cancer Treat. Rep.* **69** *1431-1432*

16. Sugarbaker D J, Heher E C, Lee T H , Couper G, Mentzer S, Corson J M, Collins J J, Shemin R, Pugatch R, Weissman L, Antman KH (1991) Extrapleural pneumonectomy, chemotherapy, and radiotherapy in the treatment of diffuse malignant pleural mesothelioma. *J. Thorac. Cardiovasc. Surg.* **102** *10-156*

17. Takita H, Mang T S, Loewen G M, Antkowiak J G, Raghaven D, Grajek J R, Dougherty T J (1994) Operation and intracavitary photodynamic therapy for malignant mesothelioma: A phase II study. *Ann. Thorac. Surg.* **58** *995-998*

18. Van Staveren H J, Beek J F, Ramaekers J W H, Keijzer M and Star W M (1994) Integrating sphere effect in whole bladder wall photodynamic therapy: I. 532 nm versus 630 nm optical irradiation. *Phys. Med. Biol.* **39** *947-959*

19. Van Staveren H J, Marijnissen J P A, Aalders M C G, Star W M (1995) Construction, quality control and calibration of spherical isotropic fibre-optic light diffusers. *Las. Med. Sci.* **10** *137-147*

Summary and Concluding Remarks

Overview

The work in this thesis is an attempt to develop light delivery and calculate and measure the light distribution during Endo-Bronchial Photodynamic therapy (EB-PDT). The fluence rate distribution resulting from illumination of the lumina of the trachea-bronchial tree has been investigated. The influence of the following parameters was studied:

- linear diffuser output characteristics
- on- or off-axis positioning of the diffuser in the lumen
- length of the diffuser
- diameter of the treated lumen
- wavelength of light used for illumination
- optical properties of the bronchial mucosa

An applicator for *in situ* light delivery and light dosimetry has been developed and been used to perform the first fluence rate measurements in humans. The applicator has been used to determine a fluence-response relationship of the healthy bronchial mucosa in pigs.

Finally, the techniques of *in vivo* fluence rate measurements have been applied to the integral illumination of the thorax after resection of the pleura and/or the lung.

Ex vivo fluence rate measurements and Monte Carlo simulations

In **chapter 2**, the light distribution during Photodynamic Therapy of the bronchial tree has been estimated by measuring the fluence rate in *ex vivo* experiments on dissected pig bronchi. The trachea was illuminated (630 nm) with a linear diffuser and the fluence rate was measured with an isotropic probe. The results from ex vivo experiments and Monte Carlo simulations of the experiment were found to agree within the error of measurement ($\pm$15%), indicating that the Monte Carlo technique can be used to estimate the light distribution for varying geometries and optical properties.

The results showed that the light fluence rate in the mucosa of the (*ex vivo*) trachea may increase by a factor of 6 compared to the fluence rate in air (in the absence of tissue), caused by multiple (diffuse) backscattering from the tissue bulk and multiple specular reflections in the trachea.

Further experiments showed that the positioning of the diffuser is critical for the fluence rate in the lesion to be treated. When the position of the diffuser was changed from the central axis to nearby the lesion, the fluence rate in the mucosa increased significantly by several orders of magnitude as compared to the initial (central) illumination. The inter- and intra- specimen variations in this increase were large (± 35 %) because of variations in optical and geometrical properties and light source positioning, respectively. These variations might cause under- or overdosage resulting in either insufficient tumour-necrosis or excessive normal-tissue damage. These results indicate that it may be wiser to illuminate the lumen always with on-axis positioning of the diffuser.

Light delivery by linear diffusers

The distribution of the light emitted by linear light diffusers commonly employed in PhotoDynamic Therapy (PDT) has been investigated in **chapter 3**. A device is presented which measures the angular distribution of the exiting light at each point of the diffuser. With these data the fluence rate in air or in a cavity at some distance from the diffuser can be predicted. The results show that the light is scattered from the diffuser predominantly in the forward direction. Experiments and calculations show that the fluence rate in air and in a cavity of scattering tissue at some distance from the diffuser has a maximum near the tip of the diffuser, instead of near the middle. However, the fluence rate resulting from an interstitial diffuser in a purely scattering tissue phantom shows a maximum in the bisecting plane of the diffuser as would be predicted when each element of the diffuser emitted light isotropically. The scattering nature of the tissue is expected to cancel the anisotropy of the light emitted by the diffuser.

In **chapter 4** the angular radiance distribution of several linear diffusers used for PhotoDynamic Therapy (PDT) was measured. The forward scattering found previously (chapter 3) was not observed in these designs. The improved isotropy leads to a better agreement between intended treatment site and actual maximum of the fluence rate profile when the linear diffuser is used in a hollow, cylindrical, organ.

Applicator for endobronchial light delivery and light dosimetry

A design of an applicator for light delivery and light dosimetry during Endo-Bronchial PhotoDynamic Therapy (EB-PDT) is presented in **chapter 5**. The design incorporates a linear diffuser that is fixed in the centre of the lumen by a steel spring basket that does not block the air flow. The fixation system ensures central positioning of the diffuser for optimal light distri-

bution (chapter 2). An isotropic probe is a part of the design, to measure the light fluence actually delivered to the bronchial mucosa surface. The applicator is designed for use with common bronchoscopy equipment, and can be used with bronchoscopes with a large biopsy channel ($\approx$ 3 mm). The first clinical measurements were performed and caused no additional discomfort to the bronchoscopy of (non-photosensitized) patients.

The data showed a considerable inter-patient variability of the fluence rate measured for a given output power of the diffuser. This fact and the expected strong dependence of the fluence rate on the lumen diameter stress the importance of *in situ* fluence rate measurement for a proper evaluation of the relationship between light fluence and biological response of EB-PDT.

Monte Carlo calculations for varying geometry, optical properties and diffuser characteristics

In **chapter 6** a Monte Carlo model is presented for the illumination of a cylindrical cavity by a linear diffuser. It is employed to compute the fluence rate distribution during endo-bronchial PhotoDynamic Therapy. The influence of geometrical parameters such as the diameter of the treated lumen, the length of the linear diffuser and the possible off-axis position of the diffuser on the fluence rate have been investigated, as well as the consequences of varying output characteristics of the diffusers. For on-axis isotropic diffusers some simple practical rules are derived to estimate the fluence rate profile on the wall for varying diffuser length and lumen diameter.

With linear diffusers that can be modelled as a row of isotropic point sources, a constant fluence rate build-up factor can be employed for varying diffuser lengths and lumen diameters. Extreme off-axis placement of the diffuser causes a highly variable, considerable increase in the maximum fluence rate as well as a highly asymmetrical fluence rate profile on the circumference of the illuminated lumen (as already observed in chapter 2). The measured radiance profiles of real diffusers can be incorporated in the model, which provides a means of evaluating the fluence rate distribution resulting from realistic (non-ideal) light sources.

The influence of the optical properties of the bronchial mucosa on the fluence rate build-up factor was also investigated. The changes in fluence rate could be accounted for by diffusion theory.

Fluence-response experiment for normal tissue damage of the bronchial mucosa in pigs

In **chapter 7** the damage to normal pig bronchial mucosa caused by Photo-Dynamic Therapy (PDT) using mTHPC and Photofrin as photosensitisers has been evaluated. The endobronchial applicator from chapter 5 was used to deliver the light with a linear diffuser and to measure the light fluence *in situ*. The applied fluences were varied, based on existing protocols. A fluence finding experiment with short-term (1-2 days) response as an end-point showed considerable damage to the mucosa with the use of Photofrin (fluences 50-275 J/cm^2, drug dose 2 mg/kg) with oedema and blood vessel damage as most important features. In the short-term mTHPC experiment the damage found was slight (fluences 12.5-50 J/cm^2, drug dose 0.15 mg/kg). For both sensitisers atrophy and acute inflammation of the epithelium and the submucosal glands was observed. The damage was confined to the mucosa and submucosa leaving the cartilage intact. A long-term experiment showed that fluences of 50 J/cm^2 for mTHPC and 65 J/cm^2 for Photofrin treated animals caused damage that recovered within 14 days, with sporadic slight fibrosis and occasional inflammation of the submucosal glands. Limited data on the pharmacokinetics of mTHPC show that drug levels in the trachea are similar at 6 and 20 days post injection. The importance of *in situ* light dosimetry was stressed by the inter-animal variations in fluence rate for comparable illumination conditions.

Intra-operative adjuvant Photodynamic Therapy for Malignant Mesothelioma

Chapter 8 describes the treatment of five patients with a pleural malignancy with maximal surgical resection of the tumour followed by intra-operative adjuvant photodynamic therapy (PDT). The additional photodynamic treatment was performed with mTHPC as photosensitiser. The light delivery to the thoracic cavity was monitored by *in situ* isotropic light detectors. The position of the spherical diffuser was adjusted to achieve optimal light distribution, taking account of reflected and scattered light in this hollow cavity.

There was no 30 day postoperative mortality and only one patient suffered from a major complication (diaphragmatic rupture and haematopericardium). The operation time was increased by a maximum of one hour to illuminate the total hemithoracic surface with 10 J/cm^2 (incident plus scattered light). The effect of the adjuvant PDT was monitored by examination of biopsies taken 24 hours after surgery under thoracoscopic guidance. Sig-

nificant damage, including necrosis, was observed in the marker lesions with remaining malignancy, compared to normal tissue samples which showed only an infiltration with PMN cells and oedema of the striated muscles cells.

Of the five patients treated, four are alive with no signs of recurrent tumour with a follow-up of 9-11 months. One patient was diagnosed to have a tumour dissemination in the skin around the thoracoscopy scar and died of abdominal tumour spread.

Concluding Remarks

The fluence rate distribution during EB-PDT (and all other applications of PDT) depends on many factors, some of which are difficult to determine *in situ* in a routine manner (eg. the optical properties of the tissue). Therefore it essential that an *in situ* measurement is performed during each treatment to ensure that a reproducible light fluence is delivered to the tissue. Only in this way one can hope to obtain a correlation between the amount of applied light and the observed therapeutic effect.

In this thesis two ways of performing *in situ* light dosimetry are presented, one for the trachea-bronchial tree and one for the integral illumination of the thorax. The fluence rate measurements can be used to estimate the fluence rate distribution although the number of measurement sites is limited especially in the bronchus applicator. Monte Carlo models can help to expand those few measurement points to an estimate of the distribution at the tissue surface and *in* the tissue. The latter is very important, because invasive measurements are seldom performed, and one has to rely on measurements on the surface.

The dimensions of the isotropic probes used for the measurements are such that they can be applied for dosimetry in virtually any area. Every target organ for PDT will require a specific device for light delivery and light dosimetry. The knowledge of the pharmacokinetics of the photosensitiser is also very important for the final therapeutic effect. Combination of *in situ* light dosimetry with measurement of the fluorescence of the photosensitiser before and during treatment will give a better prediction of the therapeutic effect.

Samenvatting

Inleiding

Het werk in dit proefschrift beschreven is een poging om de lichtapplicatie te ontwikkelen en de lichtverdeling te meten en berekenen tijdens Fotodynamische Therapie van de bovenste luchtwegen. De fluentie tempo verdeling als gevolg van de belichting van een van de lumina van de bovenste luchtwegen werd onderzocht. De invloed van de volgende parameters werd bestudeerd:

- emissie profielen van de lineaire diffuse lichtbron (diffuser)
- de positionering van de diffuser in het lumen (gecentreerd of excentrisch)
- de lengte van de gebruikte diffuser
- de diameter van het behandelde lumen
- de golflengte van het licht waarmee behandeld wordt
- optische eigenschappen van het longslijmvlies

Voor *in situ* licht applicatie en dosimetrie is een applicator ontwikkeld, en deze is gebruikt om de eerste fluentie tempo metingen uit te voeren in de mens. De applicator is vervolgens gebruikt om een fluentie('licht-dosis')-schade relatie te bepalen in het gezonde longslijmvlies van het varken.

Tenslotte zijn de technieken voor *in vivo* fluentie tempo metingen toegepast bij het integraal belichten van de thorax na resectie van het longslijmvlies en/of de long.

Ex vivo fluentie tempo metingen en Monte Carlo simulaties

In **hoofdstuk 2** wordt de licht verdeling tijdens Fotodynamische Therapie van de bronchi bestudeerd door middel van meting van het *ex vivo* fluentie tempo in de trachea van een varken. De trachea wordt belicht (rood licht, 630 nm) met een lineaire diffuser en het fluentie tempo wordt gemeten met een isotrope detector. De resultaten van de metingen komen binnen de meetfout ($\pm$15%) overeen met die van een Monte Carlo simulatie van het experiment. Dit geeft aan dat de Monte Carlo techniek gebruikt kan worden om een schatting te doen van de lichtverdeling voor verschillende geometrieën en optische eigenschappen.

De resultaten laten zien dat het fluentie tempo in het slijmvlies van de *ex vivo* trachea een factor 6 meer kan zijn dan het fluentie tempo op die plaats

in lucht. Dit wordt veroorzaakt door meervoudige (diffuse) terugstrooiing uit het weefsel en meervoudige spiegelende reflecties in de trachea.

Verdere experimenten tonen aan dat het positioneren van de lineaire diffuser bepalend is voor het fluentie tempo in de te behandelen laesie. Bij een verplaatsing van de diffuser van de centrale as tot dichtbij de laesie stijgt het fluentie tempo enkele orden van grootte vergeleken met de begintoestand. De inter- en intra- trachea variaties in deze toename waren groot ($\pm$ 35%) door variaties in respectievelijk de optische eigenschappen en geometrie en de positionering van de lineaire diffuser. Deze variaties kunnen over- en onderdosering tot gevolg hebben met als consequentie onvoldoende tumornecrose of te veel schade aan het normale weefsel. De resultaten geven aan dat het verstandiger lijkt om de belichting altijd uit te voeren met de lineaire diffuser op de centrale as.

Licht applicatie met lineaire diffusers

De verdeling van het licht uitgezonden door lineaire diffusers die gebruikt worden voor Fotodynamische Therapie werd onderzocht in **hoofdstuk 3**, waarin een apparaat wordt gepresenteerd dat de hoekverdeling meet van het uitgezonden licht op ieder punt van het diffuseroppervlak. Met deze gegevens kan het fluentie tempo in lucht of in een holte op zekere afstand van de diffuser voorspeld worden. De resultaten laten zien dat het licht van de diffuser voornamelijk in de voorwaartse richting uitgezonden wordt. Experimenten en berekeningen tonen aan dat het fluentie tempo in lucht en in een holte in verstrooiend weefsel op enige afstand van de diffuser een maximum heeft nabij de voorkant van de diffuser, in plaats van tegenover het midden. Een meting van het fluentie tempo met de diffuser interstitieel in een puur verstrooiend weefselfantoom laat zien dat het maximum ligt tegenover het midden van de diffuser, hetgeen te verwachten is indien ieder element van het diffuseroppervlak het licht isotroop uit zou zenden. De verstrooiing van het weefsel zelf zal er voor zorgen dat de anisotropie van het uitgezonden licht teniet wordt gedaan.

In **hoofdstuk 4** werd de radiantie-hoekverdeling gemeten van enkele lineaire diffusers die voor Fotodynamische Therapie gebruikt worden. De voorwaartse verstrooiing die voorheen gevonden werd (hoofdstuk 3) was afwezig in deze diffusers. De verbeterde isotropie leidt tot een beter overeenstemming tussen de bedoelde en de werkelijke plaats van behandeling in het geval van een belichting van een hol, cylindervormig orgaan.

Applicator voor endobronchiale licht applicatie en licht dosimetrie

In **hoofdstuk 5** wordt een applicator gepresenteerd voor het toedienen en het *in situ* meten van licht tijdens EndoBronchiale Fotodynamische therapie. Dit ontwerp bevat een lineaire diffuser die middels een mandje van stalen veren gecentreerd wordt in het te behandelen lumen, zonder dat de luchttoevoer geblokkeerd wordt. De centrale positionering van de diffuser zorgt voor een optimale lichtverdeling (hoofdstuk 2). Een isotrope detector is onderdeel van de applicator. Deze meet het fluentie tempo dat daadwerkelijk toegediend wordt aan het longslijmvlies. De applicator is ontworpen voor gebruik met gangbare bronchoscopen, en kan gebruikt worden met bronchoscopen met een groot ($\approx$ 3 mm) werkkanaal. De eerste klinische metingen werden uitgevoerd en veroorzaakten geen extra ongemakken bij de standaard bronchoscopie van niet-lichtgevoelige gemaakte vrijwilligers.

De gegevens laten een aanzienlijke variatie tussen de patiënten zien van het gemeten fluentie tempo voor een vast uitgangsvermogen van de lineaire diffuser. Dit gegeven gecombineerd met de te verwachten afhankelijkheid van het fluentie tempo van de lumen diameter benadrukken het belang van *in situ* fluentie tempo metingen voor een verantwoorde evaluatie van de relatie tussen licht fluentie en biologisch effect bij Endobronchiale Fotodynamische Therapie.

Monte Carlo berekeningen voor variaties in geometrie, optische eigenschappen en diffuser emissie karakteristieken

In **hoofdstuk 6** wordt een Monte Carlo model gepresenteerd voor de belichting van een cylindrische holte in weefsel door een lineaire diffuser. Het model wordt gebruikt om de fluentie tempo verdeling te berekenen tijdens Endo-Bronchiale Fotodynamische Therapie. De invloed van geometrische parameters zoals de diameter van het behandelde lumen en de lengte van de lineaire diffuser en de mogelijke excentrische positionering van de diffuser worden onderzocht. Ook wordt er gekeken naar de invloed van variaties in de emissie karakteristieken van de lineaire diffusers. Voor een centraal geplaatst diffuser worden enkele vuistregels afgeleid om de fluentie tempo verdeling op de wand van de trachea te schatten bij verschillende diffuser lengtes en lumen diameters.

Voor lineaire diffusers die gemodelleerd kunnen worden als een reeks van isotrope puntbronnen kan een constant fluentie tempo opbouwfactor gebruikt worden voor verschillende diffuser lengtes en lumen diameters. Extreme excentrische plaatsing van de diffuser veroorzaakt een aanzienlijke en zeer variabele toename in het maximum van het fluentie tempo evenals een

zeer asymmetrische fluentie tempo verdeling langs de omtrek van het lumen (zoals reeds gezien tijdens metingen in hoofdstuk 2). De gemeten emissie karakteristieken van lineaire diffusers kunnen worden ingebouwd in het model zodat de fluentie tempo verdelingen bij belichting met een niet-ideale lineaire diffuser onderzocht kunnen worden.

De invloed van de optische eigenschappen van het longslijmvlies op de fluentie tempo opbouwfactor werd ook onderzocht. De variaties in het fluentie tempo konden verklaard worden met behulp van diffusie theorie.

Fluentie-respons experiment voor normaal weefsel schade aan het longslijmvlies in varkens

In **hoofdstuk 7** wordt onderzocht welke schade er ontstaat aan het longslijmvlies van varkens na Fotodynamische Therapie met mTHPC en Photofrin als lichtgevoelige stof. De applicator uit hoofdstuk 5 werd gebruikt om het licht toe te dienen in de trachea en om een *in situ* meting van de fluentie uit te voeren. De fluenties die toegediend werden waren afgeleid van bestaande protocollen.

Een fluentie-bepalings experiment met korte-termijn schade (1-2 dagen) als eindpunt liet zien dat er aanzienlijke schade ontstaat wanneer Photofrin gebruikt wordt als lichtgevoelige stof (fluenties 50-275 J/cm^2, Photofrin dosis 2 mg/kg). Hierbij waren schade aan de bloedvaten en oedeem de belangrijkste verschijnselen. In het korte-termijn mTHPC experiment was de gevonden schade slechts gering (fluenties 12.5-50 J/cm^2, mTHPC dosis 0.15 mg/kg). Voor beide lichtgevoelige stoffen werd atrofie en acute ontsteking van zowel het epitheel als de kliertjes in de submucosa gevonden. De schade bleef beperkt tot het slijmvlies, waarbij het kraakbeen intact bleef. Een lange-termijn experiment liet zien dat fluenties van 50 J/cm^2 voor de mTHPC en 65 J/cm^2 voor de Photofrin behandelde dieren schades veroorzaakten die binnen 14 dagen hersteld was, met sporadisch lichte fibrose en af en toe ontsteking van de kliertjes.

Een beperkte set metingen van de farmaco-kinetiek van mTHPC laat zien dat de niveaus van de lichtgevoelige stof in de trachea vergelijkbaar zijn op 6 en 20 dagen na injectie. Het belang van *in situ* licht dosimetrie werd onderstreept door grote variaties in gemeten fluentie tempo tussen de dieren in vergelijkbare belichtingsomstandigheden.

Intra-operatieve adjuvante Fotodynamische Therapie voor Maligne Mesotheliomen

Hoofdstuk 8 beschrijft de behandeling van vijf patiënten met kanker aan het longslijmvlies met maximale chirurgische resectie van de tumor gevolgd door intra-operatieve adjuvante Fotodynamische Therapie. De Fotodynamische Therapie werd uitgevoerd met mTHPC als lichtgevoelige stof. De licht applicatie in de thorax werd gecontroleerd met *in situ* isotrope licht detectors. De positie van de spherische diffuser werd handmatig gevarieerd om een optimale lichtverdeling te verkrijgen, waarbij ook alle bijdragen van verstrooid licht in de thorax holte gemeten worden.

Er was geen postoperatieve mortaliteit na 30 dagen en slechts een patiënt ondervond een ernstige complicatie (scheuring van het middenrif en bloeding in het hartzakje). De operatietijd werd verlengd met maximaal een uur om de hele thoraxwand te belichten met een gemiddelde fluentie van 10 J/cm^2. Het effect van de adjuvante therapie werd onderzocht door het nemen van biopten 24 uur na de operatie middels een thoracoscopie. Significante schade (waaronder necrose) werd waargenomen in resterende tumor, terwijl bij normaal weefsel alleen acute ontstekingsinfiltraten en oedeem van het dwarsgestreepte spierweefsel gevonden werden.

Van de vijf behandelde patiënten zijn er nog 4 in leven zonder tekenen van terugkerende tumorgroei, met een opvolgtijd van 9-11 maanden. Een patiënt ontwikkelde tumor rond het litteken van de thoracoscopie, en overleed aan tumorgroei in de buikholte.

Afsluitende Opmerkingen

De fluentie tempo verdeling tijdens Endobronchiale Fotodynamische therapie (en alle andere toepassingen van PDT) wordt beïnvloed door vele factoren, waarvan sommige moeilijk *in situ* en routinematig te bepalen zijn (bijvoorbeeld de optische eigenschappen van het weefsel). Daarom is het essentieel dat er een *in situ* meting wordt gedaan tijdens de behandeling om er zeker van te zijn dat er een reproduceerbare licht fluentie aan het weefsel wordt toegediend. Alleen op deze manier zal het mogelijk zijn om een goede correlatie te verkrijgen tussen de hoeveelheid toegediend licht en het waargenomen therapeutische effect.

In dit proefschrift worden twee methodes voor *in situ* licht dosimetrie gepresenteerd, een voor de bovenste luchtwegen en een voor de belichting van de thorax. De fluentie tempo metingen kunnen gebruikt worden om een schatting te maken van de hele fluentie tempo verdeling, zij het met behulp van een beperkt aantal meetpunten (met name in het geval van de endo-

bronchiale applicator). Monte Carlo modellen kunnen helpen om met de enkele meetpunten toch een schatting van de hele lichtverdeling op en *in* het weefsel te maken. Het laatste is belangrijk omdat invasieve metingen niet goed mogelijk zijn en er van metingen aan het oppervlak uitgegaan moet worden.

De afmetingen van de isotrope detectors zijn zodanig dat ze gebruikt kunnen worden voor licht dosimetrie in vrijwel elk gebied. Voor ieder doelorgaan voor Fotodynamische Therapie is er een op dat orgaan toegesneden instrumentatie voor licht applicatie en licht dosimetrie nodig. De kennis van de farmaco-kinetiek van de lichtgevoelige stof is ook belangrijk voor het uiteindelijke therapeutische effect. De combinatie van *in situ* licht dosimetrie en meting van de fluorescentie van de lichtgevoelige stof voor en tijdens de behandeling zal een betere voorspelling geven van het te verwachten effect.

List of Publications

Murrer L H P, Marijnissen J P A, Star W M. (1998) Monte Carlo simulations for EndoBronchial PhotoDynamic Therapy: The influence of variations in optical and geometrical properties and of realistic and eccentric light sources. *Lasers Surg. Med. at press*

Murrer L H P, Marijnissen J P A, Star W M. (1997) Note: Improvements in the design of linear diffusers for Photodynamic Therapy *Phys. Med. Biol.* **42** *1461-1464*

Murrer L H P, Marijnissen J P A, Baas P, van Zandwijk N, Star W M. (1997) Applicator for light delivery and in situ light dosimetry during endobronchial Photodynamic Therapy: first measurements in humans. *Lasers Med. Sci.* **12** *253-259*

Murrer L H P, Marijnissen J P A, Star W M. (1996) Light distribution by linear diffusing sources for photodynamic therapy. *Phys. Med. Biol.* **41** *951-961*

Murrer L H P, Marijnissen J P A, Star W M. (1995) Ex vivo light dosimetry and Monte Carlo simulations for endobronchial photodynamic therapy. *Phys. Med. Biol.* **40** *1807-1817*

Baas P, Murrer L H P, Zoetmulder F A N, Stewart F A, Ris H B, van Zandwijk N and Rutgers E M. (1997) Photodynamic therapy as adjuvant therapy in surgically treated pleural malignancies. *Br. J. Cancer* **76** *819-826*

Saponaro S, Farina B, Murrer L H P, Pignoli E, Rizzo R, Star W M, Tomatis S, Marchesini R. (1996) Endoluminal photodynamic therapy: influence of optical properties on light fluence in the cilyndrical diffusing fibre geometry. *Proc. SPIE* **2923** *86-95*

Beck G, Star W M, Van Staveren H J, Murrer L H P, Rück A, Steiner R. (1996) Depth-sensitive fluorescence detection of dyes in tissue phantoms. *Proc. SPIE* **2926** *77-83*

Marijnissen J P A, Murrer L H P, Van Staveren H J. (1996) Lichtapplicatie en lichtdosimetrie voor endobronchiale fotodynamische therapie. *Klinische Fysica* **1996/3** *5-10*

Duysens J, Tax A A M, Murrer L, Dietz V. (1996) Backward and forward walking use different patterns of phase-dependent modulation of cutaneous reflexes in humans. *Journal of Neurophysiology* **76** *301-310*

Nawoord

Beste Willem, Hans, Nynke, Otto, Riette, Hugo, Jerry, Tous, Gemma, en natuurlijk Ann en Stijn.

Bedankt voor jullie bijdrage aan dit proefschrift en voor alle dingen die het leven aangenaam maken!

Curriculum Vitæ

Lars Murrer werd geboren op 12 april 1966 in Maastricht. Daar bezocht hij de Don Bosco lagere school en het Sint Maartens college, alwaar hij zijn Atheneum-β diploma behaalde in 1984. In dat zelfde jaar begon hij aan de HTS te Heerlen aan de studierichting Fysische Techniek. Tijdens stages voor deze studie begon hij zich te interesseren voor medische toepassingen van de fysica. Ook voelde hij de behoefte aan een meer fundamentele blik op de materie, zodat hij besloot na zijn afstuderen in 1988 zijn opleiding te vervolgen door natuurkunde te gaan studeren aan de Katholieke Universiteit van Nijmegen. Na het cum laude behalen van de propaedeuse koos hij voor de afstudeerrichting medische en bio-fysica, bij welke afdeling hij in 1992 cum laude afstudeerde op het onderwerp "*Modulatie van cutane reflexen in de menselijke beenspieren tijdens voor- en achteruitlopen*". Na zijn afstuderen werkte hij nog mee aan het publiceren van zijn afstudeerproject totdat hij in 1993 als Assistent In Opleiding begon bij de Erasmus Universiteit Rotterdam. Gedetacheerd bij de afdeling klinische fysica van de Daniel den Hoed Kliniek voerde hij zijn promotieonderzoek uit bij de projectgroep Fotodynamische Therapie. Het onderwerp van het onderzoek is ook het onderwerp van het proefschrift dat thans voor U ligt. Momenteel is Lars Murrer aangesteld als Klinisch Fysicus in Opleiding bij de afdeling klinische fysica van het AZR/Daniel den Hoed kliniek.